XXV SIGRAV Conference on General Relativity and Gravitation

Trieste, September 8, 2023

Tests of theories of gravitation in their weak-field and slow-motion limit with laser-tracked satellites

David Lucchesi

on behalf of the LARASE and SaToR-G experiments

Istituto Nazionale di Astrofisica (IAPS-INAF), Via Fosso del Cavaliere n. 100, 00133 Tor Vergata - Roma

Istituto Nazionale di Fisica Nucleare (INFN-RM2), Via della Ricerca Scientifica n. 1, 00133 Tor Vergata - Roma

david.lucchesi@inaf.it

Photo by Franco Ambrico (courtesy of G. Bianco, ASI-CGS)

Summary

- The LARASE and SaToR-G experiments
- Geodetic satellites and Satellite Laser Ranging
- Precise Orbit Determination
- Dynamic Model
- Measurements and constraints from pericenter and mean anomaly
- Measurements and constraints from the ascending node longitude
- Local Lorentz Invariance
- Conclusions

The LARASE and SaToR-G experiments

The **LA**ser **RA**nged **S**atellites **E**xperiment (**LARASE**, 2013-2019) and **Sa**tellite **T**ests **o**f **R**elativistic **G**ravity (**SaToR-G**, started on 2020) are two experiments devoted to measurements of the gravitational interaction in the **Weak-Field** and **Slow-Motion** (**WFSM**) limit of **General Relativity** (**GR**) by means of laser tracking to geodetic passive satellites orbiting around the Earth. The two experiments were and are funded by the **Italian National Institute for Nuclear Physics** (**INFN-CSN2**).

In particular, **SaToR-G** aims to test gravitation beyond the predictions of **Einstein's Theory** of **GR** searching for effects foreseen by **alternative theories of gravitation** (**ATG**) and possibly connected with ***''new physics''.***

SaToR-G builds on the improved dynamical model of the two **LAGEOS** and **LARES** satellites achieved within the previous project **LARASE.**

The improvements concern the modeling of both **gravitational** and **non-gravitational perturbations.**

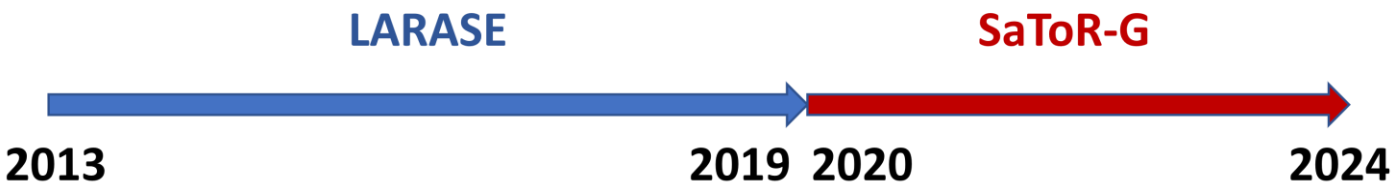

The LARASE and SaToR-G experiments

From the analysis of **satellite orbits** it is possible to obtain a series of measurements of **gravitational effects** with consequent constraints on **different theories of gravitation**. The main measures include:

1. **Relativistic precessions**
2. **Constraints on long-range interactions**
3. **Nonlinearity of the gravitational interaction**
4. **Local Lorentz Invariance**
5. **Equivalence principle**
6. **…**

From these measurements it is possible to obtain **constraints** on the **parametrized post-Newtonian** (**PPN*)* **parameters** and their combinations.

The ultimate goal is to provide **precise** and **accurate measures**, in the sense of a **robust** and **reliable** **evaluation** of **systematic errors**, in order to obtain **significant constraints** for the **different theories**.

The LARASE and SaToR-G experiments

The parametrized post-Newtonian (PPN) formalism

- Post-Newtonian formalism or **PPN** formalism details the parameters in which different metric theories of gravity, under **WFSM** conditions, can differ from Newtonian gravity.

Nordtvedt, K. *Equivalence Principle for Massive Bodies. II. Theory*. Phys. Rev. **1968**, 169, 1017–1025
Will, C.M. *Theoretical Frameworks for Testing Relativistic Gravity. II. Parametrized Post-Newtonian Hydrodynamics, and the Nordtvedt Effect*. Astrophys. J. **1971**, 163, 611–628
Will, C.M.; Nordtvedt, K. *Conservation Laws and Preferred Frames in Relativistic Gravity. I. Preferred-Frame Theories and an Extended PPN Formalism*. Astrophys. J. **1972**, 177, 757–774

Consequently, the natural theoretical framework to test gravitation will be that of the **Parameterized Post-Newtonian** (**PPN**) formalism.

However, we also try to apply, as far as possible, the approach suggested by **R. H. Dicke** more than 50 years ago, usually referred to as the **Dicke framework**:

- this is a fairly general framework that allows us to conceive experiments not connected, *a priori*, with a given physical theory and also provides a way to analyze the results of an experiment under **primary hypotheses**.

Dicke, R.H. *The Theoretical Significance of Experimental Relativity*; Blackie and Son Ltd.: London/Glasgow, UK, 1964

The LARASE and SaToR-G experiments

In 1971, **Thorne** and **Will** remarked that:

- " . . . It is important for the future that experimenters concentrate not only on measuring the **PPN** parameters. They should also perform new experiments within the **Dicke framework** to strengthen—or destroy—the foundation it lays for the **PPN framework** . . . "

Thorne, K.S.; Will, C.M. Theoretical Frameworks for Testing Relativistic Gravity. I. Foundations. Astrophys. J. **1971**, 163, 595

We analyzed these aspects in more detail in 2021 in the paper introducing the **SaToR-G** experiment:

D. Lucchesi, L. Anselmo, M. Bassan, et al., *Testing Gravitational Theories in the Field of the Earth with the SaToR-G Experiment*. Universe 7, 192, https://doi.org/10.3390/universe7060192, 2021

The LARASE and SaToR-G experiments

Gravity theories different from **GR** provide additional fields beside the metric tensor $g_{\alpha\beta}$, that act as "new" gravitational fields:

- **Scalar**
- **Vector**
- **Tensor**

The role of these gravitational fields is to "mediate" how the matter and the non-gravitational fields generate the gravitational fields and produce the metric.

In Metric theories different from GR

- spacetime geometry tells mass-energy how to move as in **GR**
- but mass-energy tells spacetime geometry how to curve in a different way from **GR**
- the metric alone acts back on the mass in agreement with **EEP** as in **GR**.

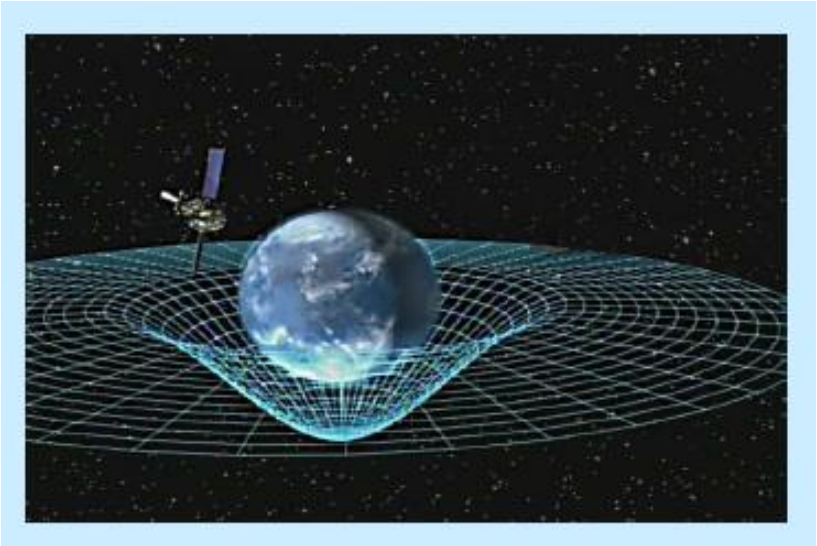

Geodetic satellites and Satellite Laser Ranging

The predictions of **GR** on the orbits of **geodetic satellites**, which play the role of **test masses**, will be compared with those of **ATG** both **metric** and **non-metric** in their essence

Parameter	Unit	Symbol	LAGEOS	LAGEOS II	LARES
Semi-major axis	km	a	12 270.00	12 162.08	7 820.31
Eccentricity	-	e	0.0044	0.0138	0.0012
Inclination	deg.	i	109.84	52.66	69.49
Radius	cm	R	30.0	30.0	18.2
Mass	kg	M	406.9	405.4	383.8
Area/Mass	m^2/kg	A/M	6.94×10^{-4}	6.97×10^{-4}	2.69×10^{-4}

LAGEOS (NASA, 1976)

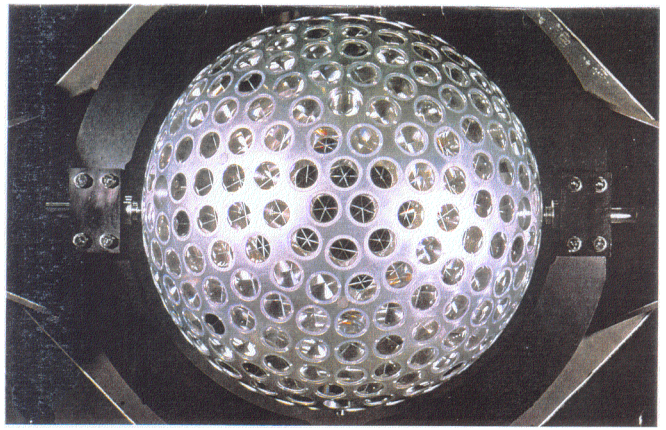

LAGEOS II (ASI/NASA, 1992)

LARES (ASI, 2012)

Geodetic satellites and Satellite Laser Ranging

The **geodetic** satellites are tracked with very high accuracy through the powerful **Satellite Laser Ranging** (**SLR**) technique.

The **SLR** represents a very impressive and powerful technique to determine the **round–trip time** between **Earth–bound laser Stations** and **orbiting passive** (and not **passive**) **satellites**.

The time series of range measurements are then a record of the motions of both the end points: the Satellite and the Station.

Thanks to the accurate modelling of both **gravitational** and **non–gravitational perturbations on** the orbit of these satellites — less than 1 cm in **range accuracy** — we are able to determine their **Keplerian elements** with about the same **accuracy**.

The precision of the measurement depends mainly from the laser pulse width, about $1 \cdot 10^{-10}$ s — $3 \cdot 10^{-11}$ s

Geodetic satellites and Satellite Laser Ranging

The **International Laser Ranging Service** (**ILRS**)

The **ILRS** was established as one of the **IAG** (**International Association of Geodesy**) measurement services in 1998, with a charter **to organize and coordinate world-wide Satellite Laser Ranging (SLR) and Lunar Laser Ranging (LLR)** activities to **support programs** in **geodesy**, **geophysics**, and **lunar and planetary science**, and to provide the data products (**Earth center of mass and scale**) important to the maintenance and improvement of the **International Terrestrial Reference Frame** (**ITRF**).
The main **scientific products** derived using **SLR** and **LLR** data include:

- **precise geocentric positions and motions of ground stations**
- **satellite orbits**
- **components of Earth's gravity field and their temporal variations**
- **tidal parameters**
- **Earth Orientation Parameters (EOP)**
- **mantle structure**
- **exchange of angular momentum between crust and atmosphere**
- **precise lunar ephemerides and information about the internal structure of the Moon**
- **Fundamental physics.**

Geodetic satellites and Satellite Laser Ranging

ilrs.gsfc.nasa.gov

The **ILRS** network

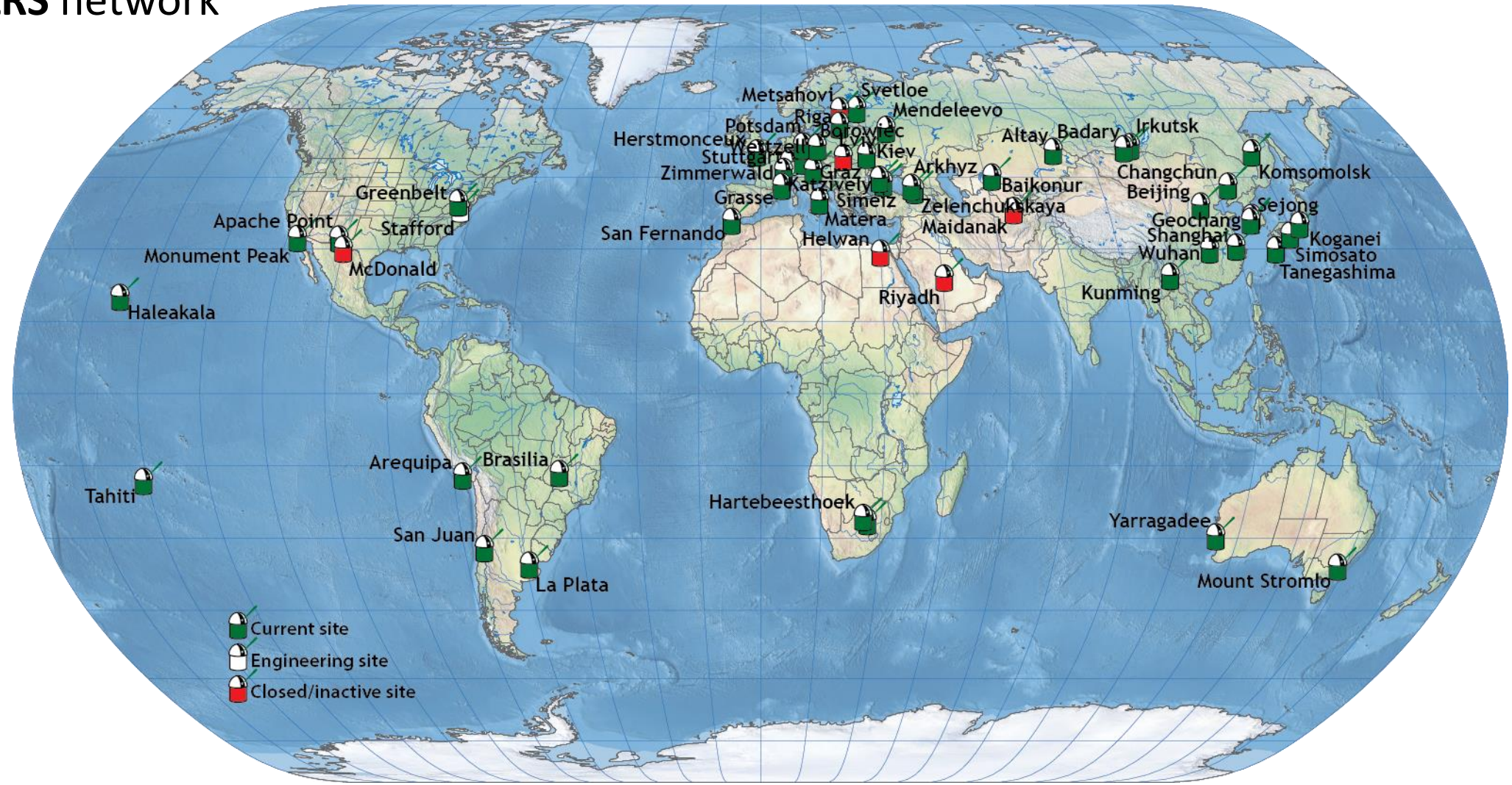

Geodetic satellites and Satellite Laser Ranging

The **ILRS** supports laser ranging measurements to **geodetic**, **remote sensing**, **navigation**, and **experimental satellites** equipped with retroreflector arrays as well as to **reflectors** on the **Moon**.

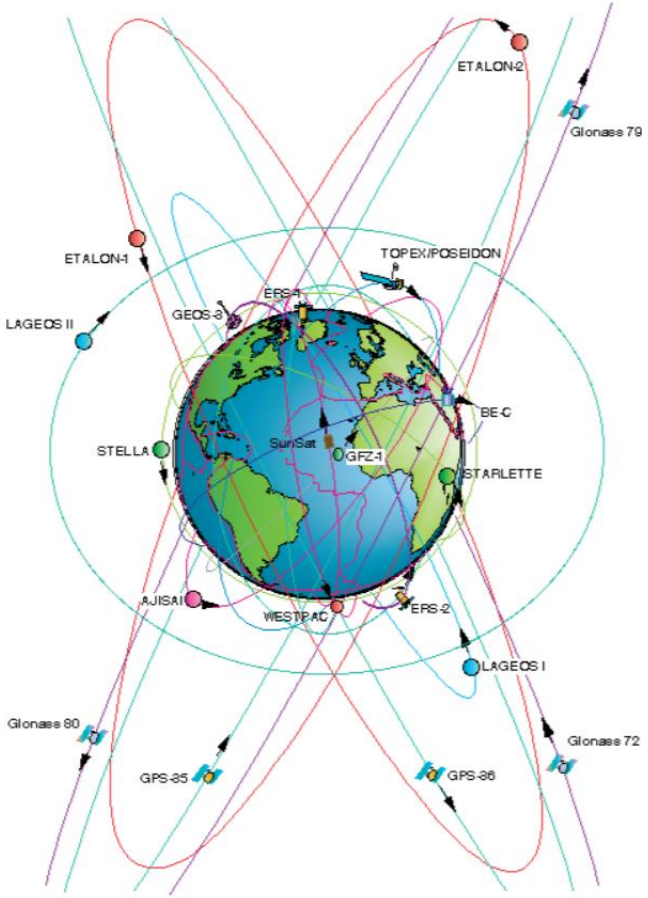

adeos	gfo1	msti
adeos2	gfz1	msti2
ajisai	giovea	oicets
alos	gioveb	paz
andec	glonass##[#] (##[#]=2/[3]-digit	pn1a
andep	satellite number)	proba2
anderra	goce	qzs#
anderrp	gpb	qzs1r
apollo11	gps35	radioastro
apollo14	gps36	reflector
apollo15	gracea	resurs
astrocst01	graceb	saral
astrocstp1	gracefo1	seasat
astrocstp2	gracefo2	sentinel3a
beaconc	hy2a	sentinel3b
beidou3m#	hy2b	sentinel6a
blits	hy2c	snet#
champ	ht2d	sohla1
chefsat	icesat	spinsat
compassg#	icesat2	starlette
compassi#	irnss1# (#=a,b,c, etc.)	starshine
compassis#	jason1	starshine2
compassm#	jason2	starshine3
compassms#	jason3	stella
cryosat2	kompsat5	stpsat2
diadem1c	lageos1	stsat2c
diadem1d	lageos2	sunsat
elsadchs	lares	swarma
elsadtgt	lares2	swarmb
envisat	larets	swarmc
ers1	lightsail1	swot
ers2	lightsail2	tandemx
etalon1	lomonosov	technosat
etalon2	lre	terrasarx
ets8	lrolr	tiangong2
fizeau	luna17	tips
galileo### (###=3-digit satellite	luna21	topex
number starting with 101)	meteor3	tubin
geoik2	meteor3m	westpac
geos3	moon	zeia
		zy3

Precise Orbit Determination

In simple words, **Precise Orbit Determination** (**POD**) has the **goal** of <u>accurately determining</u> the **position** and **velocity vectors** of an orbiting satellite.

To achieve this objective, **precise observations** of the satellite's **motion** and a **dynamic model** of the orbit as **accurate** as possible are necessary.

With these two ingredients it is possible to compute the **observable** to be **minimized** in a **least squares process**.

In the case of **SLR**, this **observable** is a **quadratic function** of the **range residuals *R***:

$$\mathcal{R}_i = O_i - C_i$$

Orbits:

$\frac{d}{dt}\vec{x} = f(\vec{x}, t, \vec{\alpha})$	Differential equation
$\begin{cases} \vec{x} \in \mathbb{R}^{\ell} \\ \vec{\alpha} \in \mathbb{R}^{m} \end{cases}$	State vector (position and velocity, …) Models dynamic parameters (C_{20}, Cr, …)
$\vec{x}(t_0 = \vec{x}_0 \in \mathbb{R}^{\ell})$	Initial condition at a given epoch: $\ell = 6+\ldots$
$\vec{x} = \vec{x}(t, \vec{x}_0, \vec{\alpha})$	General solution for the orbits (*integral flow*)

Observations:

$C = C(\vec{x}, t, \vec{\beta})$	Observation function, $\vec{\beta} \in \mathbb{R}^{n}$ kinematic parameters

$$R_i = O_i - C_i = O_i - C(\vec{x}(t_i), t_i, \vec{\beta}) = \sum_j \frac{\partial C_i}{\partial P_j}\delta P_j + \delta O_i \qquad Q(\vec{R}) = \frac{1}{q}\vec{R}^T\vec{R} = \frac{1}{q}\sum_{i=1}^{q} R_i^2$$

Precise Orbit Determination

Currently, we are using the following software in our **POD**:

- **GEODYN II** (NASA/GSFC)
- **SATAN** (NSGF, UK) in collaboration with "Observatorio de YEBES" (Spain) (under test)
- **Bernese** (Univ. Berna, CH)

1. From a least squares fit of the tracking data by means of an appropriate dynamic model, the estimate of the state vector of the satellite over 7-day arcs is obtained.
2. Then from an appropriate comparison between the state vector estimated at the beginning of each arc with the state vector estimated at the beginning of the previous arc but propagated at the same epoch, the residuals in the orbital elements are obtained: $\Delta\vec{x}_{res} = \vec{x}_{est} - \vec{x}_{pro}$

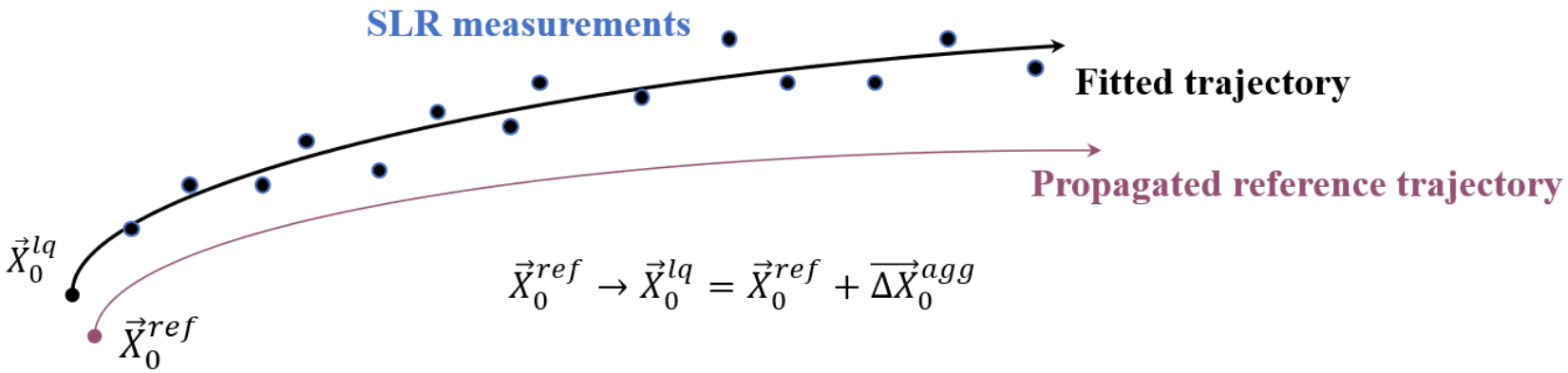

Precise Orbit Determination

Typical **POD** for the two **LAGEOS** and **LARES** satellites

- **GEODYN II s/w**
  - ❑ Arc length, 7 days
  - ❑ General Relativity: not modeled
  - ❑ Empirical accelerations, CR, …: not estimated
  - ❑ Non-gravitational perturbations: internal and external
  - ❑ Gravity field: from GRACE and GRACE-FO solutions
  - ❑ State-vector adjusted to best fit the tracking data
  - ❑ …

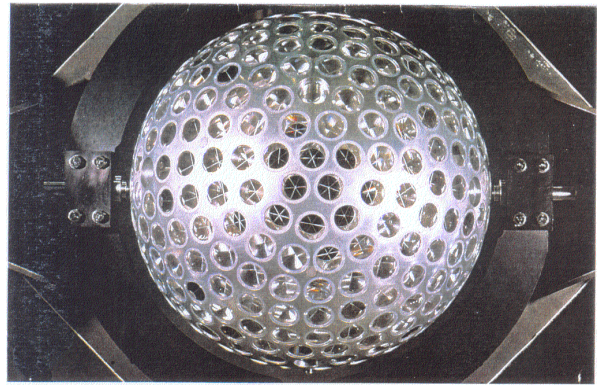

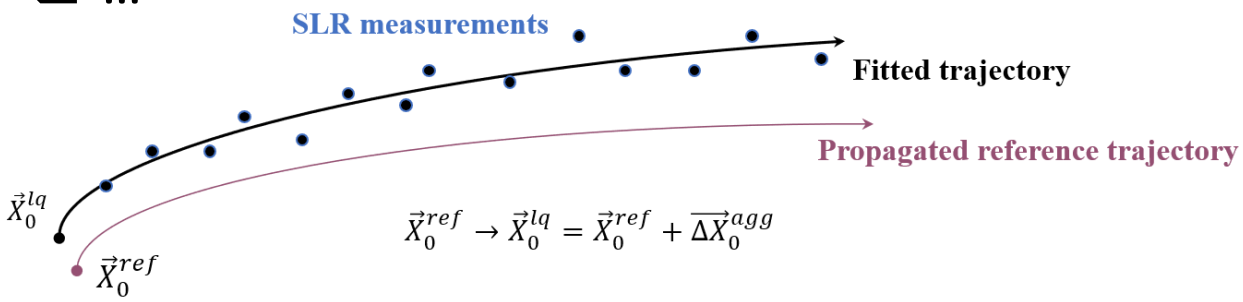

Table 2. Models currently used, within the LARASE research program, for the analysis of the orbit of the two LAGEOS and LARES satellites. The models are grouped in gravitational perturbations, non-gravitational perturbations and reference frames realizations.

Model For	Model Type	Reference
Geopotential (static)	EIGEN-GRACE02S/GGM05S	[84,90,91]
Geopotential (time-varying, tides)	Ray GOT99.2	[92]
Geopotential (time-varying, non tidal)	IERS Conventions 2010	[89]
Third–body	JPL DE-403	[93]
Relativistic corrections	Parameterized post-Newtonian	[88,94]
Direct solar radiation pressure	Cannonball	[46]
Earth albedo	Knocke-Rubincam	[63]
Earth-Yarkovsky	Rubincam	[56,64,65]
Neutral drag	JR-71/MSIS-86	[50,51]
Spin	LASSOS	[42]
Stations position	ITRF2008	[95]
Ocean loading	Schernek and GOT99.2 tides	[46,92]
Earth Rotation Parameters	IERS EOP C04	[96]
Nutation	IAU 2000	[97]
Precession	IAU 2000	[98]

Precise Orbit Determination

Orbital residuals: these are rate in the elements over 7 days

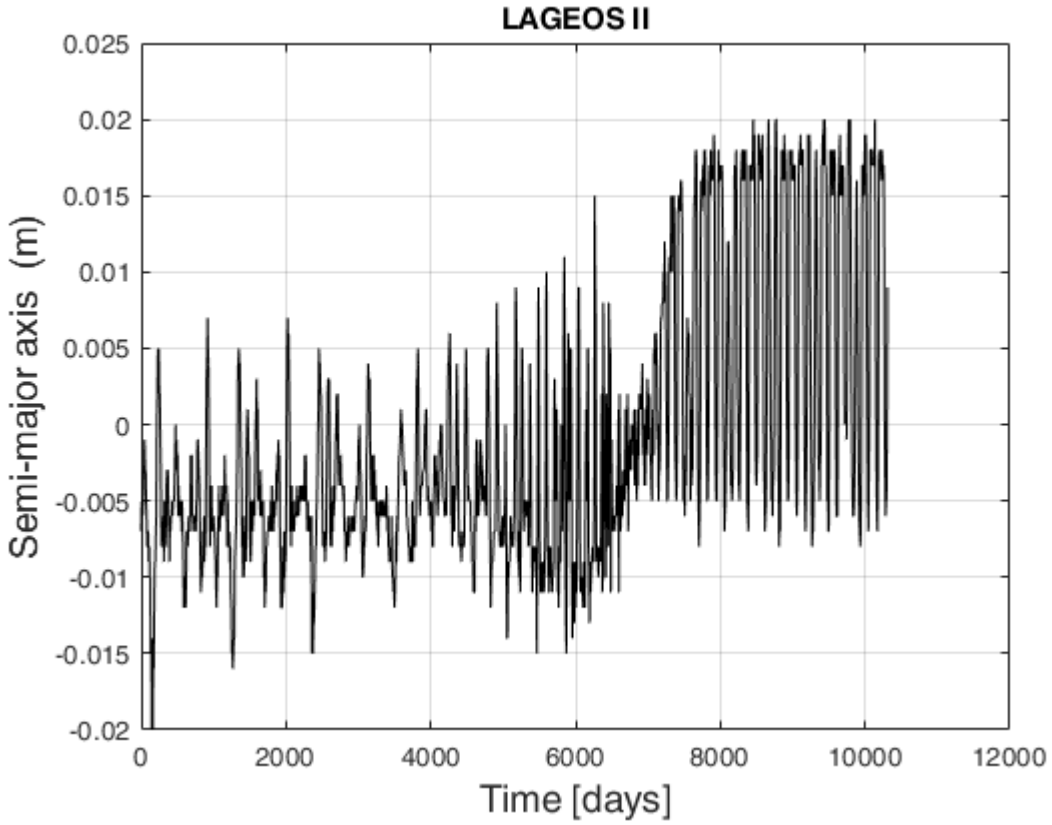

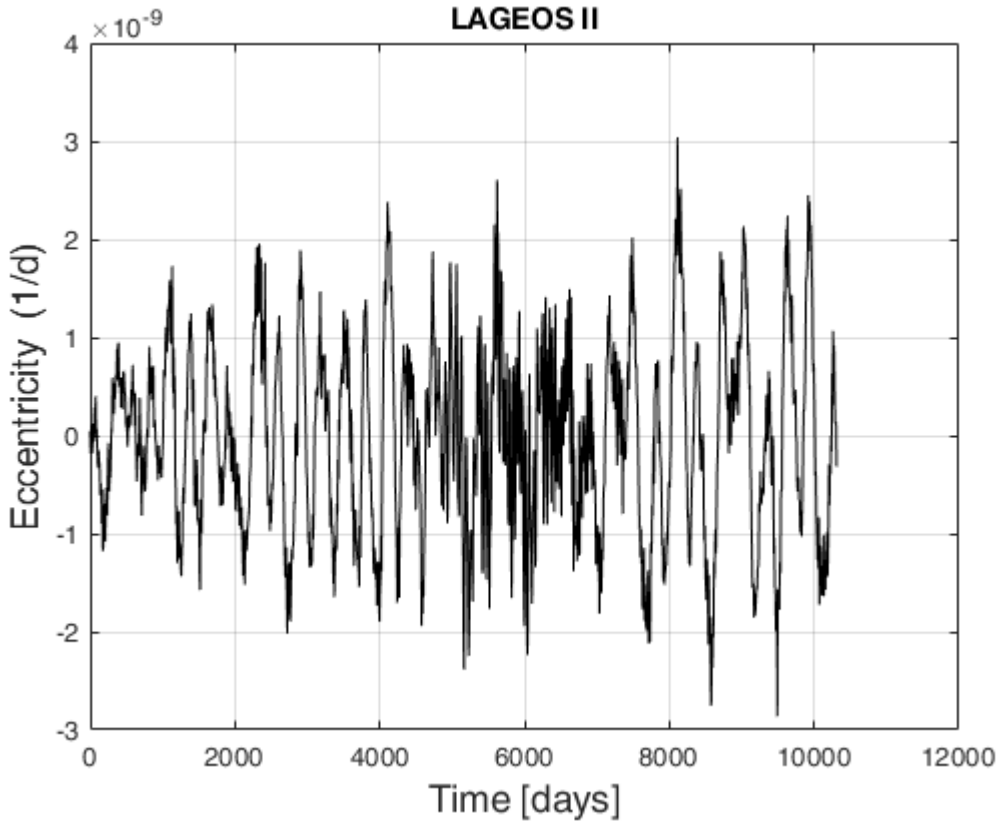

D. Lucchesi, G. Balmino, *The LAGEOS satellites orbital residuals determination and the Lense–Thirring effect measurement*. Plan. and Space Science, doi:10.1016/j.pss.2006.03.001, 2006

Precise Orbit Determination

Orbital residuals: these are rate in the elements over 7 days

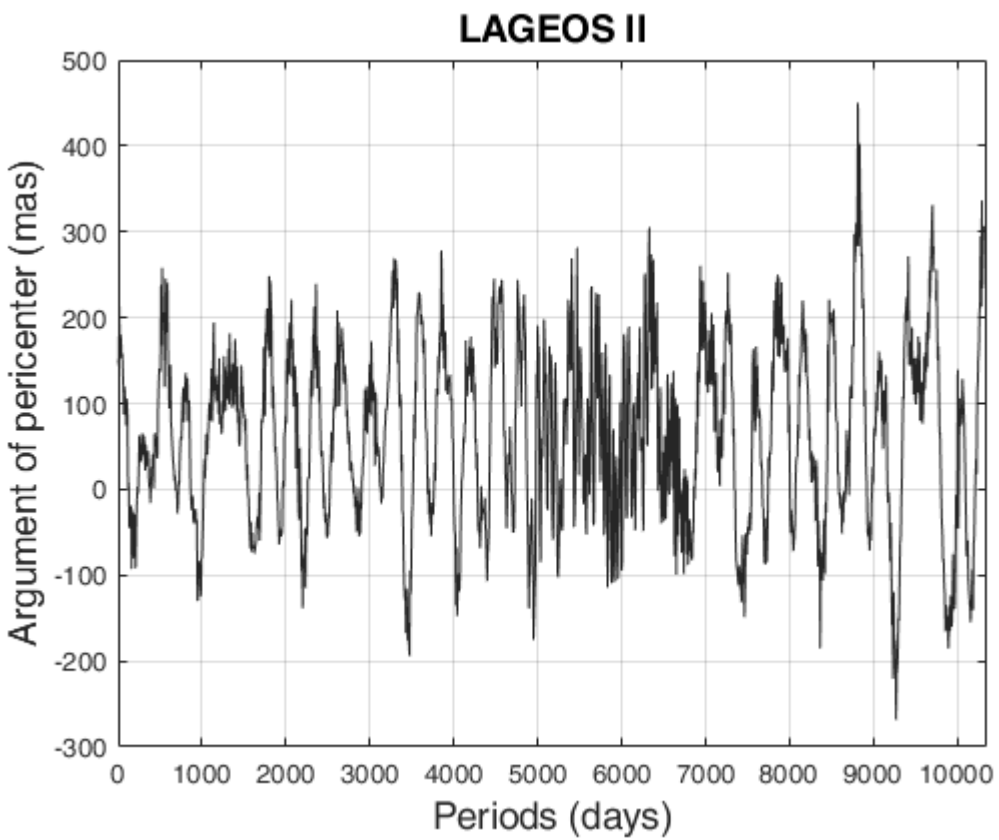

Therefore, all the computed residuals show both **periodic** and **secular effects**.

- **Periodic effects:**
  - **Gravitational effects, mainly due to the mismodeling of**
    - Gravity field
    - Tides
      - Ocean
      - Solid
  - **Non-gravitational perturbations, mainly due to**
    - Thermal thrust effects
    - Asymmetric reflectivity
- **Secular effects:**
  - **GR precession**
    - Schwarzschild
    - Lense-Thirring
    - De Sitter
    - Nonlinearity: mainly Earth's quadrupole J_2
  - **Thermal thrust effects, mainly due to**
    - Earth Yarkovsky effect
    - Solar Yarkovsky-Schach effect

Precise Orbit Determination

However, the correct separation of the various periodic effects (hence of their understanding) represents a very difficult task to achieve:

- it represents a challenge that is anything but simple to face
- the overcoming of which is of fundamental importance to better verify the gravitational interaction in the **WFSM** limit

The current periodic effects non modeled or mismodeled in the residuals:

- mask the measurement of any periodic effects of a relativistic nature
- constitute a kind of noise superimposed on the secular relativistic effects

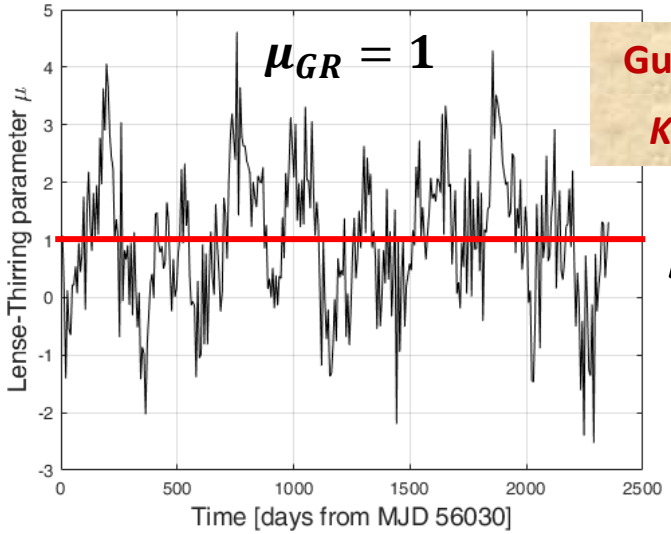

Gussian-like distribution for μ

K **≅ +3.097** ***S*** **≅ – 8.4×10⁻³**

$$\mu_{meas} = 0.99 \pm 0.13$$

S.D.=1.20

Dynamic Model

The **dynamic model** aims to reconstruct the **position** and **velocity** of the satellite taking into account **three main aspects**:

1. **gravitational perturbations**
2. **non-gravitational perturbations**
3. **reference systems.**

We will focus on the first two points:

1. **Gravitational perturbations (GPs)**
2. **Non-gravitational perturbations (NGPs).**

Dynamic Model

The **dynamic model** aims to reconstruct the position and velocity of the satellite taking into account three main aspects:

1. **gravitational perturbations**
2. **non-gravitational perturbations**
3. **reference systems.**

$$\dot{\omega}_{Schw} = \frac{3\,(GM_{\oplus})^{3/2}}{c^2\,a^{5/2}(1-e^2)}$$

$$\dot{\omega}_{LT} = -\frac{6G}{c^2a^3}\frac{J_{\oplus}}{(1-e^2)^{3/2}}\cos i$$

$$\dot{\Omega}_{LT} = \frac{2G}{c^2a^3}\frac{J_{\oplus}}{(1-e^2)^{3/2}}$$

$$\dot{M}_{Schw} = -\sqrt{1-e^2}\,\frac{3\,(GM_{\oplus})^{3/2}}{c^2\,a^{5/2}(1-e^2)}$$

We will focus on the first two points:

1. **Gravitational perturbations (GPs)**
2. **Non-gravitational perturbations (NGPs).**

In particular we are interested in knowing the effects of these perturbations on some orbital elements, those characterized by **secular effects** produced by **GR**, as:

- **Argument of pericenter, ω**
- **Right ascension of the ascending node, Ω**
- **Mean anomaly, M**

Dynamic Model: GPs

The **GR** model for the accelerations

Huang et al., Celest. Mech. & Dyn. Astron. 48, 1990

$$\vec{A}_{rel} = \vec{A}_E + \vec{A}_{dS} + \vec{A}_{LT}$$

$$\vec{A}_E = \frac{Gm_\oplus}{c^2 r^3}\left[\left(4\frac{Gm_\oplus}{r} - v^2\right)\vec{r} + 4(\vec{r} * \vec{v})\vec{v}\right]$$

$$\vec{A}_{dS} = 2(\vec{\Omega} \wedge \vec{v})$$

$$\vec{A}_{LT} = 2\frac{Gm_\oplus}{c^2 r^3}\left[\frac{3}{r^2}(\vec{r} \wedge \vec{v})(\vec{r} * \vec{J}) + (\vec{v} \wedge \vec{J})\right]$$

Relativistic perturbations

Einstein or Schwarzschild component

De Sitter (or geodetic) component

Lense–Thirring component

with:

$$\vec{\Omega} \cong \frac{3}{2}(\vec{V}_E - \vec{V}_S) \wedge \left(-\frac{GM_S}{c^2 R_{ES}^3}\right)\vec{X}_{ES}$$

Where, capital letters refer to position, velocity, acceleration and mass in the barycentric reference frame, while small letters refer to the same quantities in the non–inertial geocentric reference system (E=Earth, S=Sun)

Dynamic Model: GPs

Gravitational perturbations and their knowledge play an important role both in the satellite **POD** and in the estimation of the **error budget** of a measurement, i.e. for the valuation of the main sources of **systematic errors**

TABLE VIII: Models currently used for the POD obtained from GEODYN II. The models are grouped in gravitational perturbations, non-gravitational perturbations and reference frames realizations.

Model for	Model type	Reference
Geopotential (static)	EIGEN-GRACE02S/GGM05S	[45–47]
Geopotential (time-varying: even zonal harmonics)	GRACE/GRACE FO	[46, 47]
Geopotential (time-varying: tides)	Ray GOT99.2	[48]
Geopotential (time-varying: non tidal)	IERS Conventions 2010	[39]
Third–body	JPL DE-403	[49]
Relativistic corrections	Parameterized post-Newtonian	[44, 50]
Direct solar radiation pressure	Cannonball	[43]
Earth albedo	Knocke-Rubincam	[51]
Earth-Yarkovsky	Rubincam	[52–54]
Neutral drag	JR-71/MSIS-86	[55, 56]
Spin	LASSOS	[57]
Stations position	ITRF2008/2014	[58, 59]
Ocean loading	Schernek and GOT99.2 tides	[43, 48]
Earth Rotation Parameters	IERS EOP C04	[60]
Nutation	IAU 2000	[61]
Precession	IAU 2000	[62]

Dynamic Model: GPs

The Earth's potential development in spherical harmonics

$$V(r,\varphi,\lambda) = -\frac{GM_\oplus}{r}\left[1 + \sum_{\ell=2}^{\infty}\sum_{m=0}^{\ell}\left(\frac{R_\oplus}{r}\right)^{\ell} P_{\ell m}(\sin\varphi)(\bar{C}_{\ell m}\cos m\lambda + \bar{S}_{\ell m}\sin m\lambda)\right]$$

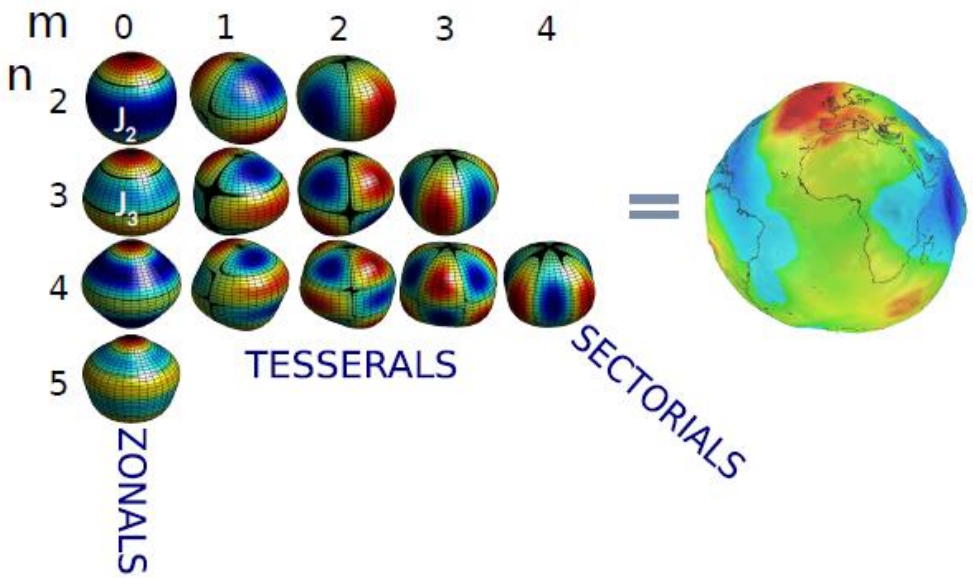

Dynamic Model: GPs

For instance, the **Einstein-Thirring-Lense** precession is very small compared to the classical precession of the orbit due to the deviation from the spherical symmetry for the distribution of the Earth's mass, or even compared to the same relativistic **Schwarzschild** precession produced by the mass of the primary (≈ 3350 mas/yr for **LAGEOS**)

$$V(r,\varphi,\lambda) = -\frac{GM_\oplus}{r}\left[1+\sum_{\ell=2}^{\infty}\sum_{m=0}^{\ell}\left(\frac{R_\oplus}{r}\right)^{\ell} P_{\ell m}(\sin\varphi)(\bar{C}_{\ell m}\cos m\lambda + \bar{S}_{\ell m}\sin m\lambda)\right]$$

$$\dot{\Omega}_{LT} = \frac{2G}{c^2a^3}\frac{J_\oplus}{(1-e^2)^{3/2}}$$

Rate (mas/yr)	LAGEOS	LAGEOS II	LARES
$\dot{\Omega}_{LT}$	30.67	31.50	118.48

The even zonal harmonics $\bar{C}_{\ell 0}$ are responsible of a secular effect

$$\langle\dot{\Omega}_{class}\rangle_{sec} = -\frac{3}{2}n\left(\frac{R_\oplus}{a}\right)^2\frac{\cos i}{(1-e^2)^2}\left\{-\sqrt{5}\bar{C}_{2,0}+\cdots\right.$$

$$\dot{\Omega}^{Obser}_{Lageos} \approx +126\ deg/yr \qquad \dot{\Omega}^{Obser}_{LageosII} \approx -231\ deg/yr \qquad \dot{\Omega}^{Obser}_{Lares} \approx -624\ deg/yr$$

Dynamic Model: GPs

Therefore, the correct modelling of the even zonal harmonics (ℓ = even, $m = 0$) represents the main challenge in this kind of measurements, since they have the same signature of the relativistic effect but much larger amplitudes. **These harmonics are the main sources of systematic errors**

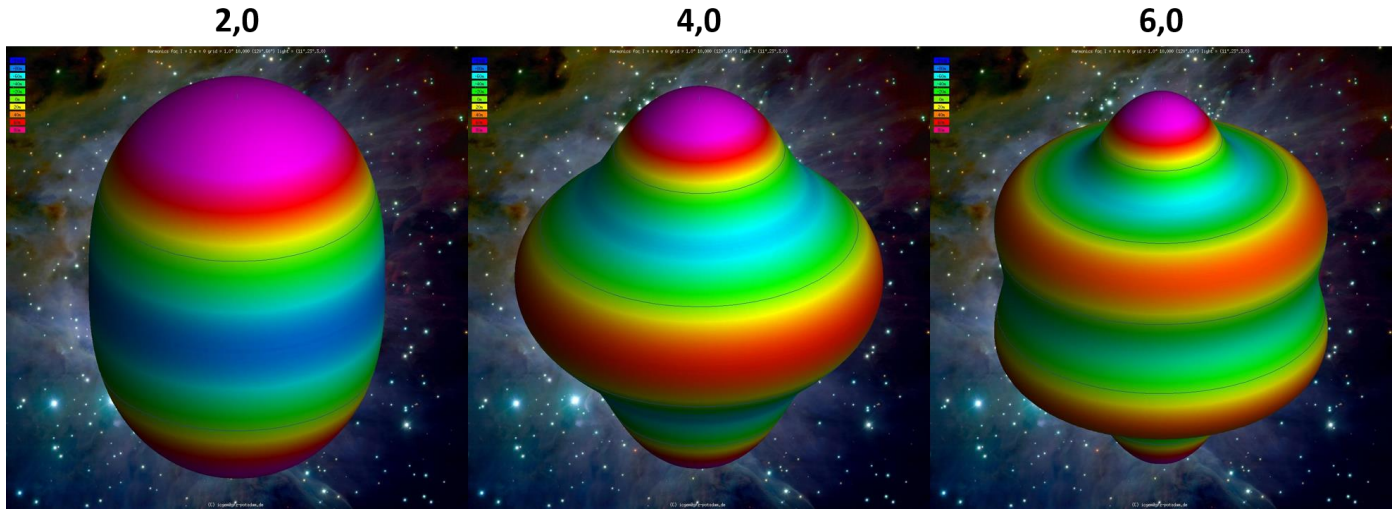

$$\langle \dot{\Omega}_{class} \rangle_{sec} = -\frac{3}{2} n \left(\frac{R_\oplus}{a}\right)^2 \frac{\cos i}{(1-e^2)^2} \left\{ -\sqrt{5}\bar{C}_{2,0} + \cdots \right.$$

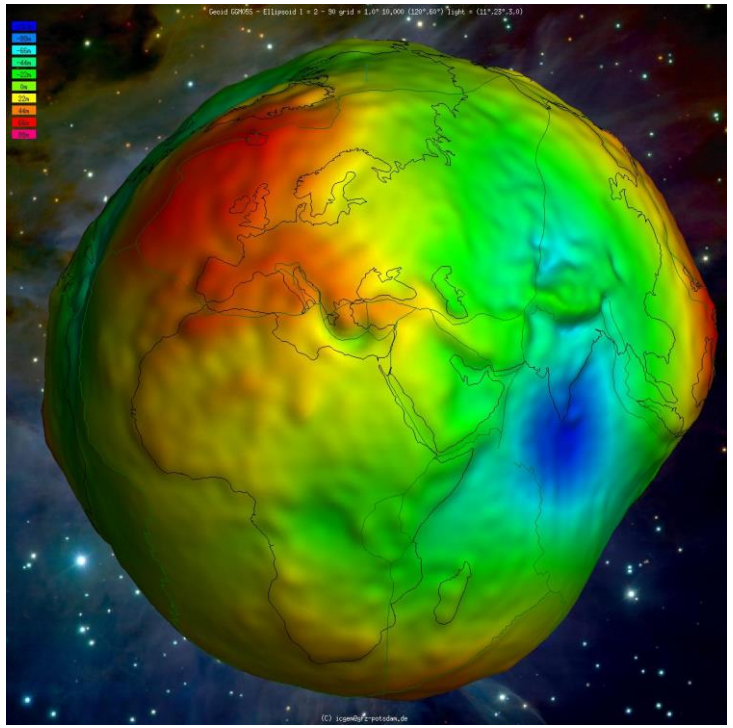

Dynamic Model: GPs

29/10/2020 ICGEM International Center for Global Gravity Field Models

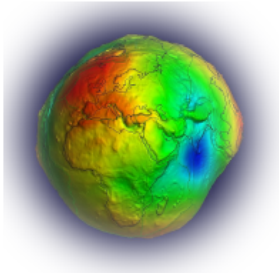

ICGEM Home

Gravity Field Models

Static Models

Temporal Models

Topographic Gravity Field Models

Calculation Service

Regular grids

User-defined points

3D Visualisation

Static Models

Temporal Models

Trend & Amplitude

Spherical Harmonics

Evaluation

Spectral domain

GNSS Leveling

Documentation

FAQ

ICGEM

GFZ Helmholtz Centre Potsdam

Global Gravity Field Models

We kindly ask the authors of the models to check the links to the original websites of the models from time to time. Please let us know if something has changed.

The table can be interactively re-sorted by clicking on the column header fields (Nr, Model, Year, Degree, Data, Reference).
In the data column, the datasets used in the development of the models are summarized, where **A** is for altimetry, **S** is for satellite (e.g., GRACE, GOCE, LAGEOS), **G** for ground data (e.g., terrestrial, shipborne and airborne measurements) and **T** is for topography.

The links calculate and show in the last columns of the table directly invoke the *Calculation Service* and *Visualization page* for the selected model.
For models with a registered **doi** ("digital object identifier") the last column contains the symbol ✓, which directly opens the page on "http://dx.doi.org/".
If you click on the reference, the complete list of references can be seen.

Nr	Model	Year	Degree	Data	References	Download	Calculate	Show	DOI
176	XGM2019e_2159	2019	2190 5540 760	A, G, S(GOCO06s), T	Zingerle, P. et al, 2019	gfc zip gfc zip gfc zip	Calculate	Show	✓
175	GO_CONS_GCF_2_TIM_R6e	2019	300	G (Polar), S(Goce)	Zingerle, P. et al, 2019	gfc zip	Calculate	Show	✓
174	ITSG-Grace2018s	2019	200	S(Grace)	Mayer-Gürr, T. et al, 2018	gfc zip	Calculate	Show	✓
173	EIGEN-GRGS.RL04.MEAN-FIELD	2019	300	S	Lemoine et al, 2019	gfc zip	Calculate	Show	✓
172	GOCO06s	2019	300	S	Kvas et al., 2019	gfc zip	Calculate	Show	✓
171	GO_CONS_GCF_2_TIM_R6	2019	300	S(Goce)	Brockmann, J. M. et al, 2014	gfc zip	Calculate	Show	✓
170	GO_CONS_GCF_2_DIR_R6	2019	300	S	Bruinsma, S. L. et al, 2014	gfc zip	Calculate	Show	✓
169	IGGT_R1C	2018	240	G, S(Goce), S(Grace)	Lu, B. et al., 2019	gfc zip	Calculate	Show	✓
168	Tongji-Grace02k	2018	180	S(Grace)	Chen, Q. et al, 2018	gfc zip	Calculate	Show	
167	SGG-UGM-1	2018	2159	EGM2008, S(Goce)	Liang, W. et al., 2018 & Xu, X. et al. (2017)	gfc zip	Calculate	Show	✓
166	GOSG01S	2018	220	S(Goce)	Xu, X. et al., 2018	gfc zip	Calculate	Show	✓
165	IGGT_R1	2017	240	S(Goce)	Lu, B. et al, 2017	gfc zip	Calculate	Show	✓
164	IfE_GOCE05s	2017	250	S	Wu, H. et al, 2017	gfc zip	Calculate	Show	✓
163	GO_CONS_GCF_2_SPW_R5	2017	330	S(Goce)	Gatti, A. et al, 2016	gfc zip	Calculate	Show	✓

icgem@gfz-potsdam.de

icgem.gfz-potsdam.de/tom_longtime 1/1

Static Models

Dynamic Model: GPs

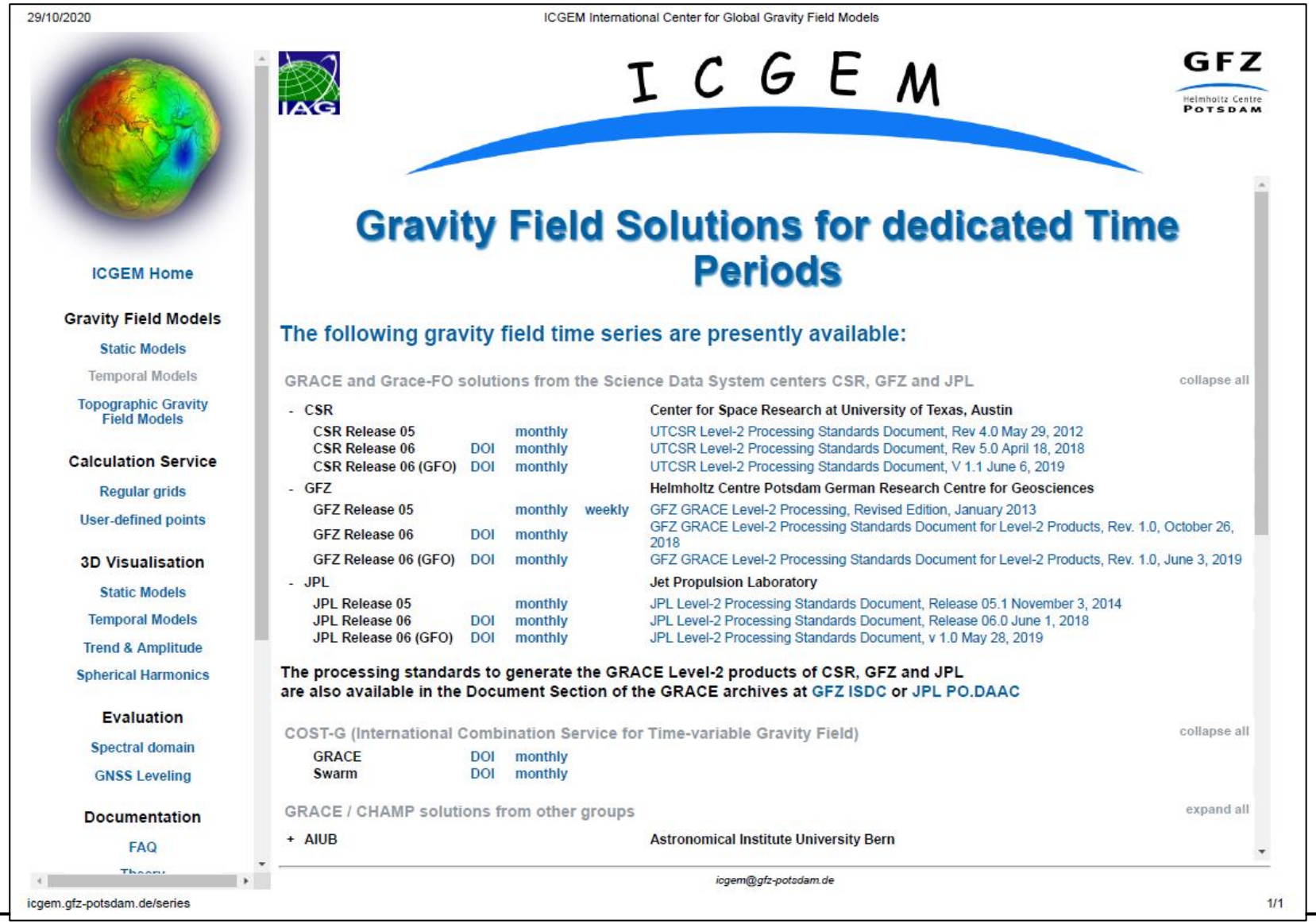

29/10/2020 ICGEM International Center for Global Gravity Field Models

ICGEM Home

Gravity Field Models

Static Models

Temporal Models

Topographic Gravity Field Models

Calculation Service

Regular grids

User-defined points

3D Visualisation

Static Models

Temporal Models

Trend & Amplitude

Spherical Harmonics

Evaluation

Spectral domain

GNSS Leveling

Documentation

FAQ

I C G E M

Gravity Field Solutions for dedicated Time Periods

The following gravity field time series are presently available:

GRACE and Grace-FO solutions from the Science Data System centers CSR, GFZ and JPL — collapse all

- CSR				Center for Space Research at University of Texas, Austin
CSR Release 05		monthly		UTCSR Level-2 Processing Standards Document, Rev 4.0 May 29, 2012
CSR Release 06	DOI	monthly		UTCSR Level-2 Processing Standards Document, Rev 5.0 April 18, 2018
CSR Release 06 (GFO)	DOI	monthly		UTCSR Level-2 Processing Standards Document, V 1.1 June 6, 2019
- GFZ				Helmholtz Centre Potsdam German Research Centre for Geosciences
GFZ Release 05		monthly	weekly	GFZ GRACE Level-2 Processing, Revised Edition, January 2013
GFZ Release 06	DOI	monthly		GFZ GRACE Level-2 Processing Standards Document for Level-2 Products, Rev. 1.0, October 26, 2018
GFZ Release 06 (GFO)	DOI	monthly		GFZ GRACE Level-2 Processing Standards Document for Level-2 Products, Rev. 1.0, June 3, 2019
- JPL				Jet Propulsion Laboratory
JPL Release 05		monthly		JPL Level-2 Processing Standards Document, Release 05.1 November 3, 2014
JPL Release 06	DOI	monthly		JPL Level-2 Processing Standards Document, Release 06.0 June 1, 2018
JPL Release 06 (GFO)	DOI	monthly		JPL Level-2 Processing Standards Document, v 1.0 May 28, 2019

The processing standards to generate the GRACE Level-2 products of CSR, GFZ and JPL are also available in the Document Section of the GRACE archives at GFZ ISDC or JPL PO.DAAC

COST-G (International Combination Service for Time-variable Gravity Field) — collapse all

GRACE	DOI	monthly
Swarm	DOI	monthly

GRACE / CHAMP solutions from other groups — expand all

+ AIUB — Astronomical Institute University Bern

icgem@gfz-potsdam.de

icgem.gfz-potsdam.de/series 1/1

Temporal Models

Dynamic Model: GPs

The modeling of the even zonal harmonics

To reduce the impact of the knowledge of these coefficients on the relativistic precession measurement, we modeled them accounting for their significant time dependency as well evidenced by their **Temporal Solutions** (**TS**) provided by the **GRACE** (**NASA/DLR**) and **GRACE-FO** missions

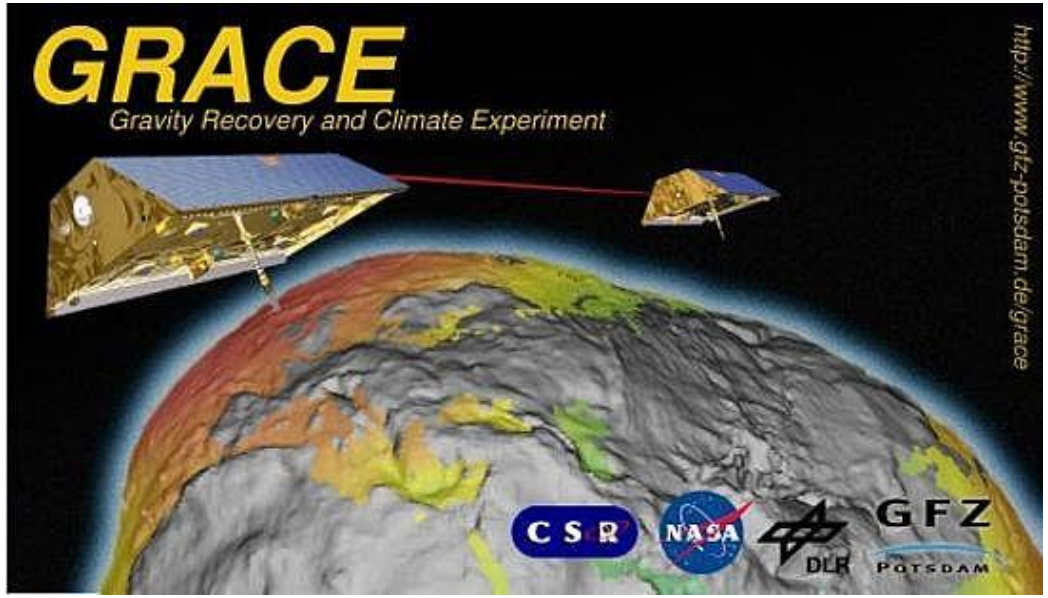

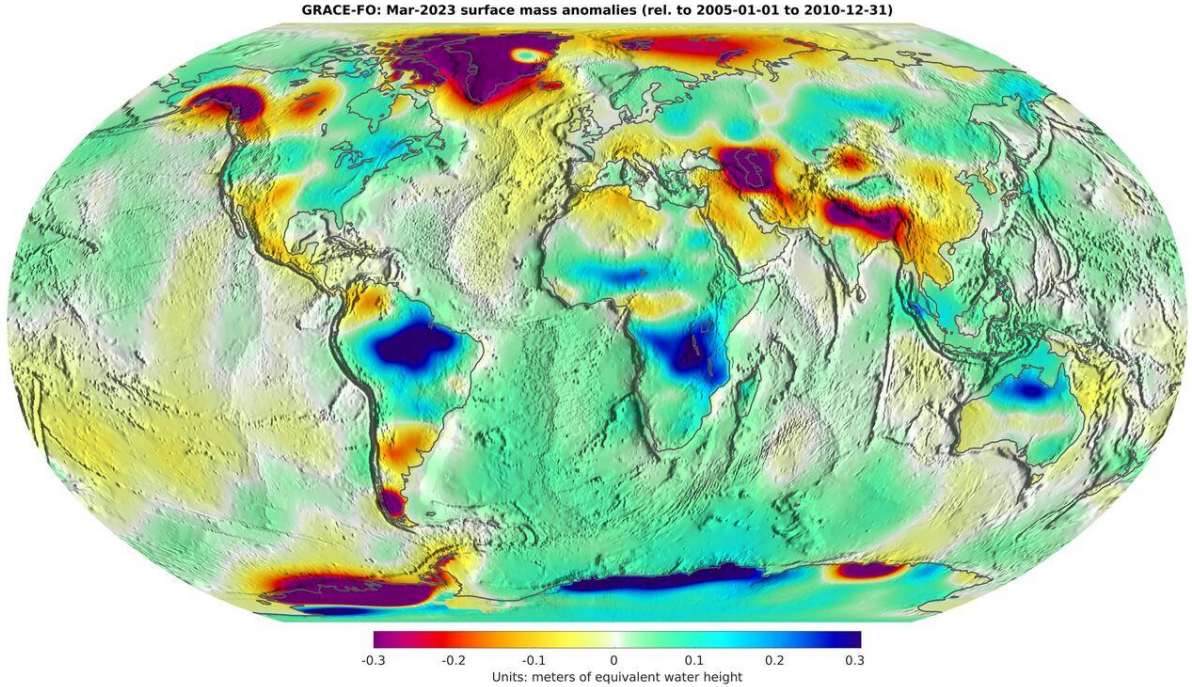

Dynamic Model: GPs

The modeling of the even zonal harmonics

To reduce the impact of the knowledge of these coefficients on the relativistic precession measurement, we modeled them accounting for their significant time dependency as well evidenced by their **Temporal Solutions** (**TS**) provided by the **GRACE** (**NASA/DLR**) and **GRACE-FO** missions

- we started this activity in 2017
- this activity has been fundamental to **reduce** the impact of the **systematic error** related to the **knowledge** of the **Earth's gravitational field**

Dynamic Model: GPs

The modeling of the even zonal harmonics

To reduce the impact of the knowledge of these coefficients on the relativistic precession measurement, we modeled them accounting for their significant time dependency as well evidenced by their **Temporal Solutions** (**TS**) provided by the **GRACE** (**NASA/DLR**) and **GRACE-FO** missions

- we started this activity in 2017
- this activity has been fundamental to reduce the impact of the systematic error related to the knowledge of the Earth's gravitational field
  - **in the error budget**

$$x = x_{meas} \pm \delta x \pm \Delta x_{sys}$$

Dynamic Model: GPs

The modeling of the even zonal harmonics

To reduce the impact of the knowledge of these coefficients on the relativistic precession measurement, we modeled them accounting for their significant time dependency as well evidenced by their **Temporal Solutions** (**TS**) provided by the **GRACE** (**NASA/DLR**) and **GRACE-FO** missions

- we started this activity in 2017
- this activity has been fundamental to reduce the impact of the systematic error related to the knowledge of the Earth's gravitational field
  - **in the error budget**
  - **In the measurement itself (nonlinear fit vs linear fit)**

$$x = \underbrace{x_{meas} \pm \delta x} \pm \Delta x_{sys}$$

Dynamic Model: GPs

From **GRACE** Temporal Solutions

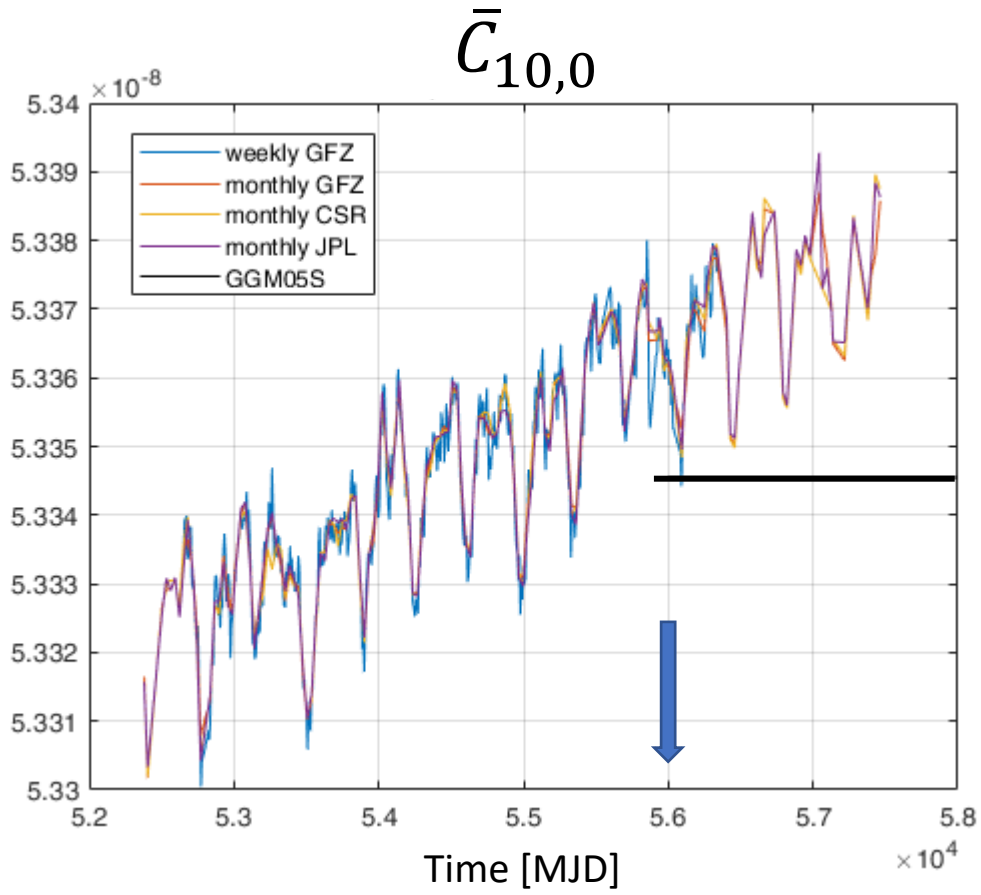

March 14, 2012

$$V(r,\varphi,\lambda) = -\frac{GM_\oplus}{r}\left[1 + \sum_{\ell=2}^{\infty}\sum_{m=0}^{\ell}\left(\frac{R_\oplus}{r}\right)^{\ell} P_{\ell m}(\sin\varphi)(\bar{C}_{\ell m}\cos m\lambda + \bar{S}_{\ell m}\sin m\lambda)\right]$$

$$\langle\dot{\Omega}_{class}\rangle_{sec} = -\frac{3}{2}n\left(\frac{R_\oplus}{a}\right)^2\frac{\cos i}{(1-e^2)^2}\left\{-\sqrt{5}\bar{C}_{2,0} + \cdots\right.$$

$$\dot{\Omega}_{LT} = \frac{2G}{c^2a^3}\frac{J_\oplus}{(1-e^2)^{3/2}}$$

$$\langle\dot{\omega}_{class}\rangle_{sec} = -\frac{3}{4}n\left(\frac{R_\oplus}{a}\right)^2\frac{1-5cos^2 i}{(1-e^2)^2}\left\{-\sqrt{5}\bar{C}_{2,0} + \cdots\right.$$

$$\dot{\omega}_{Schw} = \frac{3\,(GM_\oplus)^{3/2}}{c^2\,a^{5/2}(1-e^2)} = 3352.58\ mas/yr$$

Dynamic Model: GPs

From **GRACE** Temporal Solutions

$$V(r,\varphi,\lambda) = -\frac{GM_\oplus}{r}\left[1+\sum_{\ell=2}^{\infty}\sum_{m=0}^{\ell}\left(\frac{R_\oplus}{r}\right)^{\ell} P_{\ell m}(\sin\varphi)(\bar{C}_{\ell m}\cos m\lambda + \bar{S}_{\ell m}\sin m\lambda)\right]$$

$\bar{C}_{10,0}$

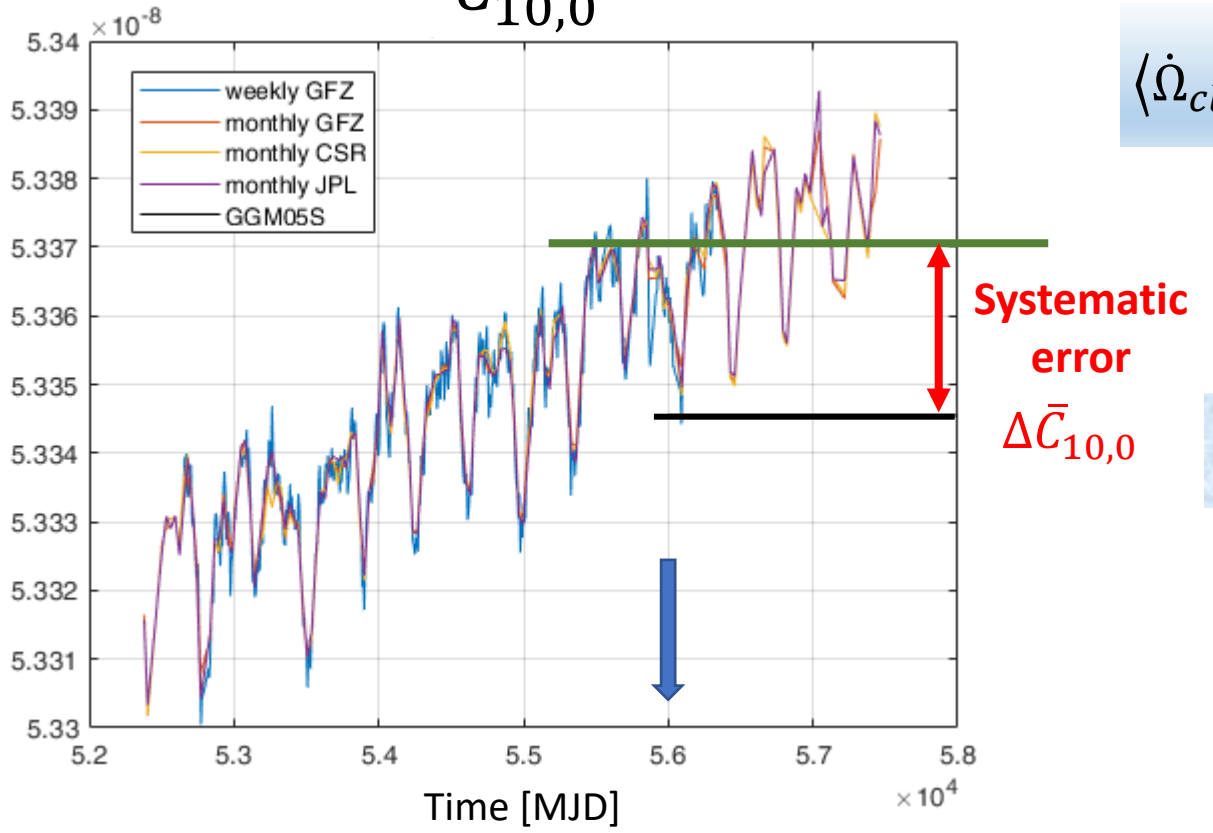

March 14, 2012

$$\langle\dot{\Omega}_{class}\rangle_{sec} = -\frac{3}{2}n\left(\frac{R_\oplus}{a}\right)^2\frac{\cos i}{(1-e^2)^2}\left\{-\sqrt{5}\bar{C}_{2,0}+\cdots\right.$$

$$\dot{\Omega}_{LT} = \frac{2G}{c^2a^3}\frac{J_\oplus}{(1-e^2)^{3/2}}$$

$$\langle\dot{\omega}_{class}\rangle_{sec} = -\frac{3}{4}n\left(\frac{R_\oplus}{a}\right)^2\frac{1-5cos^2 i}{(1-e^2)^2}\left\{-\sqrt{5}\bar{C}_{2,0}+\cdots\right.$$

$$\dot{\omega}_{Schw} = \frac{3\,(GM_\oplus)^{3/2}}{c^2\,a^{5/2}(1-e^2)} = 3352.58\ mas/yr$$

$$\Delta\bar{C}_{\ell,0} \Rightarrow \Delta\dot{\Omega}_{LT}^{sys} \quad and \quad \Delta\dot{\omega}_{LT}^{sys}$$

Dynamic Model: GPs

Some articles concerning the modeling of Gravitational Perturbations in relation to measurements in the field of gravitation and of gravity theories

D. Lucchesi, *THE IMPACT OF THE EVEN ZONAL HARMONICS SECULAR VARIATIONS ON THE LENSE THIRRING EFFECT MEASUREMENT WITH THE TWO LAGEOS SATELLITES*. International Journal of Modern Physics D, Vol. 14, No. 12, 1989-2023; doi: 10.1142/S0218271805008169, 2005

D. Lucchesi, R. Peron, LAGEOS II pericenter general relativistic precession (1993-2005): Error budget and constraints in gravitational physics. Phys. Rev. D 89, 082002, doi:10.1103/PhysRevD.89.082002, 2014

G. Pucacco, D. Lucchesi, *Tidal effects on the LAGEOS–LARES satellites and the LARASE program*. Celest. Mech. And Dyn. Astron., 130:66, https://doi.org/10.1007/s10569-018-9861-5, 2018

D. Lucchesi, L. Anselmo, et al., *General Relativity Measurements in the Field of Earth with Laser-Ranged Satellites: State of the Art and Perspectives*. Universe, 5, 141; doi:10.3390/universe5060141, 2019

D. Lucchesi, M. Visco, et al., *A 1% Measurement of the Gravitomagnetic Field of the Earth with Laser-Tracked Satellites*. Universe, 6, 139; doi:10.3390/universe6090139, 2020

Dynamic Model: NGPs

In recent years, as part of the previous experiment **LARASE**, we have developed several models to take into account some **perturbations** of **non-gravitational origin** acting on the **LAGEOS**, **LAGEOS II** and **LARES** satellites:

- **Spin model**
- **General model for thermal thrust forces due to the Sun and the Earth (to be published)**
- **Neutral drag model**

M. Visco, D. Lucchesi, *Review and critical analysis of mass and moments of inertia of the LAGEOS and LAGEOS II satellites for the LARASE program*. Adv. in Space Res. 57, 044034 doi:10.1016/j.asr.2016.02.006, 2016

M. Visco, D. Lucchesi, *Comprehensive model for the spin evolution of the LAGEOS and LARES satellites*. Phys. Rev. D 98, 044034 doi:10.1103/PhysRevD.98.044034, 2018

Pardini, C.; Anselmo, L.; Lucchesi, D.M.; Peron, R., *On the secular decay of the LARES semi-major axis*. Acta Astronautica **2017**, 140, 469–477. doi:10.1016/j.actaastro.2017.09.012

Dynamic Model: NGPs

M. Visco, D. Lucchesi, *Review and critical analysis of mass and moments of inertia of the LAGEOS and LAGEOS II satellites for the LARASE program*. Adv. in Space Res. 57, 044034 doi:10.1016/j.asr.2016.02.006, 2016

Table 1
Materials used for the construction of the two LAGEOS satellites (Cogo, 1988) and their nominal densities.

Satellite	Material density ρ_n (kg/m^3)		
	Hemispheres	Core	Stud
LAGEOS	AA6061 2700[a]	QQ-B-626 COMP.11 8440[a]	Cu-Be 8230[b]
LAGEOS II	AlMgSiCu UNI 6170 2740[c]	PCuZn39Pb2 UNI 5706 8280[c]	Cu-Be QQ-C-172 8250[c]

[a] ASM International Handbook Committee (1990).
[b] Bauccio (1993).
[c] It is the value calculated in Cogo (1988) starting from the measured averaged composition.

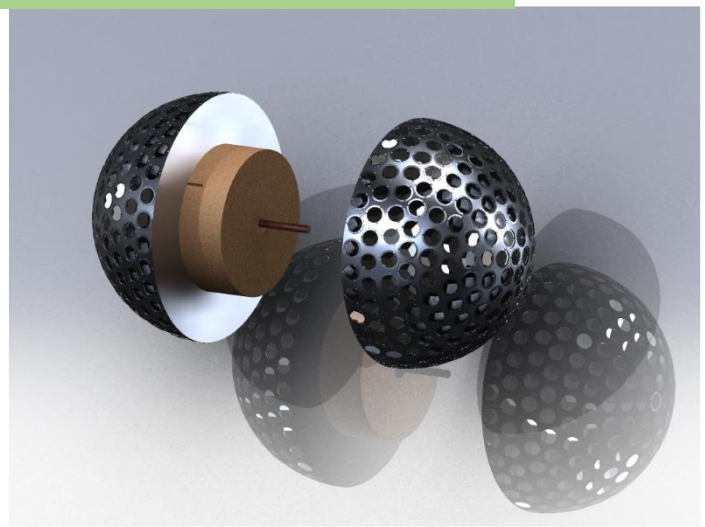

LAGEOS

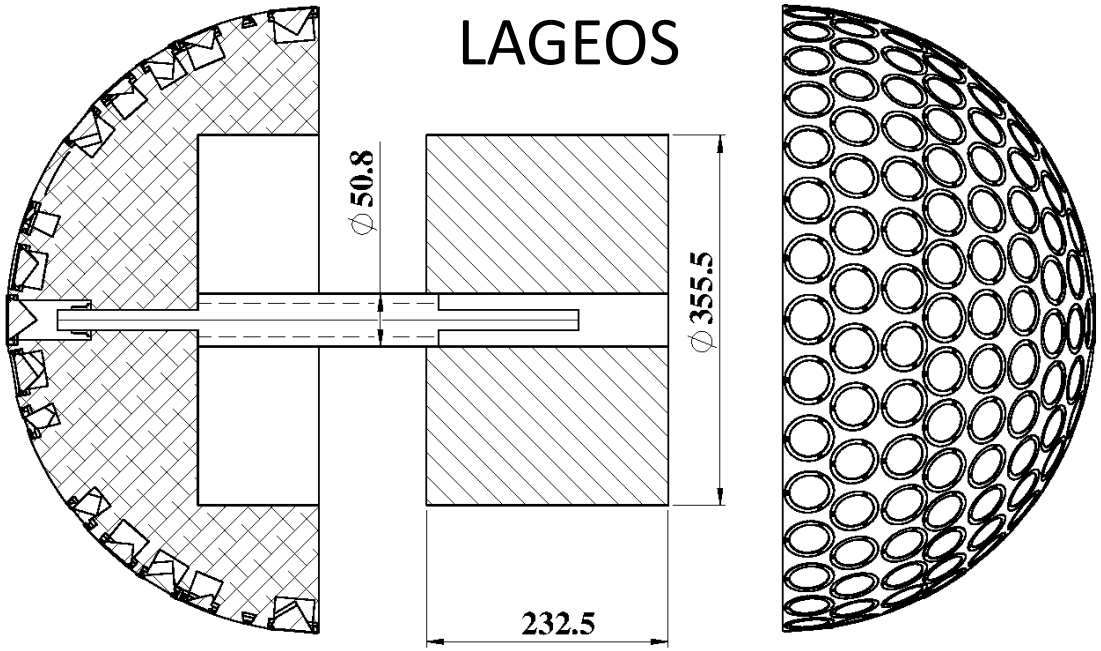

Table 1. Principal moments of inertia of LAGEOS, LAGEOS II and LARES in their flight arrangement.

Satellite	Moments of Inertia (kg m^2)		
	I_{zz}	I_{xx}	I_{yy}
LAGEOS	11.42 ± 0.03	10.96 ± 0.03	10.96 ± 0.03
LAGEOS II	11.45 ± 0.03	11.00 ± 0.03	11.00 ± 0.03
LARES	4.77 ± 0.03	4.77 ± 0.03	4.77 ± 0.03

- The two **LAGEOS** have almost the same oblateness of about 0.04
- **LARES** is practically spherical in shape, even if an oblateness as small as 0.002 is however possible

Dynamic Model: NGPs

M. Visco, D. Lucchesi, *Review and critical analysis of mass and moments of inertia of the LAGEOS and LAGEOS II satellites for the LARASE program*. Adv. in Space Res. 57, 044034 doi:10.1016/j.asr.2016.02.006, 2016

Documents on LAGEOS

- NASA, 1975. LAGEOS Phase B Technical Report, NASA Technical Memorandum X-64915. Technical Report TMX-64915. Marshall Space Flight Center. Marshall Space Flight Center, Alabama 35812. February 1975
- Siry, J.W., 1975. The LAGEOS system. Technical Report TM-X-73072. NASA
- LAGEOS Press Kit, 1976. NASA (1976) Project LAGEOS Press Kit release 76/67. Technical Report 76/67. NASA. National Aeronautics and Space Administration, Washington, DC
- Fitzmaurice, M.W., Minott, P.O., Abshire, J.B., Rowe, H.E., 1977. Prelaunch Testing of the Laser Geodynamic Satellite. Technical Report TP-1062. NASA
- Wong, C., 1978. Watching the Earth move from space. Sky Telesc., 198–202

Documents on LAGEOS II

- Cogo, F., 1988. Weight discrepancy analysis between LAGEOS 1 and LAGEOS 2 satellites. Technical Report LG-TN-AI-035. Aeritalia
- Fontana, F., 1989. Physical properties of LAGEOS II satellite. Technical Report LG-TN-AI-037. Aeritalia
- Fontana, F., 1990. Physical properties of LAGEOS II satellite. Technical Report LG-TN-AI-037. Aeritalia
- Minott, P.O., Zagwodzki, T.W., Varghese, T., Seldon, M., 1993. Prelaunch Optical Characterization of the Laser Geodynamic Satellite (LAGEOS 2). Technical Report 3400. NASA Technical Paper 3400. National Aeronautics and Space Administration, Washington, DC

Dynamic Model: NGPs

M. Visco, D. Lucchesi, *Comprehensive model for the spin evolution of the LAGEOS and LARES satellites*. Phys. Rev. D 98, 044034 doi:10.1103/PhysRevD.98.044034, 2018

LASSOS Spin Model: results for LAGEOS II

Blue = LASSOS model for the rapid-spin
Red = LASSOS general model

LArase **S**atellites **S**pin m**O**del **S**olutions (**LASSOS**)

Andrés de la Fuente, J.I., 2007. *Enhanced Modelling of LAGEOS Non-Gravitational Perturbations* (Ph.D. thesis). Delft University Press. Sieca Repro, Turbineweg 20, 2627 BP Delft, The Netherlands.
Kucharski, D., **Lim**, H.C., **Kirchner**, G., **Hwang**, J.Y., 2013. *Spin parameters of LAGEOS-1 and LAGEOS-2 spectrally determined from Satellite Laser Ranging data*. Adv. Space Res. 52, 1332–1338.

Spin Orientation: α, δ

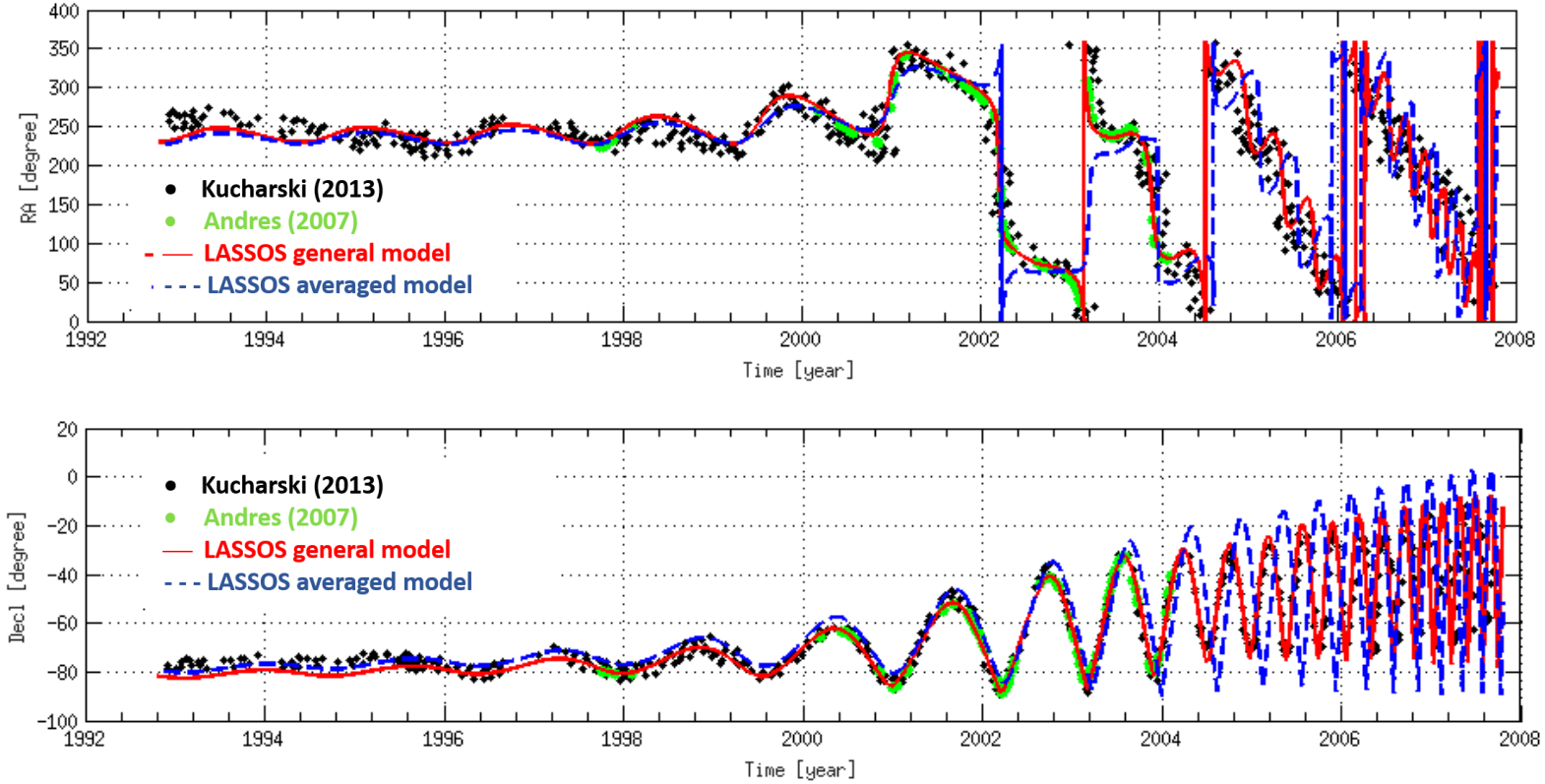

Dynamic Model: NGPs

M. Visco, D. Lucchesi, *Comprehensive model for the spin evolution of the LAGEOS and LARES satellites*. Phys. Rev. D 98, 044034 doi:10.1103/PhysRevD.98.044034, 2018

LASSOS Spin Model: results for LAGEOS II

Blue = LASSOS model for the rapid-spin
Red = LASSOS general model

LArase **S**atellites **S**pin m**O**del **S**olutions (**LASSOS**)

Andrés de la Fuente, J.I., 2007. *Enhanced Modelling of LAGEOS Non-Gravitational Perturbations* (Ph.D. thesis). Delft University Press. Sieca Repro, Turbineweg 20, 2627 BP Delft, The Netherlands.
Kucharski, D., **Lim**, H.C., **Kirchner**, G., **Hwang**, J.Y., 2013. *Spin parameters of LAGEOS-1 and LAGEOS-2 spectrally determined from Satellite Laser Ranging data*. Adv. Space Res. 52, 1332–1338.

Rotational Period: P

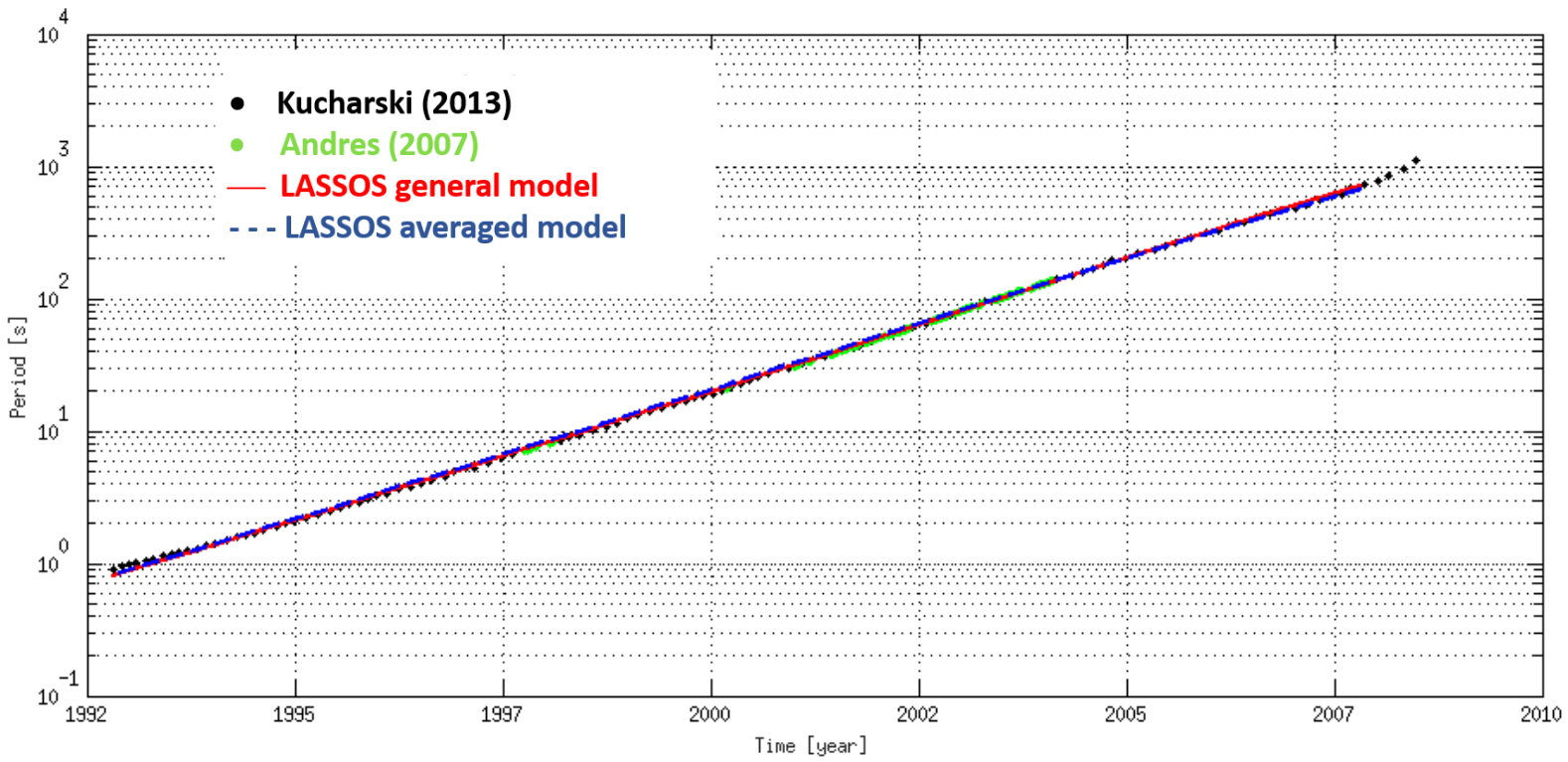

Dynamic Model: NGPs

Thermal thrust perturbations

We have tackled the problem following the two approaches considered in the past in the literature (but with some differences):

- We developed a simplified thermal model of the satellite based on
  - the energy balance equation on its surface
  - a linear approach for the distribution of the temperature with respect to its equilibrium (mean) temperature

- A general thermal model based on
  - a satellite (metallic structure) in thermal equilibrium
  - the CCRs rings are at the same temperature of the satellite
  - for each CCR the thermal exchange with the satellite is computed

$$\mathbf{dF_T} = -\frac{2}{3}\frac{\epsilon\sigma T^4 dA}{c}\mathbf{n}$$

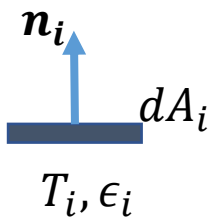

$$\frac{dQ_i}{dt} \cong \sum_j \left(P_j - \varepsilon_j \sigma A_{ext,j} T_i^4\right) + \sum_k R_{i,k}\left(T_k^4 - T_i^4\right) + \sum_k C_{i,k}(T_k - T_i) + \cdots = \mathcal{H}_i \frac{\partial T_i}{\partial t}$$

Absorbed power | Emitted power | Power exchanged by radiation | Power exchanged by conduction

Dynamic Model: NGPs

LArase Thermal mOdel Solutions (LATOS)

Simplified (average) thermal model

Farinella P, Vokrouhlicky D., Thermal force effects on slowly rotating, spherical artificial satellites - I. Solar heating, Plan. Space Sci. 44, 12 (1996)

Characteristic amplitude:

$$A_{YS} \cong \frac{16}{9}\frac{A}{m}\frac{\varepsilon\sigma}{c}T_0^3\Delta T$$

<u>Accelerations in body:</u>

With no eclipses

$$a_X = A_{YS}\frac{sinz_\odot}{1+\left(\omega_{spin}\tau\right)^2}$$

$$a_Y = A_{YS}\frac{sinz_\odot}{1+\left(\omega_{spin}\tau\right)^2}\omega_{spin}\tau$$

$$a_Z = A_{YS}cosz_\odot$$

With eclipses

$$a_X = A_{YS}\frac{sinz_\odot}{1+\left(\omega_{spin}\tau\right)^2}\Gamma_X$$

$$a_Y = A_{YS}\frac{sinz_\odot}{1+\left(\omega_{spin}\tau\right)^2}\Gamma_Y$$

$$a_Z = A_{YS}cosz_\odot\Gamma_Z$$

- We used:
  - $A_{YS} \cong -1.035\times10^{-10}$ m/s^2
  - $\tau \cong 2113$ s

Lucchesi D.M., Reassessment of the error modelling of the non-gravitational perturbations on LAGEOS II and their impact in the Lense-Thirring derivation - Part II, Plan. Space Sci. 50 (2002)

Dynamic Model: NGPs

LArase Thermal mOdel Solutions (LATOS)

Thermal thrust: results for LAGEOS II

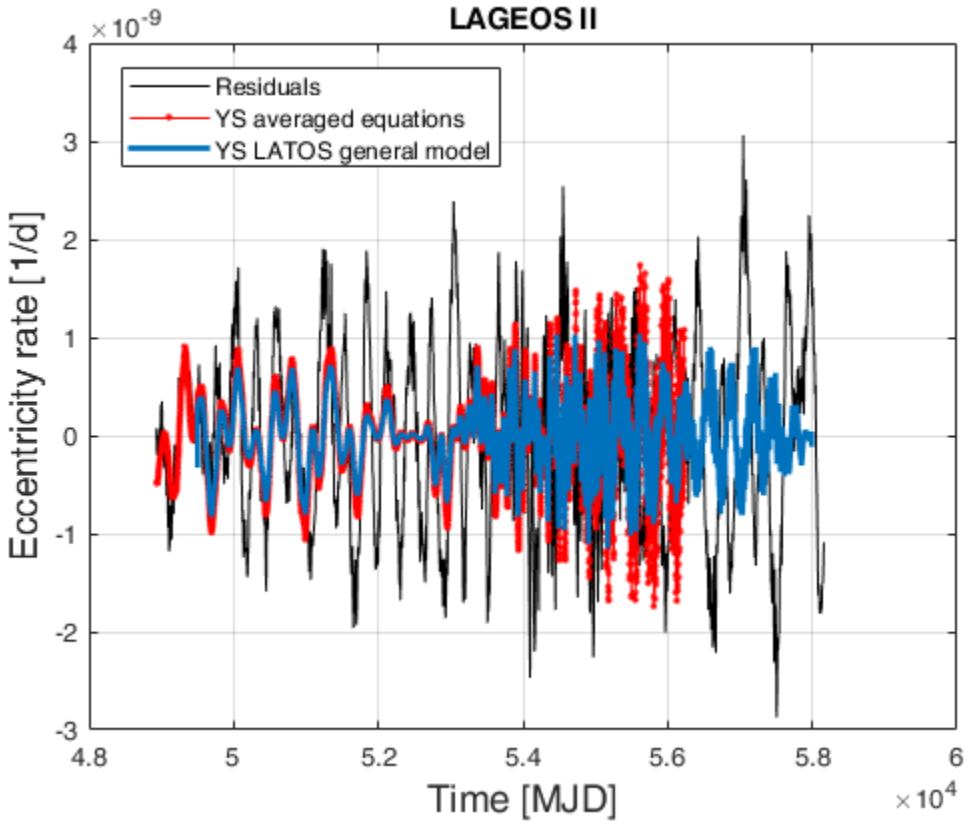

$$\frac{de}{dt} = \frac{\sqrt{1-e^2}}{na}\left[R\sin f + T(\cos f + \cos u)\right]$$

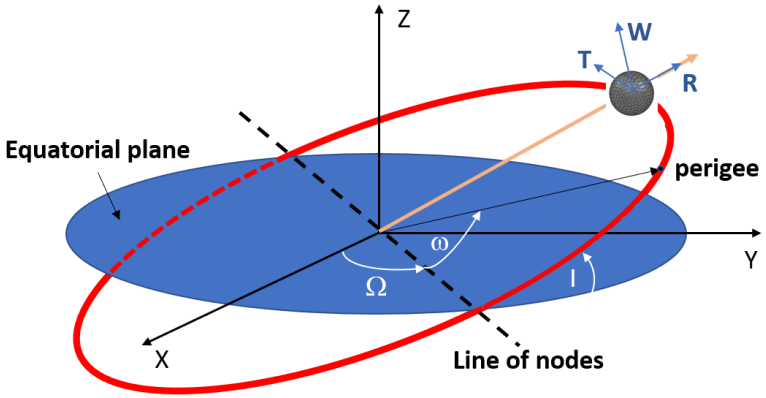

About 27 years POD of LAGEOS II with GEODYN II

Dynamic Model: NGPs

LArase Thermal mOdel Solutions (LATOS)

Thermal thrust: results for LAGEOS II

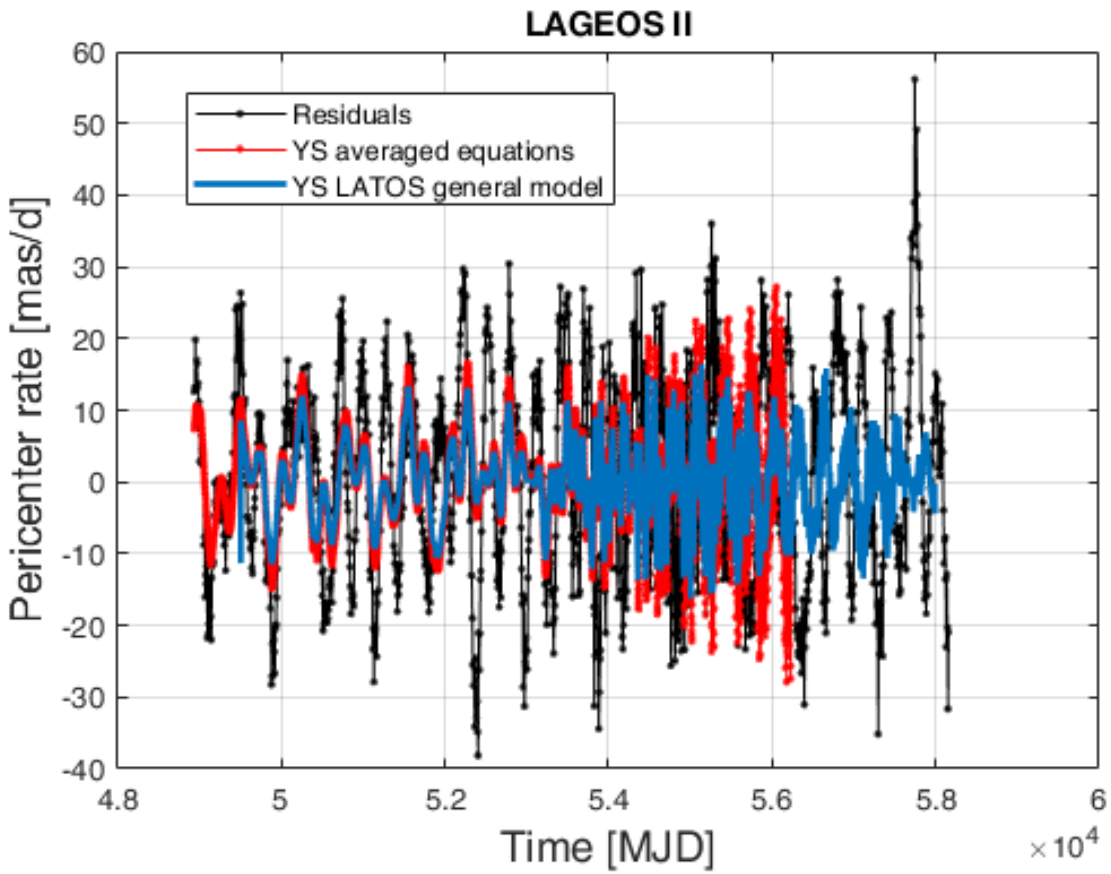

About 27 years POD of LAGEOS II with GEODYN II

$$\frac{d\omega}{dt} = \frac{\sqrt{1-e^2}}{nae}\left[-R\cos f + T\left(\sin f + \frac{\sin u}{\sqrt{1-e^2}}\right)\right] - \frac{W}{H\sin i} r \sin(\omega + f)\cos i$$

Being able to clean up this parameter has a particular importance for us: it contains a secular effect from **General Relativity**, due to the **Gravitoelectric** field (M) and to the **Gravitomagnetic** field (J)

Dynamic Model: NGPs

It is as if a certain mechanism is pumping energy to the satellite !

Residuals in the semi-major axis (m/7d)

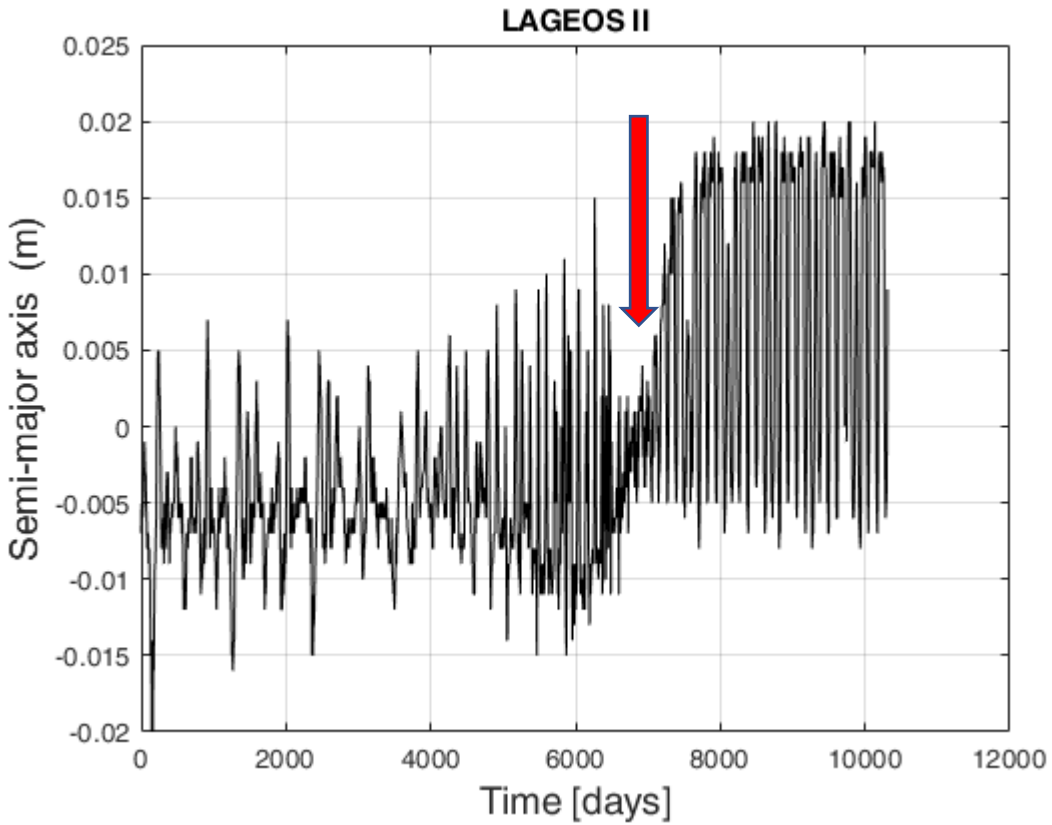

Integrated residuals in the semi-major axis (m)

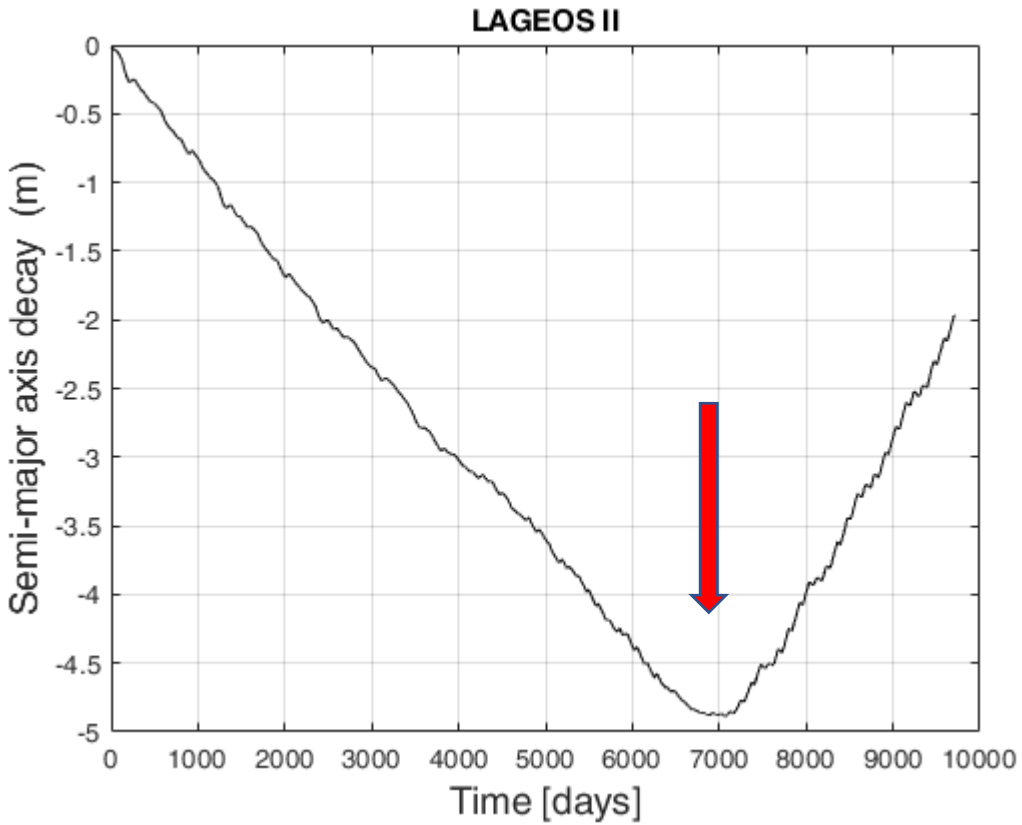

March 14, 2012

Dynamic Model: NGPs

The former (old) explanation:

In the late 1980s and early 1990s, the observed decay for the semi-major axis of the two **LAGEOS** satellites was explained in terms of:

- **Earth-Yarkovsky thermal drag ≈ 70%**
- **Charged particles drag ≈ 20%**
- **Neutral particles drag ≈ 10 %.**

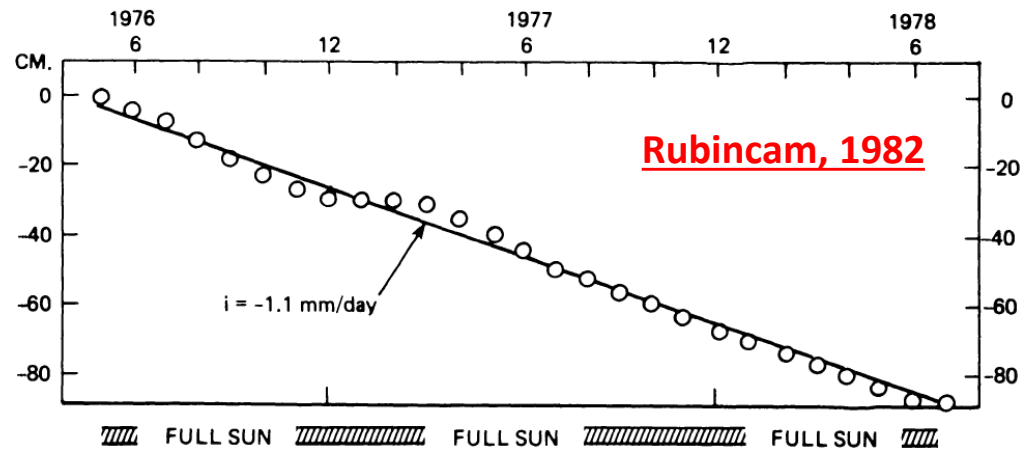

Fig. 1. The secular decrease in the semimajor axis of Lageos's orbit. The straight line fitted through the data points has a slope of -1.1 mm day^{-1}. When the orbit is in full sunlight and shadow is shown along the horizontal axis.

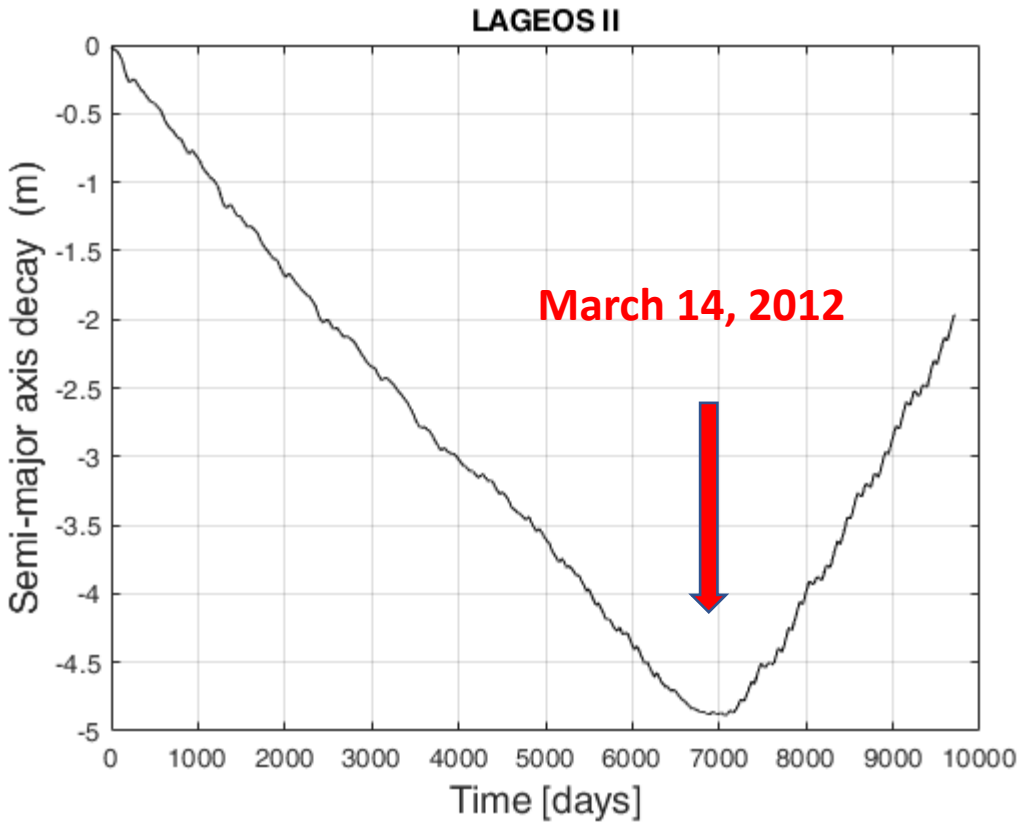

Dynamic Model: NGPs

The former (old) explanation:

In the late 1980s and early 1990s, the observed decay for the semi-major axis of the two **LAGEOS** satellites was explained in terms of:

- **Earth-Yarkovsky thermal drag ≈ 70%**
- **Charged particles drag ≈ 20%**
- **Neutral particles drag ≈ 10 %.**

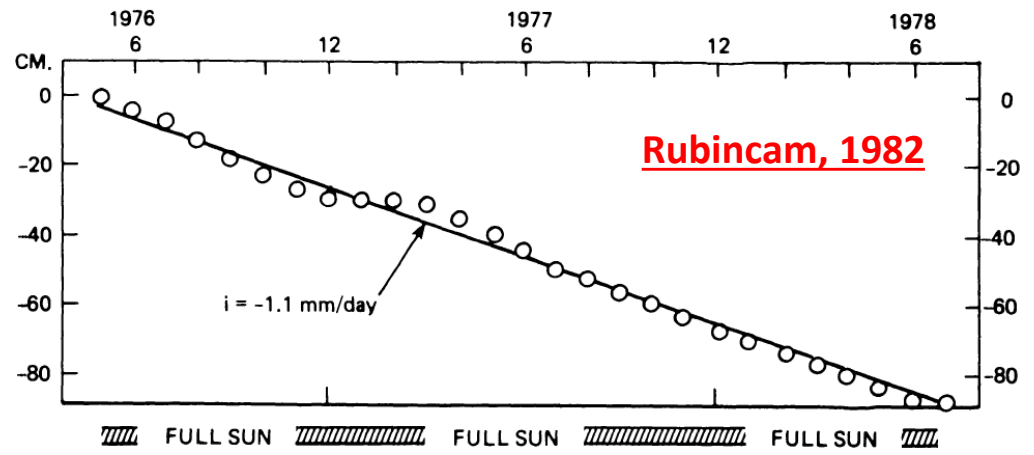

Fig. 1. The secular decrease in the semimajor axis of Lageos's orbit. The straight line fitted through the data points has a slope of -1.1 mm day^{-1}. When the orbit is in full sunlight and shadow is shown along the horizontal axis.

Based on the results of our analyzes and the models we have developed for **NGPs**, we believe that the possible explanation for the observed phenomenon lies in the evolution of the **Spin** of **LAGEOS II** and its consequent impact on the **solar Yarkovsky** effect.

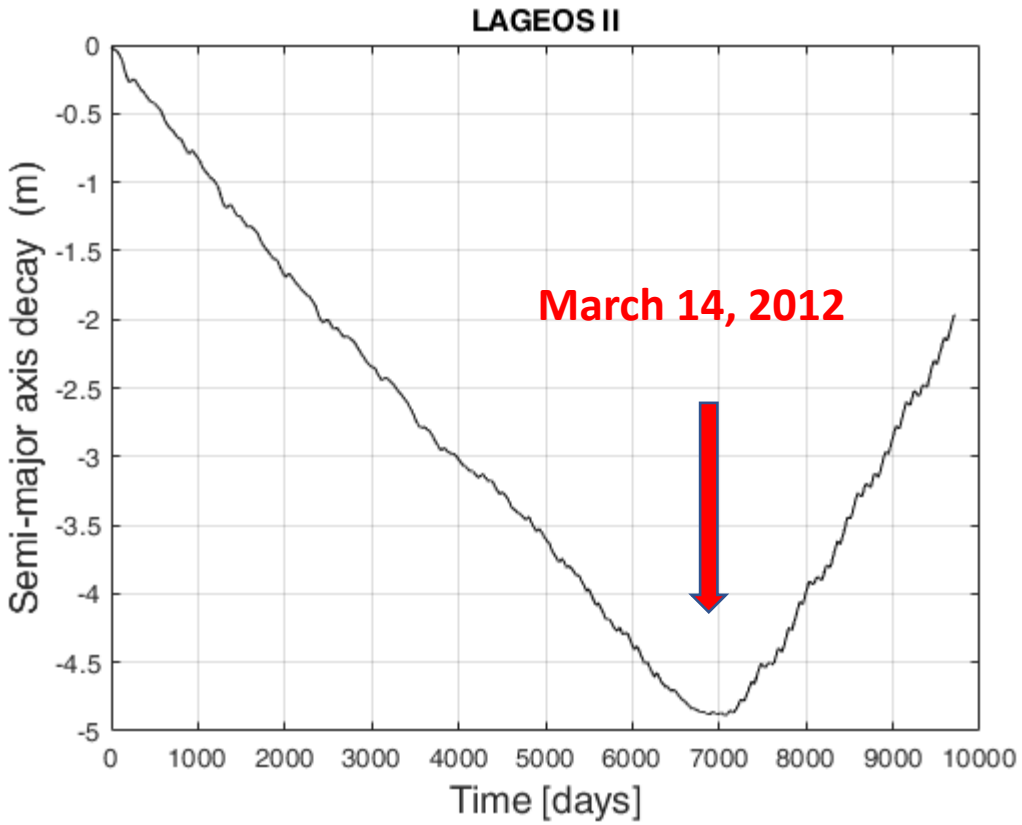

Dynamic Model: NGPs

Residuals in the semi-major axis and their comparison with the solar Yarkovsky-Schach effect

Earth-Yarkovsky deceleration vs. solar Yarkovsky-Schach acceleration

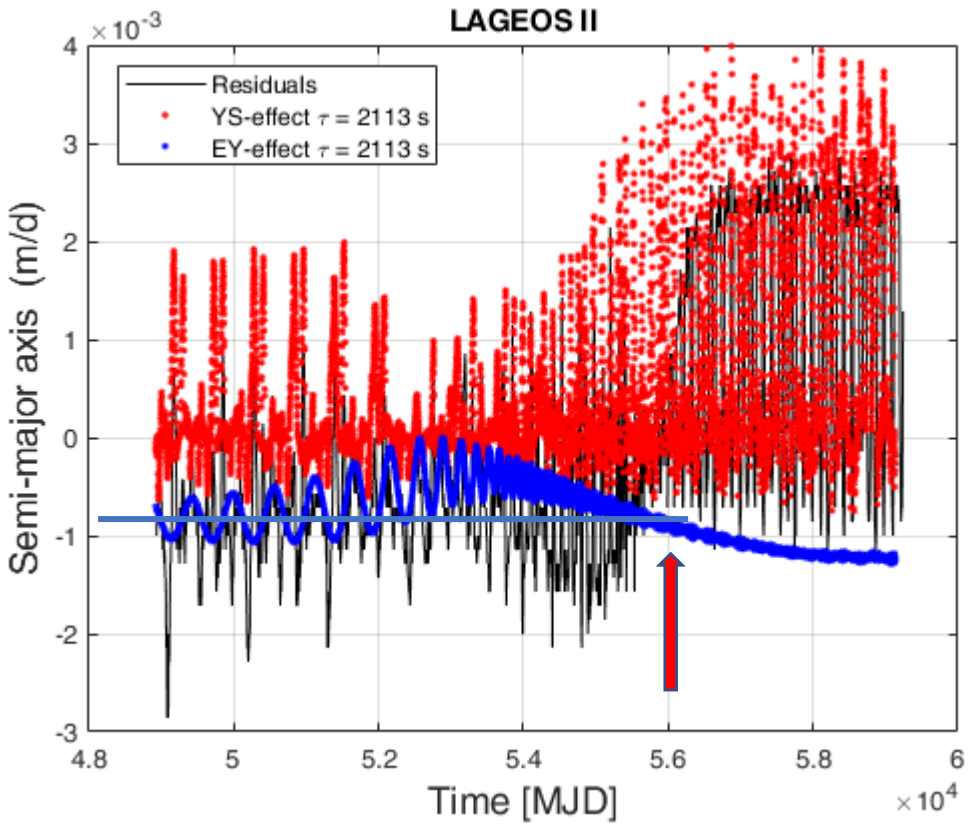

$$\dot{a} \cong \frac{2}{n} T$$

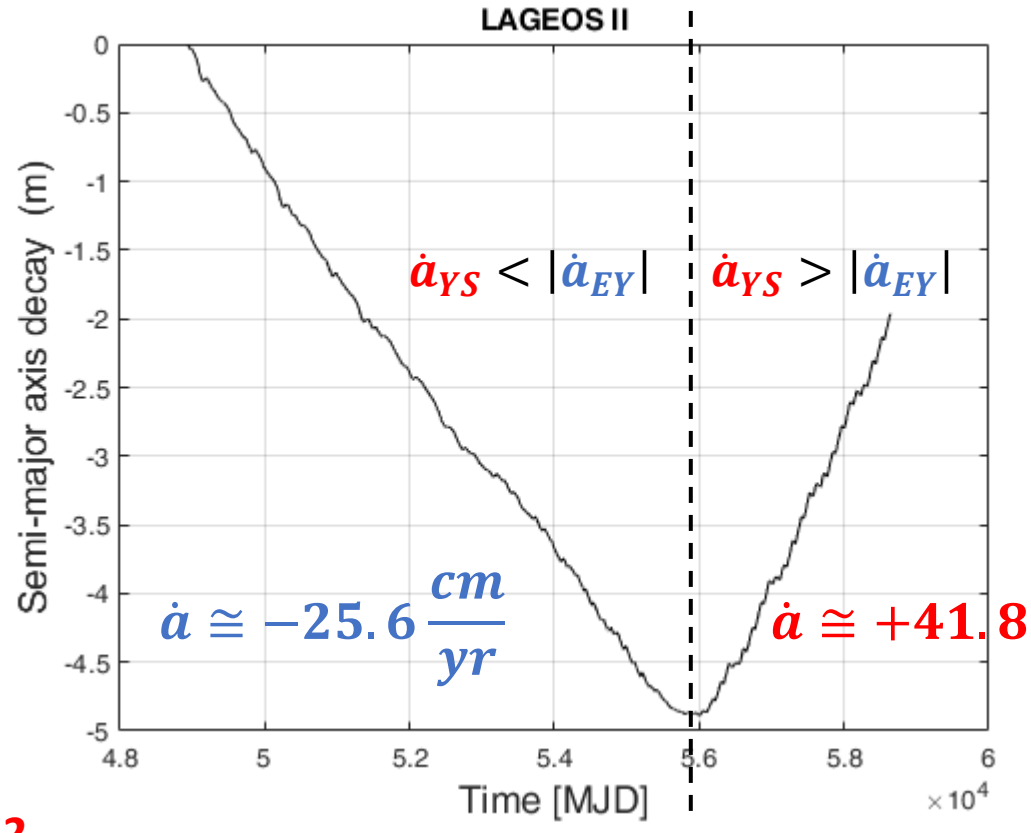

March 14, 2012

Dynamic Model: NGPs

Residuals in the semi-major axis and their comparison with the solar **Yarkovsky-Schach** and **Earth-Yarkovsky** effects

CCRs Thermal inertia:

- τ = 2113 s
- τ = 3000 s
- τ = 300 s

The role of the Thermal Inertia

$$\frac{da}{dt} = \frac{2}{n\sqrt{1-e^2}}[T + e(T\cos f + R\sin f)]$$

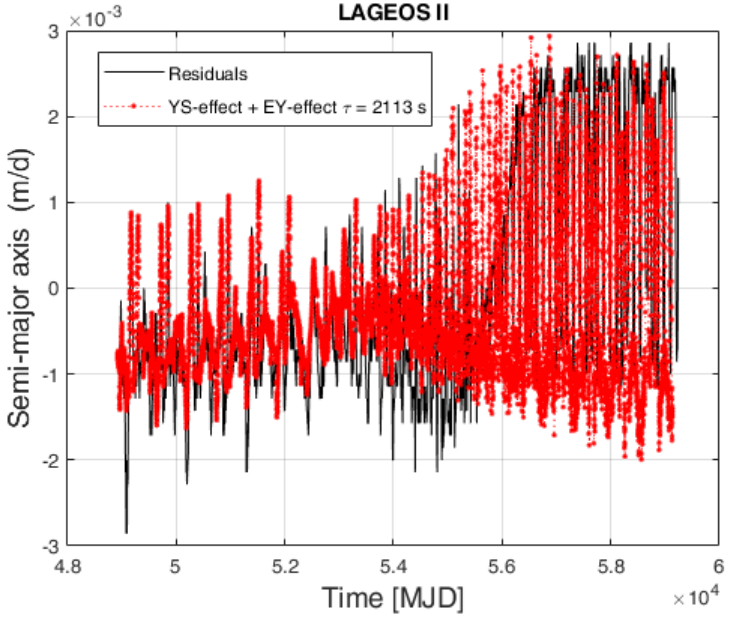

$\tau = 2113\ s$

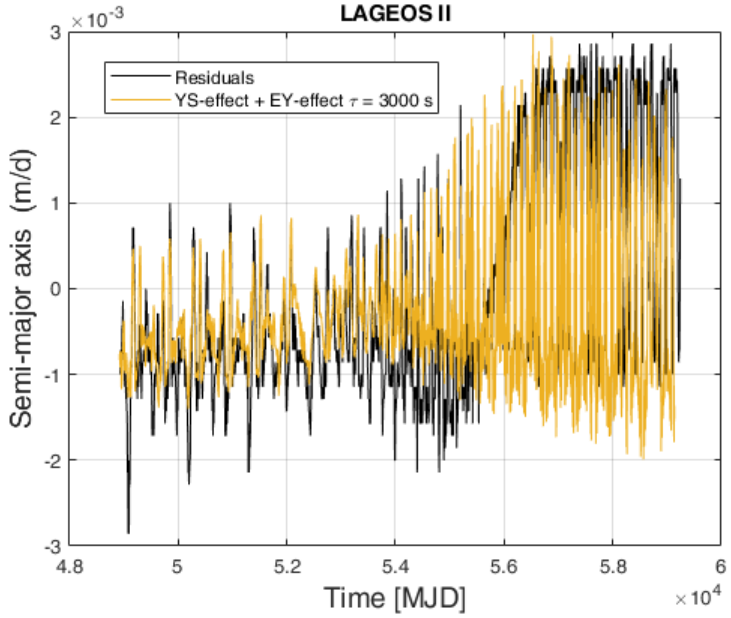

$\tau = 3000\ s$

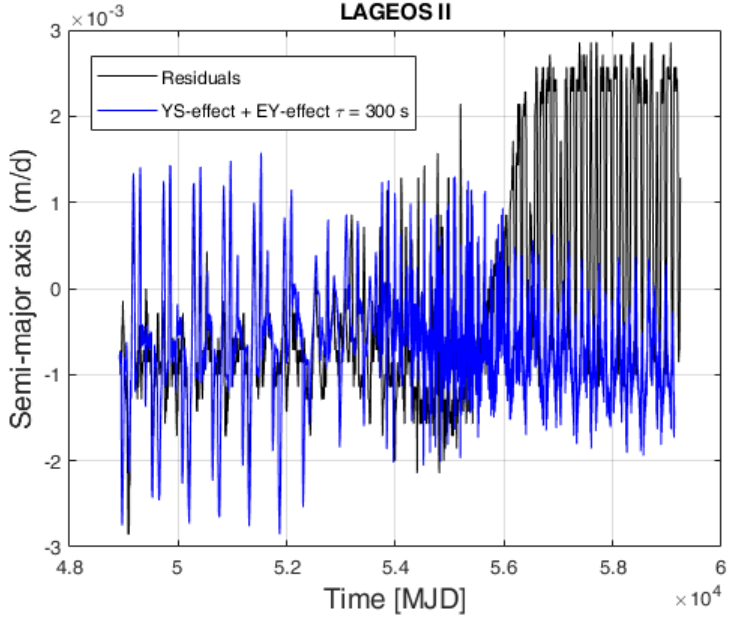

$\tau = 300\ s$

Dynamic Model: NGPs

Neutral Drag: results for LARES

A modified version of the **SATRAP** (**SAT**ellite **R**entry **A**nalysis **P**rogram) tool, developed at **ISTI/CNR** in Pisa, was used to compute the **neutral drag acceleration** acting on **LARES**, as a function of time, taking into account the real evolution of **solar** and **geomagnetic activities** and the observed secular semi-major axis decay

Several **thermospheric** density models were used in **SATRAP** to compute the components of the **neutral drag acceleration** in the **Gauss** reference system **R** (Radial), **T** (Transverse) and **W** (Out-of-Plane): **JR-71**, **MSIS-86**, **MSISE-90**, **NRLMSISE-00**, **GOST-2004** and **JB2008**

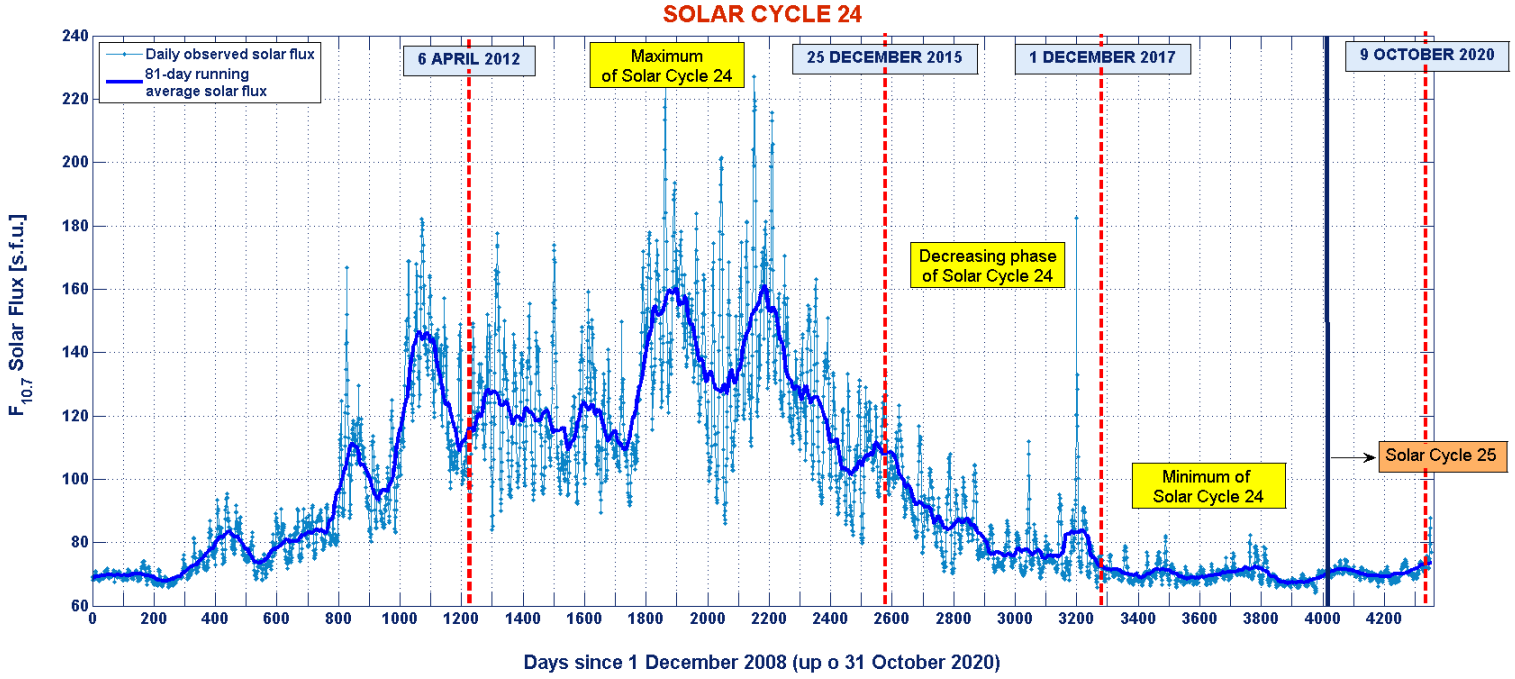

Pardini, C.; Anselmo, L.; Lucchesi, D.M.; Peron, R., *On the secular decay of the LARES semi-major axis*. Acta Astronautica **2017**, 140, 469–477. doi:10.1016/j.actaastro.2017.09.012

Dynamic Model: NGPs

Neutral Drag: results for LARES

$$\vec{\mathcal{A}}_{drag} = -\frac{1}{2}\frac{A}{M}\rho C_D V_r^2 \hat{V}_r$$

In an analysis of about 6.5 years (April 6, 2012 → October 26, 2018) we investigated the effects of the neutral drag on all the orbital elements of **LARES**. In particular:

- from the perturbing accelerations obtained from **SATRAP** we computed the effects on the orbit via Gauss equations
- we compared these orbital effects with the orbit residuals obtained from **GEODYN**

Accelerations (in Gauss co-moving frame) due to neutral drag obtained with SATRAP (MSIS-86): $\langle C_D \rangle \cong 4.07$

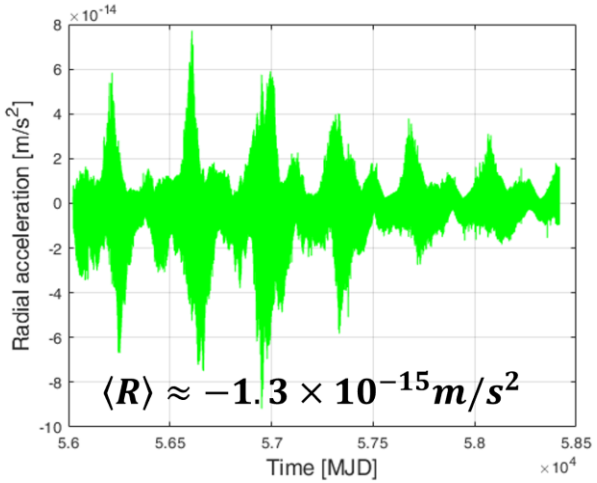

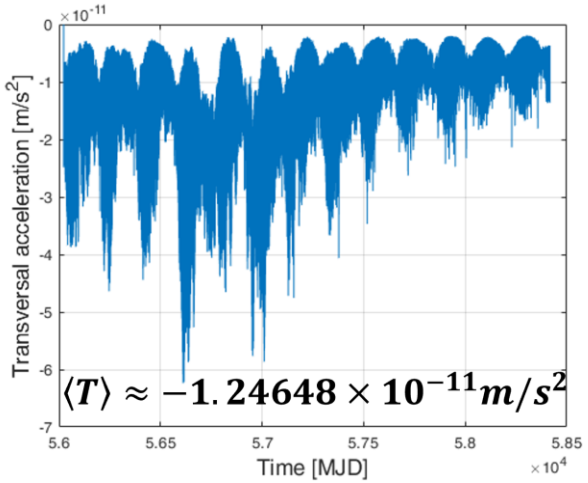

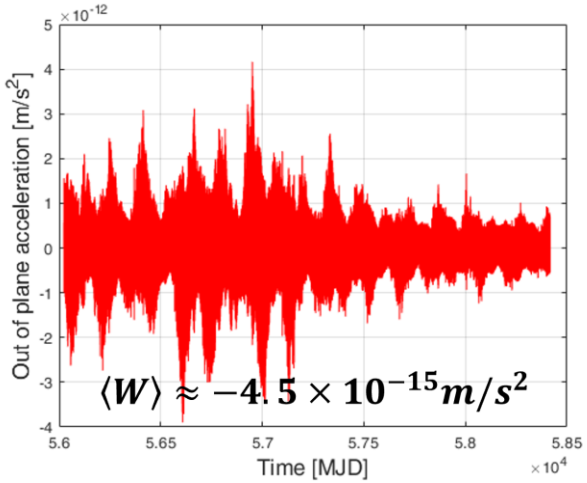

Dynamic Model: NGPs

Neutral Drag: results for LARES

$$\frac{da}{dt} = \frac{2}{n\sqrt{1-e^2}}[T + e(T\cos f + R\sin f)]$$

Model from SATRAP

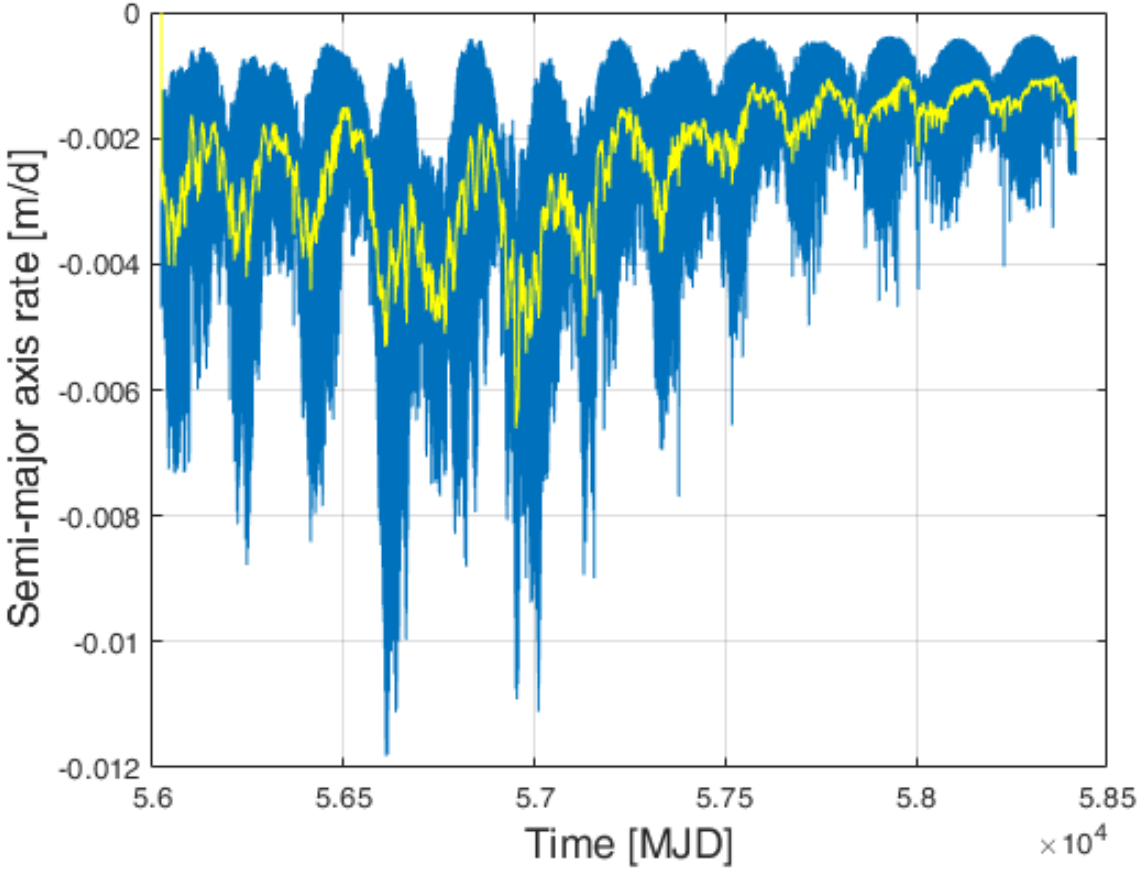

Model vs. GEODYN Residuals

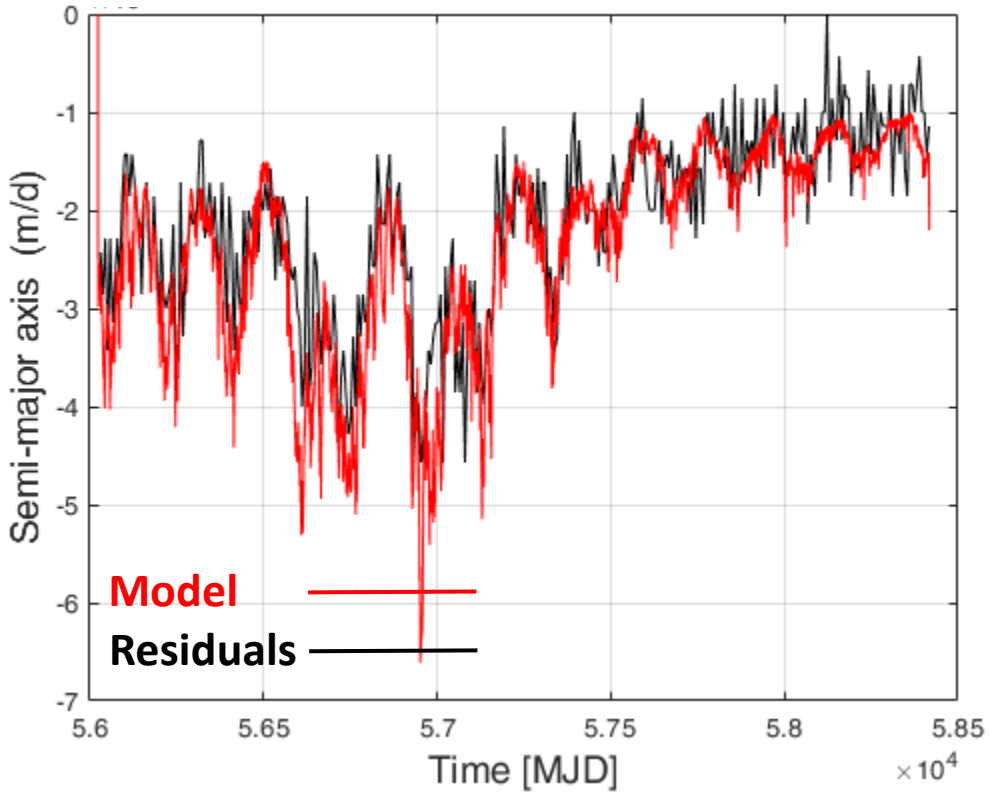

Measurements and constraints from pericenter and mean anomaly

We have at our disposal **three main observables** to investigate the effects produced by the different theories of **gravitation**, starting with those of **GR**, on the orbits of artificial satellites:

- **The argument of pericenter: ω**
- **The mean anomaly: M**
- **The right ascension of the ascending node: Ω**

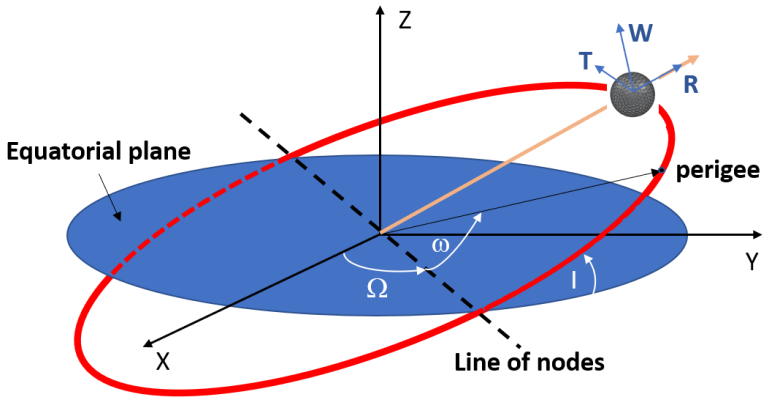

Therefore, the main targets of our analyses have been the measurement of:

- **Schwarzschild precession**
- **Lense-Thirring precession**

Measurements and constraints from pericenter and mean anomaly

We have at our disposal **three main observables** to investigate the effects produced by the different theories of **gravitation**, starting with those of **GR**, on the orbits of artificial satellites:

- **The argument of pericenter: ω**
- **The mean anomaly: M**
- **The right ascension of the ascending node: Ω**

Rate (mas/yr)	LAGEOS	LAGEOS II	LARES
$\dot{\omega}_{Schw}$	+ 3270.78	+ 3352.58	+ 10,110.15
$\dot{\omega}_{LT}$	+ 31.23	– 57.33	– 124.53
$\dot{\omega}_{J2}^{dir}$	– 3.26	+ 2.85	– 23.38
$\dot{\omega}_{J2}^{indir}$	– 0.36	+ 0.16	– 2.65
Total	+ 3306.38	+ 3298.26	+ 9959.59
$\dot{M}_{Schw}$	– 3278.75	– 3352.26	– 10,110.14
$\dot{M}_{J_2rel}$	– 0.92	+ 0.15	– 6.71
Total	– 3278.75	– 3352.11	– 10,116.85
$\dot{\Omega}_{LT}$	+ 30.67	+ 31.51	+ 118.47
$\dot{\Omega}_{dS}$	+ 17.64	+ 17.64	+ 17.64
$\dot{\Omega}_{J2}^{dir}$	+ 1.95	– 3.63	– 15.31
$\dot{\Omega}_{J2}^{indir}$	+ 0.08	– 0.15	– 0.64
Total	+ 50.34	+ 45.37	+ 120.16

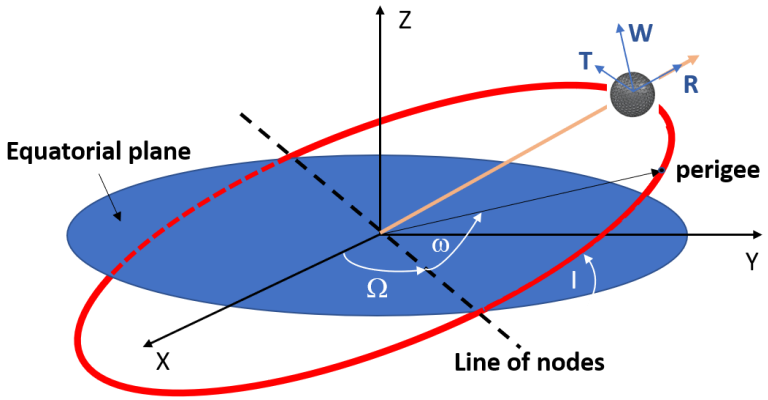

$$\dot{\omega}_{Schw} = \frac{3\,(GM_{\oplus})^{3/2}}{c^2\,a^{5/2}(1-e^2)}$$

$$\dot{M}_{Schw} = -\sqrt{1-e^2}\,\frac{3\,(GM_{\oplus})^{3/2}}{c^2\,a^{5/2}(1-e^2)}$$

$$\dot{\Omega}_{LT} = \frac{2G}{c^2 a^3}\,\frac{J_{\oplus}}{(1-e^2)^{3/2}}$$

Measurements and constraints from pericenter and mean anomaly

Observables such as the **argument of pericenter** and the **mean anomaly**, are interesting to be analyzed in the context of a possible violation of the $1/r^2$ law for gravity parametrized by a **Yukawa-like long-range interaction**:

$$V(r) = -G_\infty \frac{M_1 M_2}{r}\left(1 + \alpha e^{-r/\lambda}\right)$$

$$\vec{F}(r) = -\vec{\nabla} V(r) = -G_\infty \left[1 + \alpha\left(1 + \frac{r}{\lambda}\right) e^{-r/\lambda}\right] \frac{M_1 M_2}{r^2}\hat{r}$$

A **Yukawa-like** parameterization seems general at the lowest order interaction and in the non-relativistic limit, independently of a:

- **Scalar** field with the exchange of a spin-0 light boson
- **Vector** field with the exchange of a spin-1 light boson
- **Tensor** field with the exchange of a spin-2 light boson

$$V_{yuk} = -\alpha \frac{G_\infty M_1}{r} e^{-r/\lambda}$$

$$\alpha = \frac{1}{G_\infty}\left(\frac{K_1}{M_1} \cdot \frac{K_2}{M_2}\right)$$

$$\lambda = \frac{h}{\mu c}$$

M_1 = Mass of the primary source;

M_2 = Mass of the secondary source;

G_∞ = Newtonian gravitational constant;

r = Distance;

α = Strength of the interaction; K_1, K_2 = Coupling strengths;

λ = Range of the interaction; μ = Mass of the light-boson;

h = Planck constant; c = Speed of light

Measurements and constraints from pericenter and mean anomaly

Consequences:

1. the **deviations** from the usual 1/r law for the gravitational potential lead to **new weak interactions** **between macroscopic objects**
2. The interesting point is that these supplementary interactions may be either **consistent** with **Einstein Equivalence Principle** or **not**
3. In this second case, **non–metric** phenomena will be produced with **tiny**, but **significant**, **consequences** in the **gravitational experiments**
4. The characteristic of such very weak interactions, which are predicted by several theories, is to produce deviations for masses separations ranging through **several orders of magnitude**, starting from the **sub–millimeter** level up to the **astronomical scale**

Measurements and constraints from pericenter and mean anomaly

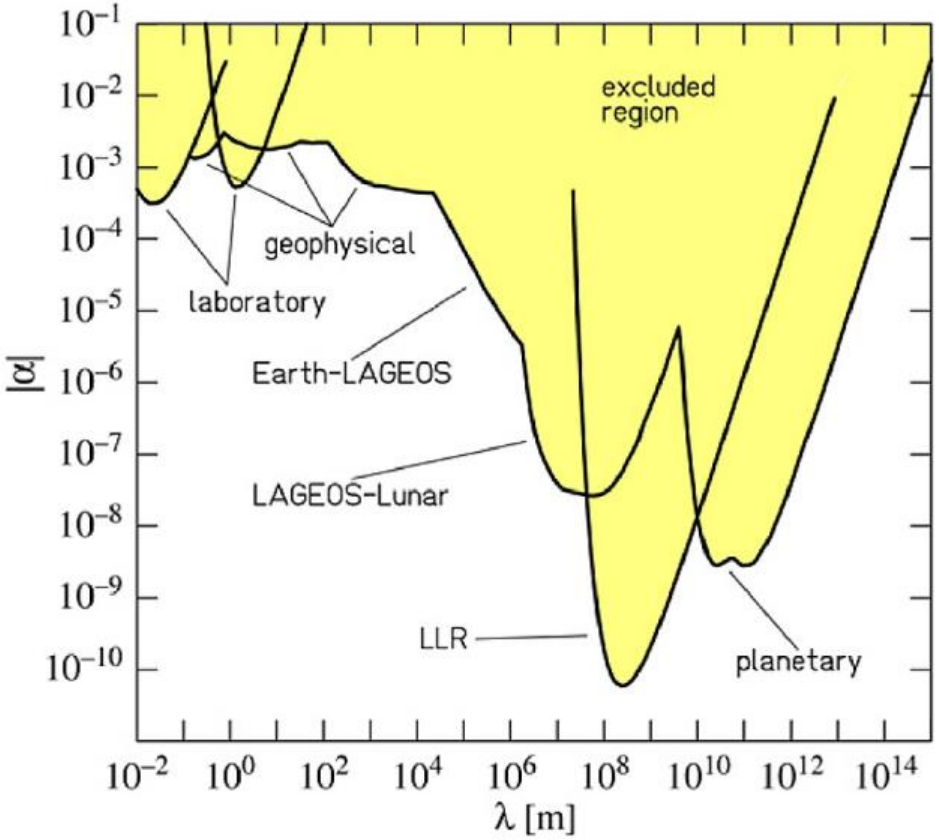

Fig. 11. Limits on the fifth force strength $|\alpha|$ for $\lambda \geq 1$ cm from laboratory, geo and astronomical measurements [Adelberger 2009].

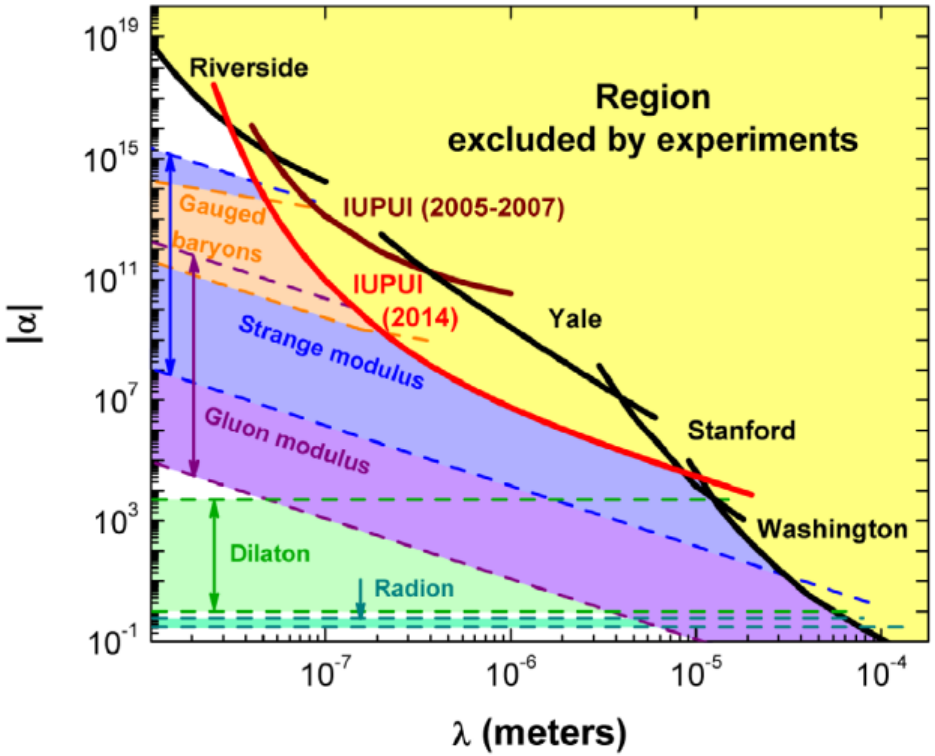

Fig. 12. Limits on the fifth force strength $|\alpha|$ for $\lambda \leq 0.1$ mm from short-distance force experiments along with predicted strengths from various theories [Chen 2014]. "IUPUI" labels constraints coming from experiments with Ricardo Decca and Daniel López utilizing "iso-electronic" effect experiments.

scale distances between 10^{-4} m — 10^{15} m have been tested during the last 35 years with null results for a possible violation of NISL and for the WEP

Measurements and constraints from pericenter and mean anomaly

We are therefore interested in new analyzes of the long-term and secular effects on the orbits of the two **LAGEOS** and (possibly) of **LARES** to further constrain a possible **long-range force** described by a **Yukawa-like** potential

The main objectives are:

- Perform the analysis over the entire life of **LAGEOS II**, about 32 years
- Consider as observables both the **argument of pericenter** and the **mean anomaly** of **LAGEOS II**
- Include in the analysis also the older **LAGEOS** satellite
- Improve the results of a previous measurement (**2010/2014**) obtained with **LAGEOS II** **argument of pericenter**
- Compare the results with the predictions of **GR** and of other **ATG**

D. Lucchesi, R. Peron, *Accurate Measurement in the Field of the Earth of the General-Relativistic Precession of the LAGEOS II Pericenter and New Constraints on Non-Newtonian Gravity*. Phys. Rev. Lett. 105, 231103, doi:10.1103/PhysRevLett.105.231103, 2010

D. Lucchesi, R. Peron, *LAGEOS II pericenter general relativistic precession (1993-2005): Error budget and constraints in gravitational physics*. Phys. Rev. D 89, 082002, doi:10.1103/PhysRevD.89.082002, 2014

Measurements and constraints from pericenter and mean anomaly

$$\dot{\omega}_{Schw} = \frac{3\,(GM_{\oplus})^{3/2}}{c^2\,a^{5/2}(1-e^2)} = 3352.58\ mas/yr$$

The total relativistic precession of the argument of pericenter: 28 years

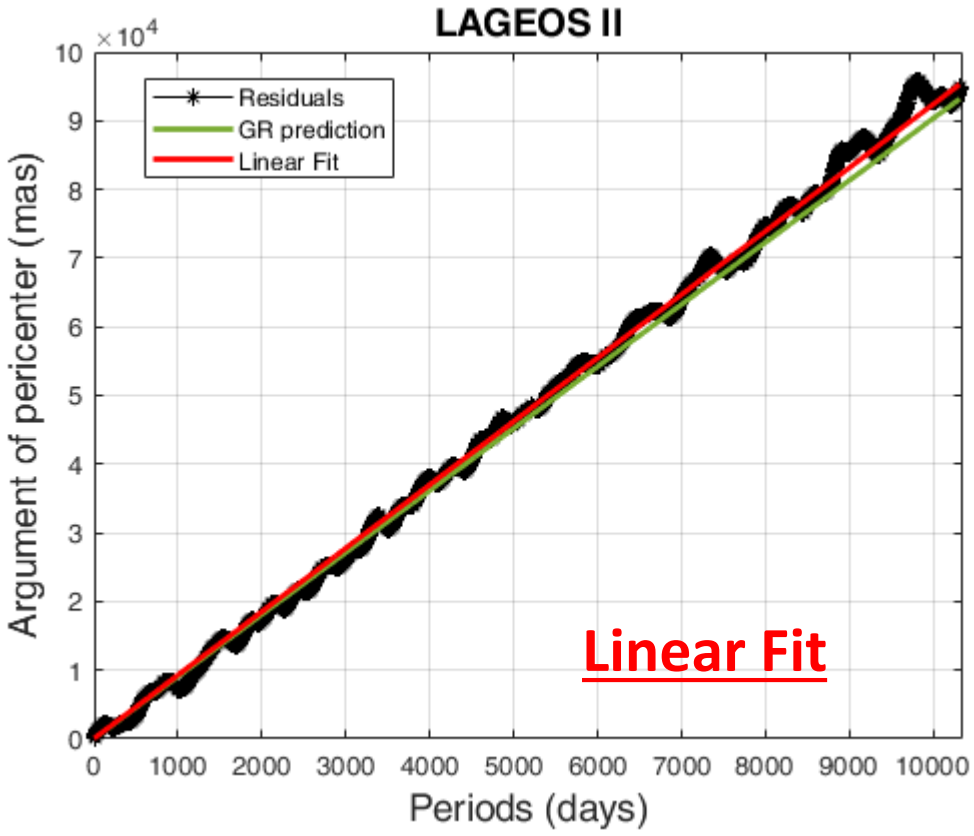

Although the **POD** performed on the **LAGEOS II** satellite is **not yet optimized**, the preliminary results are encouraging:

$$\dot{\omega}_{GR} = \dot{\omega}_{Schw} + \dot{\omega}_{LT} + \dot{\omega}_{J_2}^{dir} + \dot{\omega}_{J_2}^{indir} = 3298.26\ mas/yr$$

$$\dot{\omega}_{tot} = \dot{\omega}_{GP} + \dot{\omega}_{NGP} + \varepsilon\dot{\omega}_{GR} + \cdots$$

$$\boldsymbol{\varepsilon - 1 \cong 2.3 \times 10^{-2}}$$

One of the main point to face is that of a reliable model for the time behavior of the coefficients of the gravity field of the Earth on a so long timespan

Measurements and co y

To reduce the impact of the gravitational field mismodeling, the time interval in which the analysis is carried out can be reduced

The total relativistic precession of the argument of pericenter: 13.7 years (5000 days)

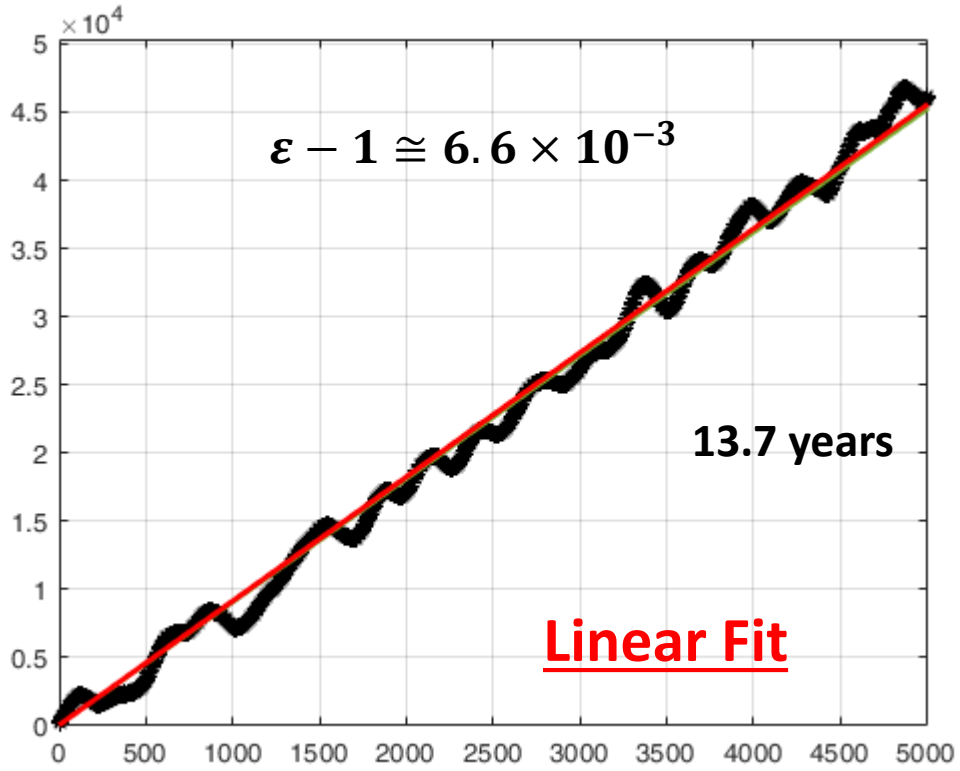

The previous measurement in 2014

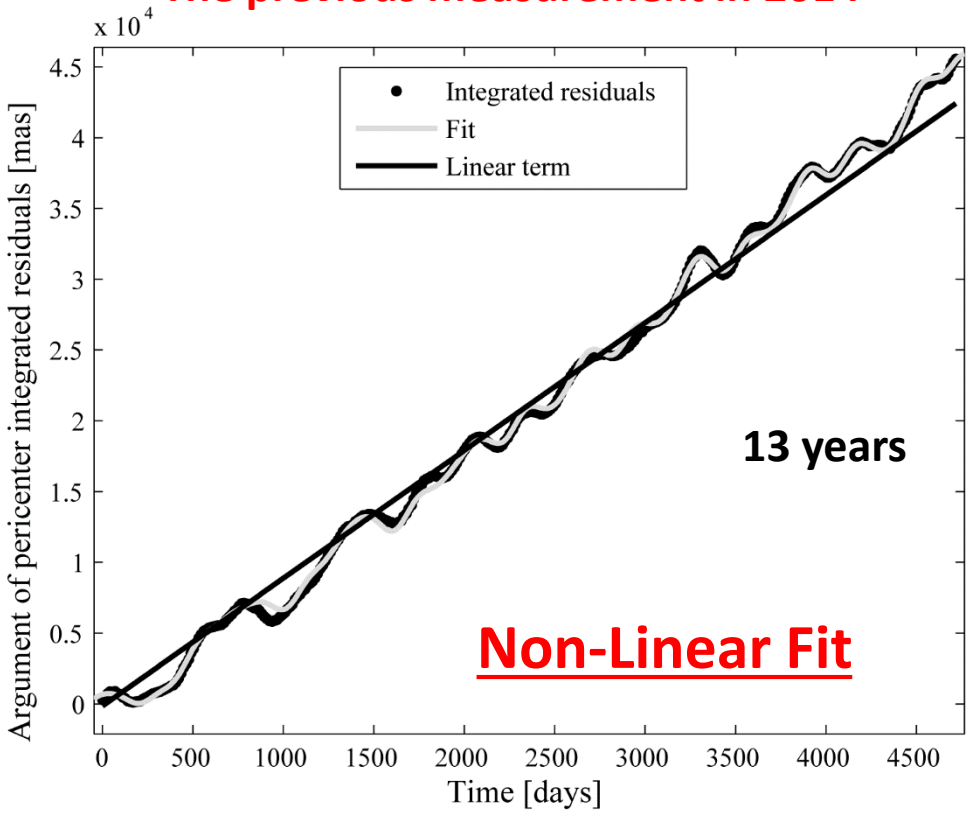

$$\varepsilon - 1 = (-0.12 \pm 2.10) \cdot 10^{-3} \pm 2.5 \cdot 10^{-2}$$

Measurements and constraints from pericenter and mean anomaly

Combination of the **argument of pericenter** and the **mean anomaly** of **LAGEOS II**: cancels the errors related to J_2

$$\dot{\omega}_{Schw} = \frac{3\,(GM_{\oplus})^{3/2}}{c^2\,a^{5/2}(1-e^2)} = 3352.58\ mas/yr$$

$$\dot{M}_{Schw} = -\sqrt{1-e^2}\,\frac{3\,(GM_{\oplus})^{3/2}}{c^2\,a^{5/2}(1-e^2)}$$

$$\dot{M}_{Schw} = -\sqrt{1-e^2}\,\dot{\omega}_{Schw} = -3352.26\ \ mas/yr$$

$$\langle\dot{\omega}_{class}\rangle_{sec} = -\frac{3}{4}n\left(\frac{R_{\oplus}}{a}\right)^2\frac{1-5cos^2 i}{(1-e^2)^2}\left\{-\sqrt{5}\bar{C}_{2,0}+\cdots\right.$$

$$\langle\dot{M}\rangle_{sec} = n_0 + \frac{3}{2}\left(\frac{R_{\oplus}}{a}\right)^2 n_0\frac{\left(1-\frac{3}{2}sin^2 i\right)}{(1-e^2)^{3/2}}\left\{-\sqrt{5}\bar{C}_{2,0}+\cdots\right.$$

$$\dot{M}^{L2}_{res} + k\dot{\omega}^{L2}_{res}$$

$$k \cong -0.123500$$

$$\varepsilon - 1 \cong (+0.35 \pm 2.42)\times 10^{-3} \pm \varepsilon_{sys}$$

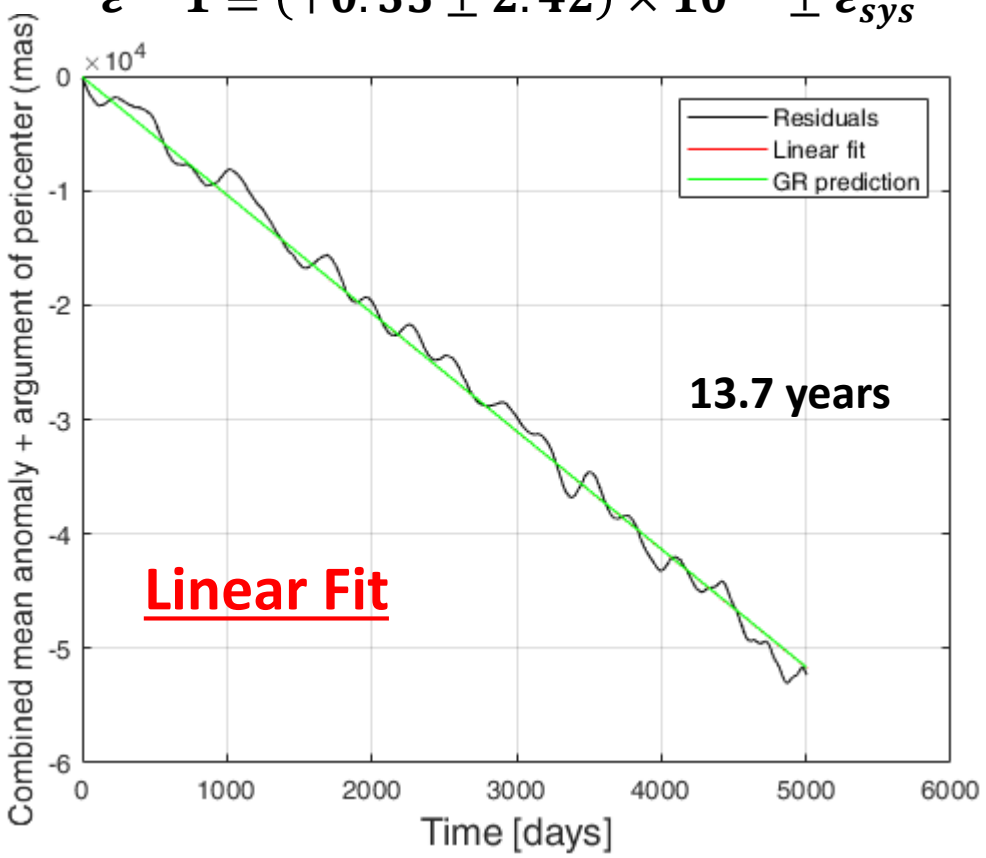

The previous measurement in 2014, on 13 years: $\varepsilon - 1 = (-0.12 \pm 2.10)\cdot 10^{-3} \pm 2.5\cdot 10^{-2}$

Measurements and constraints from pericenter and mean anomaly

The total relativistic precession of the argument of pericenter: **a previous result on 13 years**

D. Lucchesi, R. Peron, *LAGEOS II pericenter general relativistic precession (1993-2005): Error budget and constraints in gravitational physics*. Phys. Rev. D 89, 082002, doi:10.1103/PhysRevD.89.082002, 2014

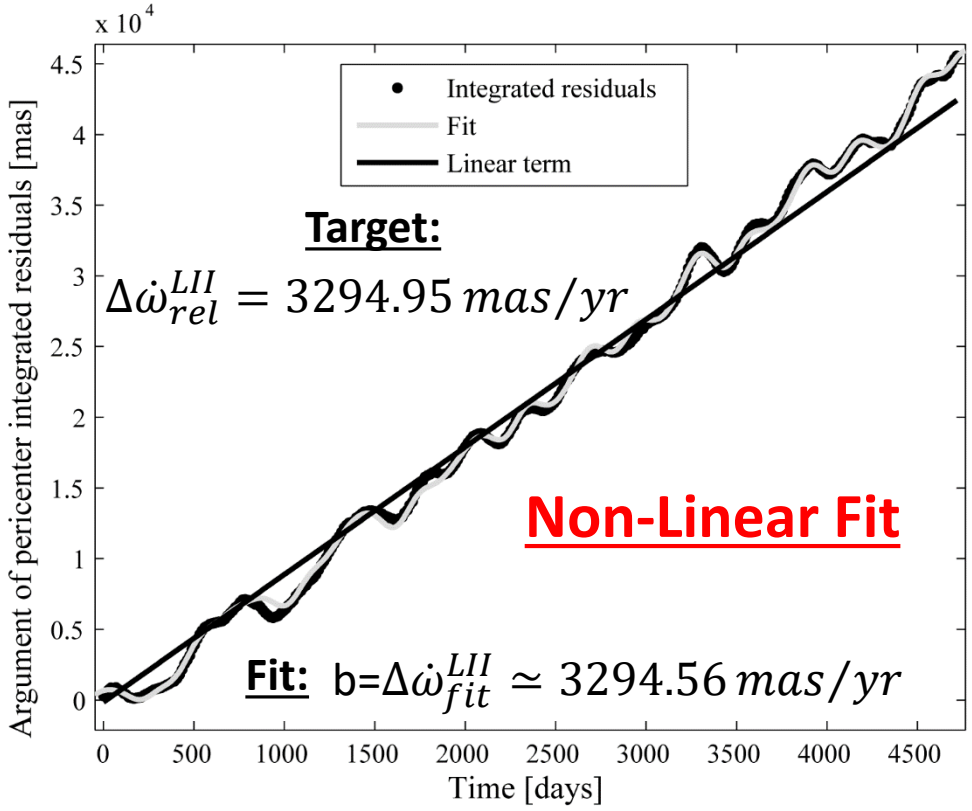

We obtained b ≅ 3294.6 mas/yr, very close to the prediction of **GR**

The discrepancy is just **0.01%**

From a sensitivity analysis, with constraints on some of the parameters that enter into the least squares fit, we obtained an upper bound of **0.2%**

$$\Delta\dot{\omega} = \Delta\dot{\omega}_{GP} + \Delta\dot{\omega}_{NGP} + \varepsilon \cdot \Delta\dot{\omega}_{GR}$$

$$\varepsilon = 1 + (-0.12 \pm 2.10) \cdot 10^{-3} \pm 2.5 \cdot 10^{-2}$$

Measurements and constraints from pericenter and mean anomaly

PHYSICAL REVIEW D **89**, 082002 (2014)

LAGEOS II pericenter general relativistic precession (1993–2005): Error budget and constraints in gravitational physics

David M. Lucchesi*

Istituto di Astrofisica e Planetologia Spaziali, Istituto Nazionale di Astrofisica, (IAPS/INAF), Via del Fosso del Cavaliere 100, 00133 Roma, Italy, Istituto di Scienza e Tecnologie dell'Informazione, Consiglio Nazionale delle Ricerche, (ISTI/CNR), Via G. Moruzzi 1, 56124 Pisa, Italy, and Istituto Nazionale di Fisica Nucleare (INFN), Sezione di Pisa, Largo B. Pontecorvo 3, 56127 Pisa, Italy

Roberto Peron

Istituto di Astrofisica e Planetologia Spaziali, Istituto Nazionale di Astrofisica, (IAPS/INAF), Via del Fosso del Cavaliere 100, 00133 Roma, Italy and Istituto Nazionale di Fisica Nucleare (INFN), Sezione di Roma Tor Vergata, Via della Ricerca Scientifica 1, 00133 Roma, Italy

(Received 16 April 2013; published 7 April 2014)

The aim of this paper is to extend, clarify, and deepen the results of our previous work [D. M. Lucchesi and R. Peron, Phys. Rev. Lett. **105**, 231103 (2010)], related to the precise measurement of LAGEOS (LAser GEOdynamics Satellite) II pericenter shift. A 13-year time span of LAGEOS satellites' laser tracking data has been considered, obtaining a very precise orbit and correspondingly residuals time series from which to extract the relevant signals. A thorough description is provided of the data analysis strategy and the dynamical models employed, along with a detailed discussion of the known sources of error in the experiment, both statistical and systematic. From this analysis, a confirmation of the predictions of Einstein's general relativity, as well as strong bounds on alternative theories of gravitation, clearly emerge. In particular, taking conservatively into account the stricter error bound due to systematic effects, general relativity has been confirmed in the Earth's field at the 98% level (meaning the measurement of a suitable combination of β and γ PPN parameters in weak-field conditions). This bound has been used to constrain possible deviations from the inverse-square law parameterized by a Yukawa-like new long range interaction with strength $|\alpha| \lesssim 1 \times 10^{-10}$ at a characteristic range $\lambda \simeq 1$ Earth radius, a possible nonsymmetric gravitation theory with the interaction parameter $\mathcal{C}_{\oplus\mathrm{LAGEOS\ II}} \lesssim (9 \times 10^{-2}\ \mathrm{km})^4$, and a possible spacetime torsion with a characteristic parameter combination $|2t_2 + t_3| \lesssim 7 \times 10^{-2}$. Conversely, if we consider the results obtained from our best fit of the LAGEOS II orbit, the constraints in fundamental physics improve by at least 2 orders of magnitude.

DOI: 10.1103/PhysRevD.89.082002 PACS numbers: 04.80.Cc, 91.10.Sp, 95.10.Eg, 95.40.+s

Selected for a Viewpoint in *Physics*

PRL **105**, 231103 (2010) PHYSICAL REVIEW LETTERS week ending 3 DECEMBER 2010

Accurate Measurement in the Field of the Earth of the General-Relativistic Precession of the LAGEOS II Pericenter and New Constraints on Non-Newtonian Gravity

David M. Lucchesi[1,2] and Roberto Peron[1]

[1]*Istituto di Fisica dello Spazio Interplanetario, Istituto Nazionale di Astrofisica, IFSI/INAF, Via del Fosso del Cavaliere 100, 00133 Roma, Italy*

[2]*Istituto di Scienza e Tecnologie dell'Informazione, Consiglio Nazionale delle Ricerche, ISTI/CNR, Via G. Moruzzi 1, 56124 Pisa, Italy*

(Received 18 July 2010; published 29 November 2010)

The pericenter shift of a binary system represents a suitable observable to test for possible deviations from the Newtonian inverse-square law in favor of new weak interactions between macroscopic objects. We analyzed 13 years of tracking data of the LAGEOS satellites with GEODYN II software but with no models for general relativity. From the fit of LAGEOS II pericenter residuals we have been able to obtain a 99.8% agreement with the predictions of Einstein's theory. This result may be considered as a 99.8% measurement in the field of the Earth of the combination of the γ and β parameters of general relativity, and it may be used to constrain possible deviations from the inverse-square law in favor of new weak interactions parametrized by a Yukawa-like potential with strength α and range λ. We obtained $|\alpha| \lesssim 1 \times 10^{-11}$, a huge improvement at a range of about 1 Earth radius.

Physics *Physics* **3**, 100 (2010)

Viewpoint

Via satellite

David Rubincam
Planetary Geodynamics Laboratory NASA Goddard Space Flight Center, Greenbelt, MD 20771, USA

Published November 29, 2010

More than a decade's worth of data collected from the LAGEOS II satellite is offering a new way to test general relativity.

Subject Areas: **Gravitation**

A Viewpoint on:
Accurate Measurement in the Field of the Earth of the General-Relativistic Precession of the LAGEOS II Pericenter and New Constraints on Non-Newtonian Gravity
David M. Lucchesi and Roberto Peron
Phys. Rev. Lett. **105**, 231103 (2010) – Published November 29, 2010

Measurements and constraints from pericenter and mean anomaly

The total relativistic precession of the argument of pericenter: **a previous result on 13 years**

Summary of the constraints obtained

TABLE XVIII. Summary of the results obtained in the present work; together with the measurement error budget, the constraints on fundamental physics are listed and compared with the literature.

	Parameter	Values and uncertainties (this study)	Uncertainties (literature)	Remarks
	$\epsilon_\omega - 1$	$-1.2\times10^{-4}\pm2.10\times10^{-3}\pm2.54\times10^{-2}$	$\cdots$	Error budget of the perigee precession measurement in the field of the Earth
PPN →	$\frac{\lvert 2+2\gamma-\beta\rvert}{3}-1$	$-1.2\times10^{-4}\pm2.10\times10^{-3}\pm2.54\times10^{-2}$	$\pm(1.0\times10^{-3})\pm(2\times10^{-2})$[a]	Constraint on the combination of PPN parameters
Yukawa →	$\lvert\alpha\rvert$	$\lesssim\lvert 0.5\pm8.0\pm101\rvert\times10^{-12}$	$\pm1\times10^{-8}$[b]	Constraint on a possible (Yukawa-like) NLRI
ATGs →	$\mathcal{C}_{\oplus\mathrm{LAGEOSII}}$	$\leq(0.003\ \mathrm{km})^4\pm(0.036\ \mathrm{km})^4\pm(0.092\ \mathrm{km})^4$	$\pm(0.16\ \mathrm{km})^4$[c]; $\pm(0.087\ \mathrm{km})^4$[d]	Constraint on a possible NSGT
	$\lvert 2t_2+t_3\rvert$	$\lesssim3.5\times10^{-4}\pm6.2\times10^{-3}\pm7.49\times10^{-2}$	3×10^{-3}[e]	Constraint on torsion

[a]From the preliminary estimate of the systematic errors of [166] for the perihelion precession of Mercury.
[b]From [167] with Lunar-LAGEOS GM measurements.
[c]From [5] and based on a partial estimate for the systematic errors.
[d]From [7] and based on the analysis of the systematic errors only.
[e]From [168] with no estimate for the systematic errors.

Measurements and constraints from pericenter and mean anomaly

The previous measurement in 2014, on 13 years: $\varepsilon - 1 = (-0.12 \pm 2.10) \cdot 10^{-3} \pm 2.5 \cdot 10^{-2}$

Violation of 1/r^2 law: Yukawa-like potential

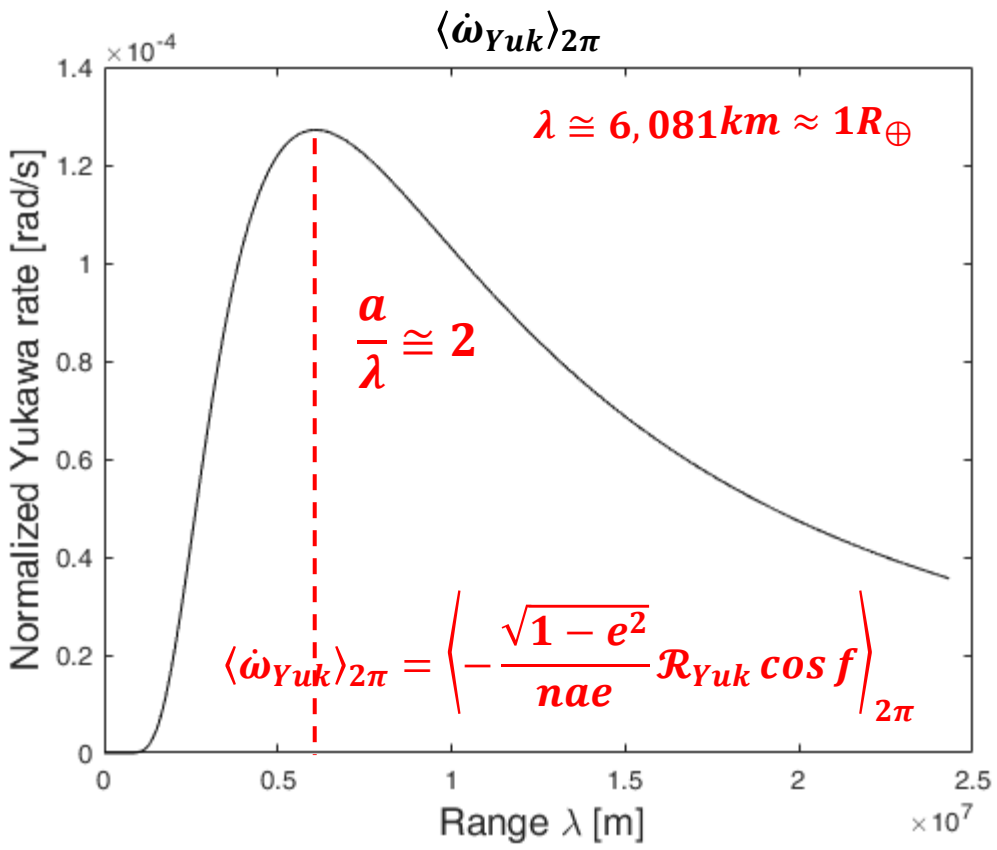

$$\left\langle \frac{d\omega}{dt} \right\rangle_{2\pi}^{Peak} \cong 1.27394 \cdot 10^{-4} \cdot \alpha \, rad/s$$

$$\vec{\mathcal{R}}_{Yuk} = -\alpha \frac{G_{\infty} M_{\oplus}}{r^2} \left(1 + \frac{r}{\lambda}\right) e^{-r/\lambda} \hat{r}$$

$$|\alpha| \cong \left| (0.5 \pm 8) \cdot 10^{-12} \pm 101 \cdot 10^{-12} \right|$$

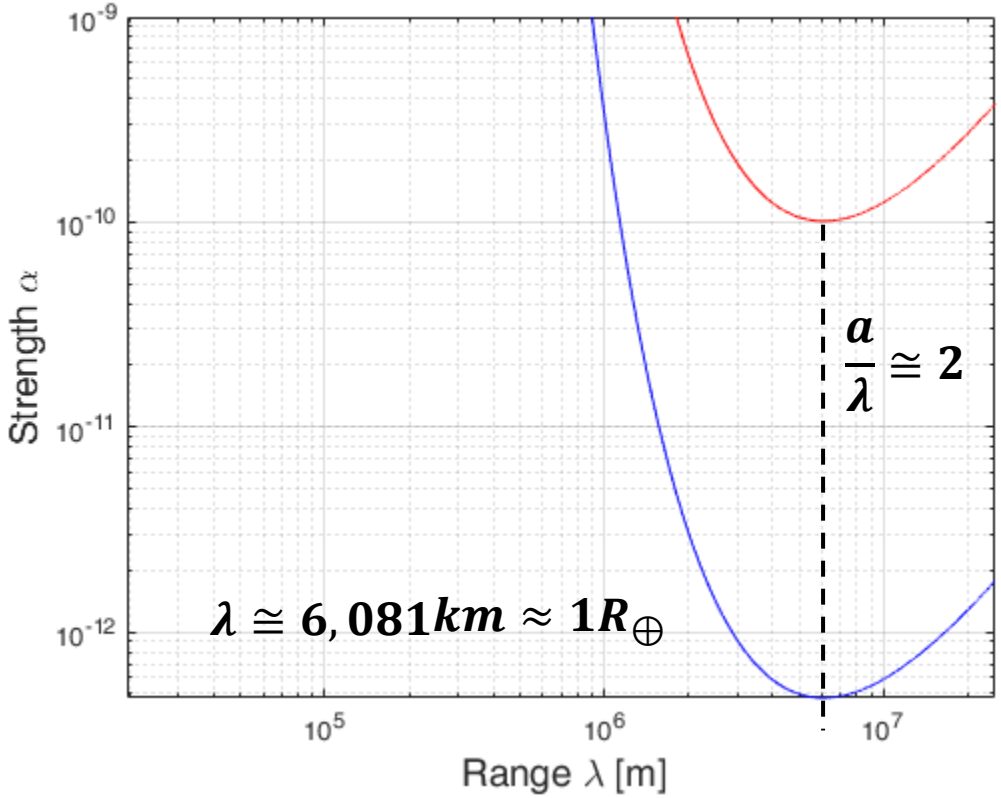

Measurements and constraints from pericenter and mean anomaly

Constraints on a long-range force: Yukawa like interaction

The region above each curve is ruled out at the 95.5% confidence level

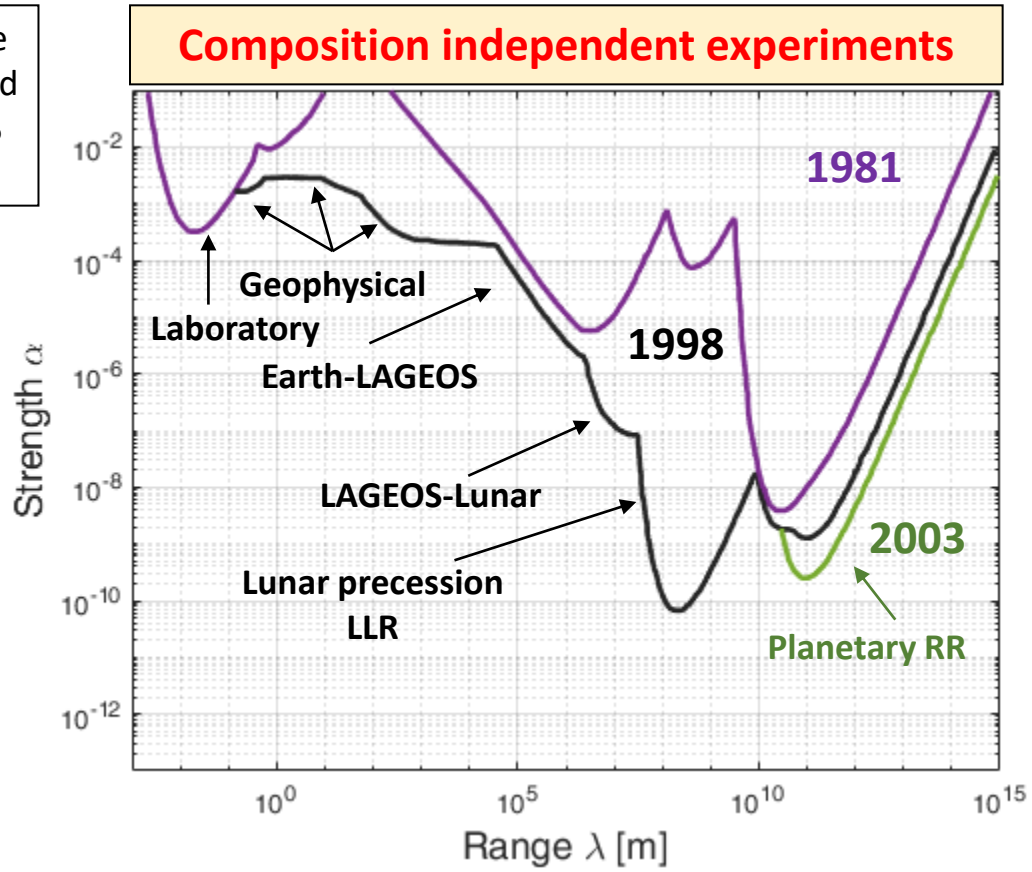

Previous limits with **LAGEOS's** from **GM** measurements:

$$|\alpha| < 10^{-5} \div 10^{-8}$$

Measurements and constraints from pericenter and mean anomaly

Constraints on a long-range force: Yukawa like interaction

$$|\alpha| \cong \left|(0.5 \pm 8) \cdot 10^{-12} \pm 101 \cdot 10^{-12}\right|$$

The region above each curve is ruled out at the 95.5% confidence level

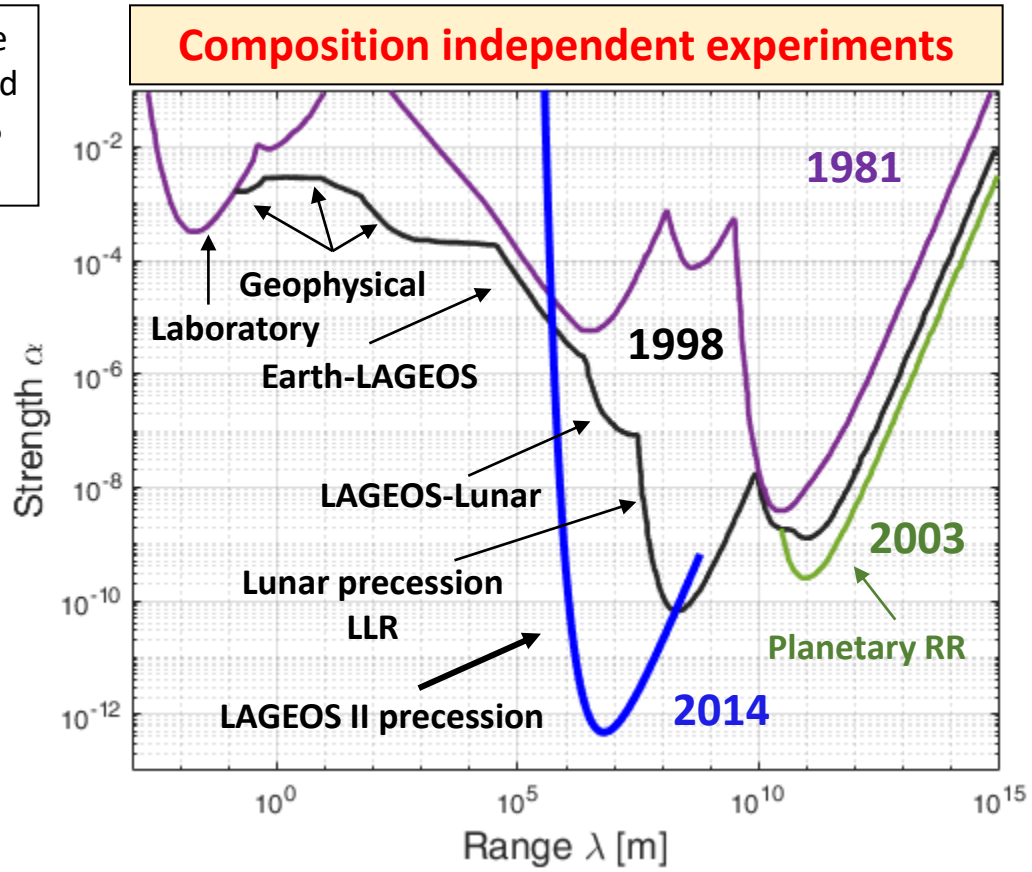

Previous limits with **LAGEOS's** from **GM** measurements:

$$|\alpha| < 10^{-5} \div 10^{-8}$$

$$|\alpha| \cong 5 \cdot 10^{-13}$$

Measurements and constraints from pericenter and mean anomaly

Constraints on a long-range force: Yukawa like interaction

$$|\alpha| \cong \left|(0.5 \pm 8) \cdot 10^{-12} \pm 101 \cdot 10^{-12}\right|$$

The region above each curve is ruled out at the 95.5% confidence level

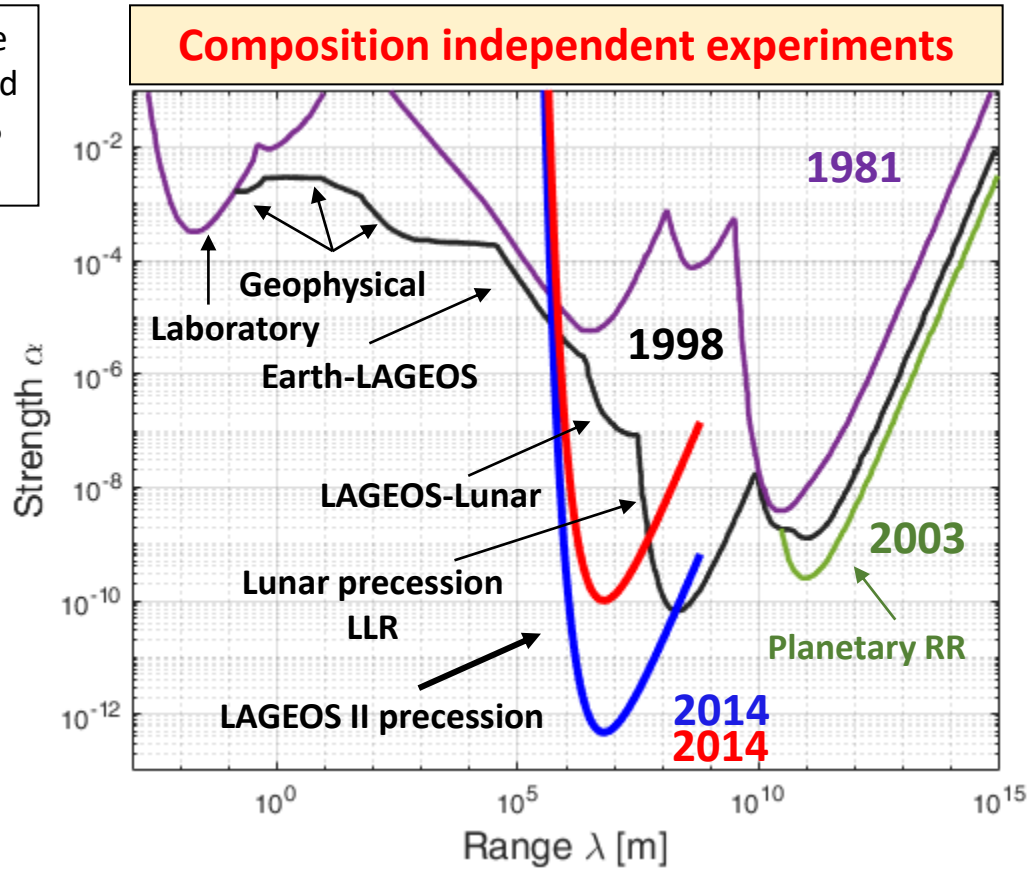

Previous limits with **LAGEOS's** from **GM** measurements:

$$|\alpha| < 10^{-5} \div 10^{-8}$$

$$|\alpha| \cong 5 \cdot 10^{-13}$$

$$|\alpha| \cong 1 \cdot 10^{-10}$$

$$\lambda \cong 6,081 km \approx 1 R_{\oplus}$$

Measurements and constraints from pericenter and mean anomaly

The previous error budget for the pericenter on 13 years

$$\varepsilon - 1 = (-0.12 \pm 2.10) \cdot 10^{-3} \pm 2.5 \cdot 10^{-2}$$

DAVID M. LUCCHESI AND ROBERTO PERON — PHYSICAL REVIEW D **89**, 082002 (2014)

TABLE XVII. Error budget of the LAGEOS II pericenter general relativity shift. Top: summary of the errors from the data reduction and the *a posteriori* best fit (see Sections VI and VII). Middle: summary of the systematic errors from the gravitational perturbations (see Section VIII). Bottom: summary of the systematic errors from the nongravitational perturbations (see Section IX).

Statistical errors		
Residuals	Mean	Standard deviation
Range	9.67 cm	3.88 cm
Pericenter	4.57 mas	1.87 mas
Adjusted $\mathcal{R}_a^2$	0.998	
Reduced χ_ν^2 test	0.14	
	$\epsilon_\omega^{\rm sta} - 1 = (-0.12 \pm 2.10) \times 10^{-3}$	

Systematic errors: gravitational perturbations		
Error source	Error value (% $\Delta\dot{\omega}_{\rm II}^{\rm rel}$)	Total not correlated (% $\Delta\dot{\omega}_{\rm II}^{\rm rel}$)
Even zonal harmonics	2.45	
Odd zonal harmonics	4.10×10^{-2}	
Tides (solid + ocean)	2.48×10^{-2}	2.46
Secular trends (ℓ = even)	3.30×10^{-2}	
Seasonal-like effects	0.24	

Systematic errors: nongravitational perturbations		
Error source	Error value (% $\Delta\dot{\omega}_{\rm II}^{\rm rel}$)	Total not correlated (% $\Delta\dot{\omega}_{\rm II}^{\rm rel}$)
Direct solar radiation	0.50	
Earth's albedo	0.39	
Thermal thrusts	0.09	0.64
Drag (neutral + charged)	negligible	
Total not correlated		2.54
	$\epsilon_\omega^{\rm sys} - 1 = \pm 2.54 \times 10^{-2}$	

Preliminary measurement

New Error Budget should be estimatd, but

$$\varepsilon - 1 \cong 0.35 \times 10^{-3} \pm 2.42 \times 10^{-3} \pm ?$$

$$\begin{cases} X_{obs} = \dot{M}_{res}^{L2} + k\dot{\omega}_{res}^{L2} \\ k \cong -0.123500 \end{cases} \longrightarrow \delta J_2 = 0$$

$$X_{rel} = \dot{M}_{rel}^{L2} + k\dot{\omega}_{rel}^{L2} \cong -3759.26 \text{ mas/yr}$$

$$\varepsilon_{GP} \approx 0$$

New Error Budget should be estimatd, but

Measurements and constraints from pericenter and mean anomaly

LAGEOS II

<u>Preliminary measurement</u>

The long-term temporal behavior is very similar in these two orbital elements

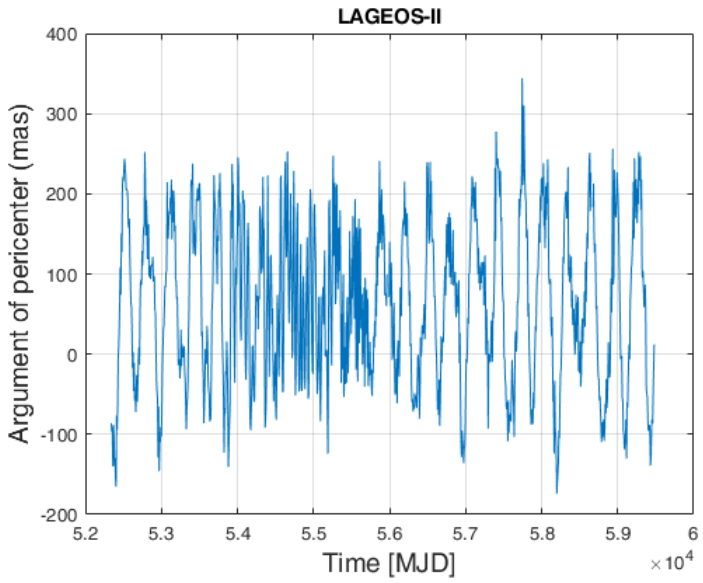

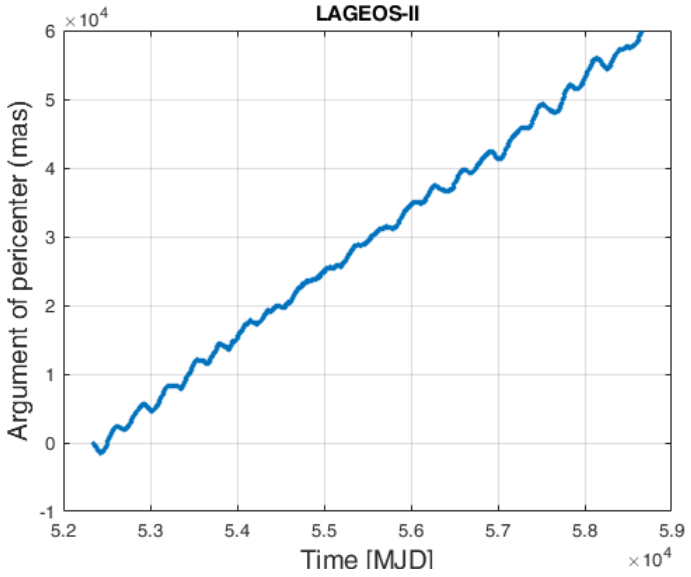

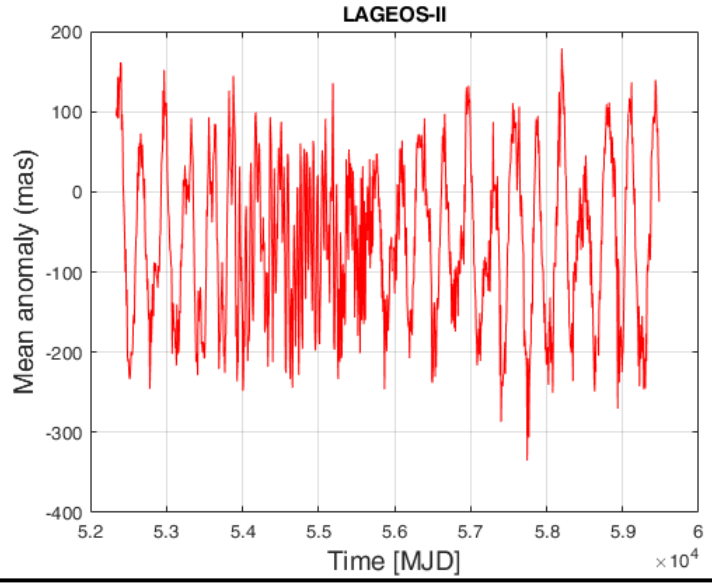

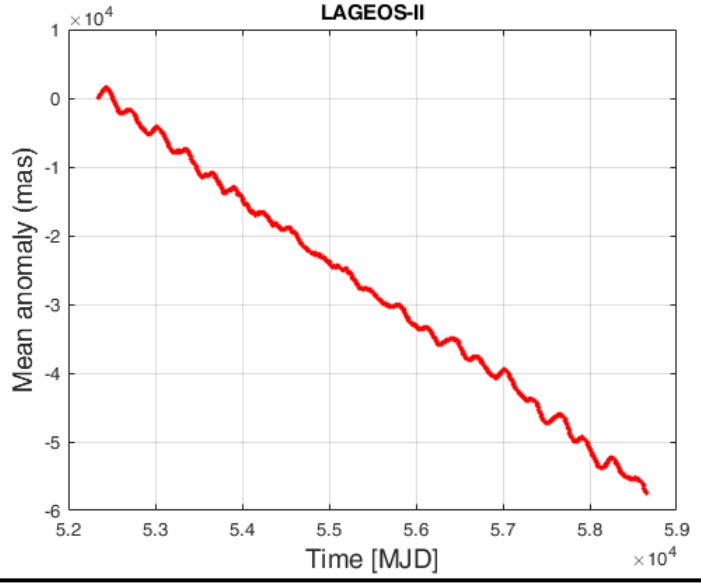

Measurements and constraints from pericenter and mean anomaly

The previous error budget for the pericenter on 13 years

$$\varepsilon - 1 = (-0.12 \pm 2.10) \cdot 10^{-3} \pm 2.5 \cdot 10^{-2}$$

DAVID M. LUCCHESI AND ROBERTO PERON — PHYSICAL REVIEW D **89**, 082002 (2014)

TABLE XVII. Error budget of the LAGEOS II pericenter general relativity shift. Top: summary of the errors from the data reduction and the *a posteriori* best fit (see Sections VI and VII). Middle: summary of the systematic errors from the gravitational perturbations (see Section VIII). Bottom: summary of the systematic errors from the nongravitational perturbations (see Section IX).

Statistical errors		
Residuals	Mean	Standard deviation
Range	9.67 cm	3.88 cm
Pericenter	4.57 mas	1.87 mas
Adjusted $\mathcal{R}_a^2$	0.998	
Reduced χ_ν^2 test	0.14	
	$\epsilon_\omega^{\rm sta} - 1 = (-0.12 \pm 2.10) \times 10^{-3}$	
Systematic errors: gravitational perturbations		
Error source	Error value (% $\Delta\dot{\omega}_{\rm II}^{\rm rel}$)	Total not correlated (% $\Delta\dot{\omega}_{\rm II}^{\rm rel}$)
Even zonal harmonics	2.45	
Odd zonal harmonics	4.10×10^{-2}	
Tides (solid + ocean)	2.48×10^{-2}	2.46
Secular trends (ℓ = even)	3.30×10^{-2}	
Seasonal-like effects	0.24	
Systematic errors: nongravitational perturbations		
Error source	Error value (% $\Delta\dot{\omega}_{\rm II}^{\rm rel}$)	Total not correlated (% $\Delta\dot{\omega}_{\rm II}^{\rm rel}$)
Direct solar radiation	0.50	
Earth's albedo	0.39	
Thermal thrusts	0.09	0.64
Drag (neutral + charged)	negligible	
Total not correlated		2.54
	$\epsilon_\omega^{\rm sys} - 1 = \pm 2.54 \times 10^{-2}$	

Preliminary measurement

New Error Budget should be estimatd, but

$$\varepsilon - 1 \cong 0.35 \times 10^{-3} \pm 2.42 \times 10^{-3} \pm ?$$

$$\begin{cases} X_{obs} = \dot{M}_{res}^{L2} + k\dot{\omega}_{res}^{L2} \\ k \cong -0.123500 \end{cases} \longrightarrow \delta J_2 = 0$$

$$X_{rel} = \dot{M}_{rel}^{L2} + k\dot{\omega}_{rel}^{L2} \cong -3759.26 \text{ mas/yr}$$

$$\varepsilon_{GP} \approx 0$$

New Error Budget should be estimatd, but since the long-term behaviour of the two elements are quite similar

$$\varepsilon_{NGP} \approx (0.7 + k0.7)\% \cong 0.8\%$$

Measurements and constraints from pericenter and mean anomaly

Comparison with previous results: literature, LARASE , SaToR-G

LARASE: pericenter

SaToR-G: pericenter + mean anomaly

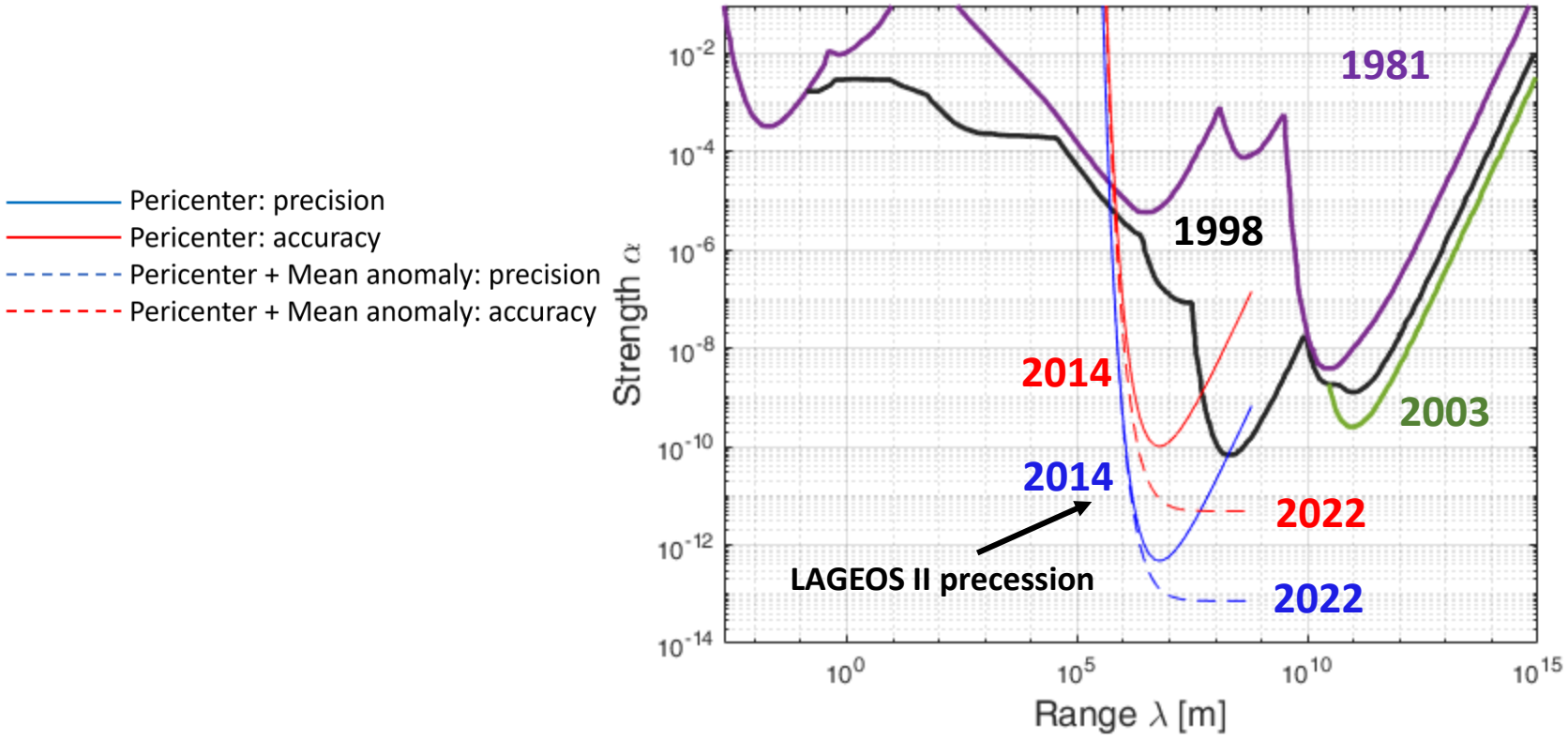

Currently, for the precision of the measurement we assumed the same as that obtained from LARASE experiment

Measurements and constraints from pericenter and mean anomaly

The total relativistic precession of the argument of pericenter: **a previous result on 13 years**

Summary of the constraints obtained

TABLE XVIII. Summary of the results obtained in the present work; together with the measurement error budget, the constraints on fundamental physics are listed and compared with the literature.

	Parameter	Values and uncertainties (this study)	Uncertainties (literature)	Remarks
	$\epsilon_\omega - 1$	$-1.2\times10^{-4}\pm2.10\times10^{-3}\pm2.54\times10^{-2}$	$\cdots$	Error budget of the perigee precession measurement in the field of the Earth
PPN →	$\frac{\lvert 2+2\gamma-\beta\rvert}{3}-1$	$-1.2\times10^{-4}\pm2.10\times10^{-3}\pm2.54\times10^{-2}$	$\pm(1.0\times10^{-3})\pm(2\times10^{-2})^{a}$	Constraint on the combination of PPN parameters
Yukawa →	$\lvert\alpha\rvert$	$\lesssim\lvert 0.5\pm8.0\pm101\rvert\times10^{-12}$	$\pm1\times10^{-8b}$	Constraint on a possible (Yukawa-like) NLRI
ATGs →	$\mathcal{C}_{\oplus\mathrm{LAGEOSII}}$	$\leq(0.003\ \mathrm{km})^4\pm(0.036\ \mathrm{km})^4\pm(0.092\ \mathrm{km})^4$	$\pm(0.16\ \mathrm{km})^{4c}$; $\pm(0.087\ \mathrm{km})^{4d}$	Constraint on a possible NSGT
	$\lvert 2t_2+t_3\rvert$	$\lesssim3.5\times10^{-4}\pm6.2\times10^{-3}\pm7.49\times10^{-2}$	3×10^{-3e}	Constraint on torsion

[a]From the preliminary estimate of the systematic errors of [166] for the perihelion precession of Mercury.
[b]From [167] with Lunar-LAGEOS GM measurements.
[c]From [5] and based on a partial estimate for the systematic errors.
[d]From [7] and based on the analysis of the systematic errors only.
[e]From [168] with no estimate for the systematic errors.

Measurements and constraints from pericenter and mean anomaly

Preliminary constraints to alternative theories of gravitation

- **Constraints beta and gamma**

$$\frac{|2+2\gamma-\beta|}{3}-1=(-0.12\pm 2.10)\cdot 10^{-3}\pm 2.5\cdot 10^{-2}$$

PRD 2014

$$\left(\frac{|2+2\gamma-\beta|}{3}-1\right)_{sys}=\pm 0.8\cdot 10^{-2}$$

Measurements and constraints from pericenter and mean anomaly

Preliminary constraints to alternative theories of gravitation

- **Constraints on Moffat non-symmetric theory for gravitation**

Moffat (1979), and Moffat and Woolgar (1988), studied the possibility of a Non-Symmetric Gravitation Theory (NSGT) starting from Einstein's idea to unify gravitation and electromagnetism introducing a non-symmetric fundamental tensor.

Among the various features of this theory, we are interested to the one which specifies that a given body **B** has associated — in addition to its mass — a NSGT charge ℓ^2_B which arises from the coupling of the non-metric with a vector current. Interesting for our study, the equation of motion of a test body is not the standard geodesic-equation, because of the presence of this new attribute. Indeed, for the pericenter rate of a binary system constituted by a primary **B** and a satellite **S**, Moffat and Woolgar (1988) obtained an additional contribution given by:

$$\langle \Delta\dot{\omega} \rangle_{sec}^{Moffat} = \frac{3\left(GM_{\oplus}\right)^{3/2}}{c^2 a^{5/2}(1-e^2)} \left[\mathcal{C}_{\oplus S} \frac{c^4(1+e^2/4)}{\left(GM_{\oplus}(1-e^2)\right)^2} \right]$$

$$\boxed{C_{\oplus S} = \left(M_{\oplus} + m_S\right)\left(\ell_{\oplus}^2/M_{\oplus} - \ell_S^2/M_S\right)\left(\ell_{\oplus}^2 - \ell_S^2\right)}$$

Measurements and constraints from pericenter and mean anomaly

Preliminary constraints to alternative theories of gravitation

- **Constraints on Moffat non-symmetric theory for gravitation**

$$\langle \Delta\dot{\omega} \rangle_{sec}^{Moffat} = \frac{3\left(GM_{\oplus}\right)^{3/2}}{c^2 a^{5/2}(1-e^2)} \left[\mathcal{C}_{\oplus s} \frac{c^4(1+e^2/4)}{\left(GM_{\oplus}(1-e^2)\right)^2} \right]$$

Therefore, with the present study we can constrain the non-symmetric interaction to the following values:

$$\mathcal{C}_{\oplus LageosII} \leq (0.003km)^4 \pm (0.036km)^4 \pm (0.092km)^4$$ **PRD 2014**

$$\mathcal{C}_{\oplus LageosII\_sys} \leq \pm(0.029km)^4$$

To compare with:

$$\mathcal{C}_{\oplus Lageos} \leq (0.16km)^4$$

Ciufolini and Matzner [**Int. J. Mod. Phys. (1992)**], from the total uncertainty in the calculated precession of **LAGEOS**

$$\mathcal{C}_{\oplus LageosII} \leq (0.087km)^4$$

Lucchesi [**Phys. Lett. A 318 (2003)**], from the systematic effects on the pericenter of **LAGEOS II**

Measurements and constraints from pericenter and mean anomaly

Preliminary constraints to alternative theories of gravitation

- **Constraints on Mao spacetime torsion**

A generalization of Einstein's **GR** may be obtained when a Riemann-Cartan spacetime is considered. In this case a non-vanishing torsional tensor is present because of **non-symmetric connection coefficients**. More recently, Mao et al. (2007) suggested that the presence of torsional effects in the solar system should be tested experimentally. Indeed, they developed a theory-independent framework based on symmetry arguments in order to parametrize both metric and connection. This theory is characterized by a set of parameters that are able to describe **torsion** and **metric**.

Subsequently, March et al. (2011) computed (in the **WFSM** limit) the corrections to the longitude of the pericenter in the case of a satellite orbiting the Earth and in the field of the Sun for the Schwarzschild, Lense-Thirring and de Sitter precessions produced by these possible spacetime torsions. For the argument of pericenter we obtain:

$$\langle \Delta\dot{\omega} \rangle_{sec}^{torsion} = \frac{3\left(GM_{\oplus}\right)^{3/2}}{c^2 a^{5/2}(1-e^2)}\left[\frac{2t_2+t_3}{3}\right] + \Delta\dot{\omega}_{LT}^{torsion}$$

Measurements and constraints from pericenter and mean anomaly

Preliminary constraints to alternative theories of gravitation

- **Constraints on Mao spacetime torsion**

$$\langle \Delta\dot{\omega} \rangle_{sec}^{torsion} = \frac{3\left(GM_{\oplus}\right)^{3/2}}{c^2 a^{5/2}(1-e^2)} \left[\frac{2t_2+t_3}{3}\right] + \Delta\dot{\omega}_{LT}^{torsion}$$

Therefore, with the present study we can constrain the torsion effects to the following values:

$$|2t_2 + t_3| \leq 3.5 \cdot 10^{-4} \pm 6.2 \cdot 10^{-3} \pm 7.49 \cdot 10^{-2}$$

PRD 2014

$$|2t_2 + t_3|_{\_sys} \leq \pm 2.40 \cdot 10^{-2}$$

To compare with:

$$|2t_2 + t_3| \cong 3 \cdot 10^{-3}$$

March et al. (2011), using the Mercury's perihelion shift measurement of Shapiro et al. (1990)

Measurements and constraints from the ascending node longitute

The 2019-2020 measurement: The Einstein-Thirring-Lense precession

- We considered several models for the background gravitational field of the Earth
  - **This allows to highlight possible systematics among the different models**
- For the first **10/15** even zonal harmonics we considered their explicit time dependency following the monthly solutions from **GRACE** measurements
  - **This has reduced the systematic error of the background gravitational field**
- Together with the relativistic **Einstein-Thirring-Lense** precession we estimated also some of the low-degree even zonal harmonics (ℓ = even and m = 0) of the background gravitational field
  - **This allows to estimate the direct correlation between the relativistic Einstein-Thirring-Lense precession with the coefficients of the gravitational field**

Measurements and constraints from the ascending node longitute

The 2019-2020 measurement: The Einstein-Thirring-Lense precession

- The relativistic **Einstein-Thirring-Lense** precession has been measured both in the residuals of the rates of the combined nodes and in their integration
  - **This is the first time that the measurement has been performed on the rate of the combined observables**
- The measurement has been obtained both via linear fits and non-linear fits
  - **This is also the first time that a reliable measurement of the Einstein-Thirring-Lense precession has been obtained by means of a simple linear fit**

Measurements and constraints from the ascending node longitute

The 2019-2020 measurement: The Einstein-Thirring-Lense precession

By solving a linear system of three equations in three unknowns, we can solve for the relativistic precession while reducing the impact in the measurement of the non perfect knowledge of the Earth's gravitational field:

$$\begin{cases} \dot{\Omega}_2^{L1}\delta\bar{C}_{2,0} + \dot{\Omega}_4^{L1}\delta\bar{C}_{4,0} + \dot{\Omega}_{LT}^{L1}\mu + \cdots = \delta\dot{\Omega}_{res}^{L1} \\ \dot{\Omega}_2^{L2}\delta\bar{C}_{2,0} + \dot{\Omega}_4^{L2}\delta\bar{C}_{4,0} + \dot{\Omega}_{LT}^{L2}\mu + \cdots = \delta\dot{\Omega}_{res}^{L2} \\ \dot{\Omega}_2^{LR}\delta\bar{C}_{2,0} + \dot{\Omega}_4^{LR}\delta\bar{C}_{4,0} + \dot{\Omega}_{LT}^{LR}\mu + \cdots = \delta\dot{\Omega}_{res}^{LR} \end{cases}$$

$$\left(\mu, \delta\bar{C}_{2,0}, \delta\bar{C}_{4,0}\right)$$

$$\dot{\Omega}_{GR}^{comb} = 50.17\ mas/yr$$

$$\mu = \frac{\dot{\Omega}^{comb}}{\dot{\Omega}_{GR}^{comb}} = \begin{cases} 1 & \bullet\ \text{In General Relativity} \\ 0 & \bullet\ \text{In Newtonian physics} \end{cases}$$

$$\dot{\Omega}^{comb} = \delta\dot{\Omega}_{res}^{L1} + k_1\delta\dot{\Omega}_{res}^{L2} + k_2\delta\dot{\Omega}_{res}^{LR}$$

$$k_1 \cong 0.345$$
$$k_2 \cong 0.073$$

- LT effect observable
- k_1 and k_2 are such that to cancel the unmodelled effects/errors of two even zonal harmonics (order m=0) of the Earth's gravitational field: quadrupole and octupole coefficients

Measurements and constraints from the ascending node longitute

The data reduction of the satellites orbit has been done with **GEODYN II** (**NASA/GSFC**) on a time span of about **6.5 years** (**2359 days**) from **MJD 56023**, that is from April 6th 2012, and we computed the residuals on the orbit elements of **LAGEOS**, **LAGESOS II** and **LARES**:

- **Background gravity model: GRACE-static and coefficients from GRACE Temporal Solutions**
- **Arc length of 7 days**
- **No empirical accelerations**
- **Thermal thrust effects (Yarkovsky Schach and Rubincam) not modelled**
- **General relativity modelled with the exception of the Lense-Thirring effect**

1. **EIGEN-GRACE02S (2004)**
2. **GGM05S (2014): official field of the ILRS**
3. **ITU_GRACE16 (2016)**
4. **Tonji-Grace02s (2017)**

Table 2. Models currently used, within the LARASE research program, for the analysis of the orbit of the two LAGEOS and LARES satellites. The models are grouped in gravitational perturbations, non-gravitational perturbations and reference frames realizations.

Model For	Model Type	Reference
Geopotential (static)	EIGEN-GRACE02S/GGM05S	[84,90,91]
Geopotential (time-varying, tides)	Ray GOT99.2	[92]
Geopotential (time-varying, non tidal)	IERS Conventions 2010	[89]
Third–body	JPL DE-403	[93]
Relativistic corrections	Parameterized post-Newtonian	[88,94]
Direct solar radiation pressure	Cannonball	[46]
Earth albedo	Knocke-Rubincam	[63]
Earth-Yarkovsky	Rubincam	[56,64,65]
Neutral drag	JR-71/MSIS-86	[50,51]
Spin	LASSOS	[42]
Stations position	ITRF2008	[95]
Ocean loading	Schernek and GOT99.2 tides	[46,92]
Earth Rotation Parameters	IERS EOP C04	[96]
Nutation	IAU 2000	[97]
Precession	IAU 2000	[98]

Measurements and constraints from the ascending node longitute

D. Lucchesi, G. Balmino, *The LAGEOS satellites orbital residuals determination and the Lense–Thirring effect measurement*. Plan. and Space Science, doi:10.1016/j.pss.2006.03.001 , 2006

GGM05S + GRACE-TS model

Gussian-like distribution for μ

$K \cong +3.097 \quad S \cong -8.4\times10^{-3}$

Results for μ from the linear system

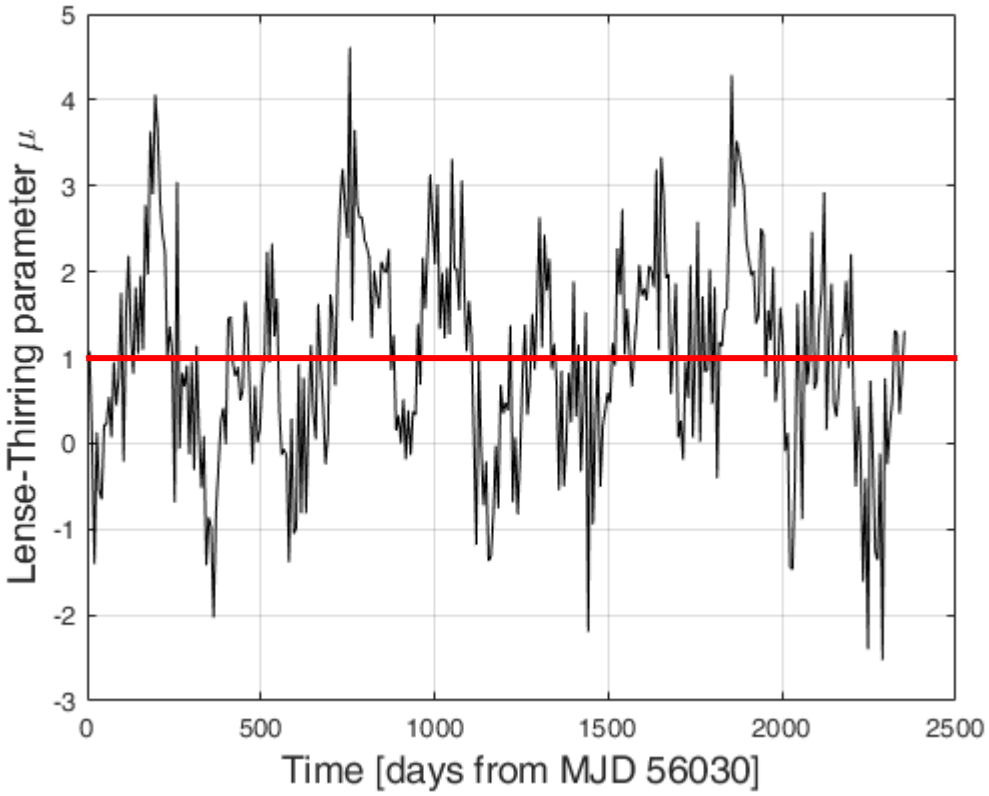

Cumulative sum for μ

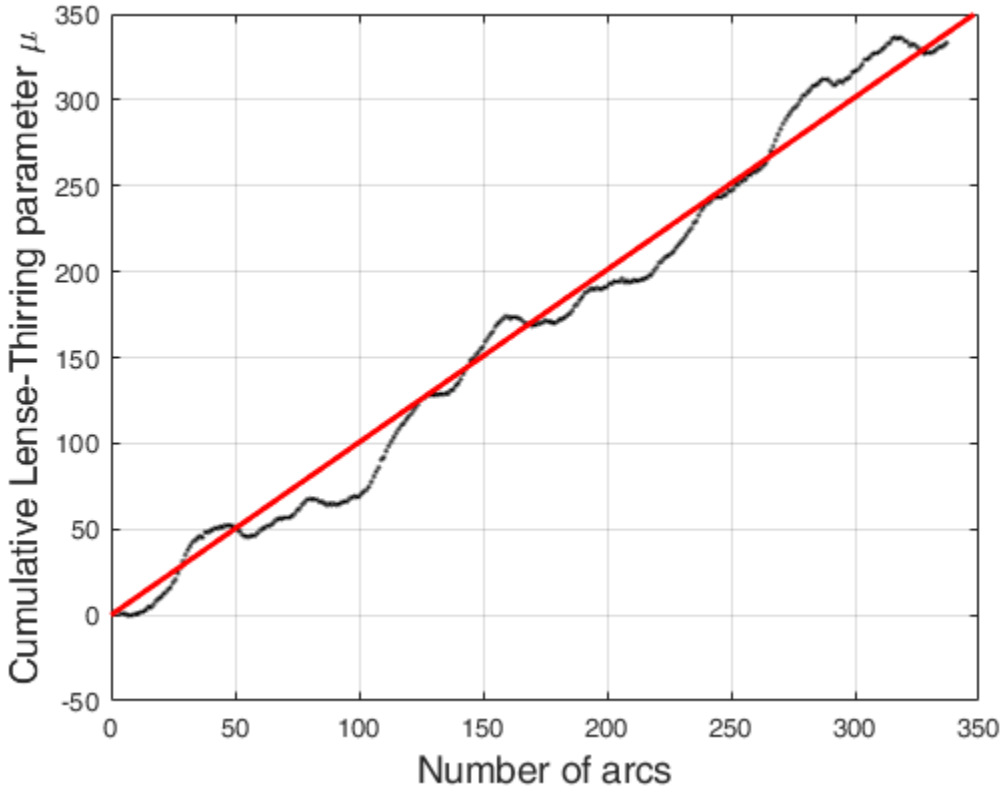

Measurements and constraints from the ascending node longitute

GGM05S / EIGEN-GRACE02S / ITU_GRACE16 / Tonj-Grace02S

+ GRACE-TS model

Results for μ from the linear system

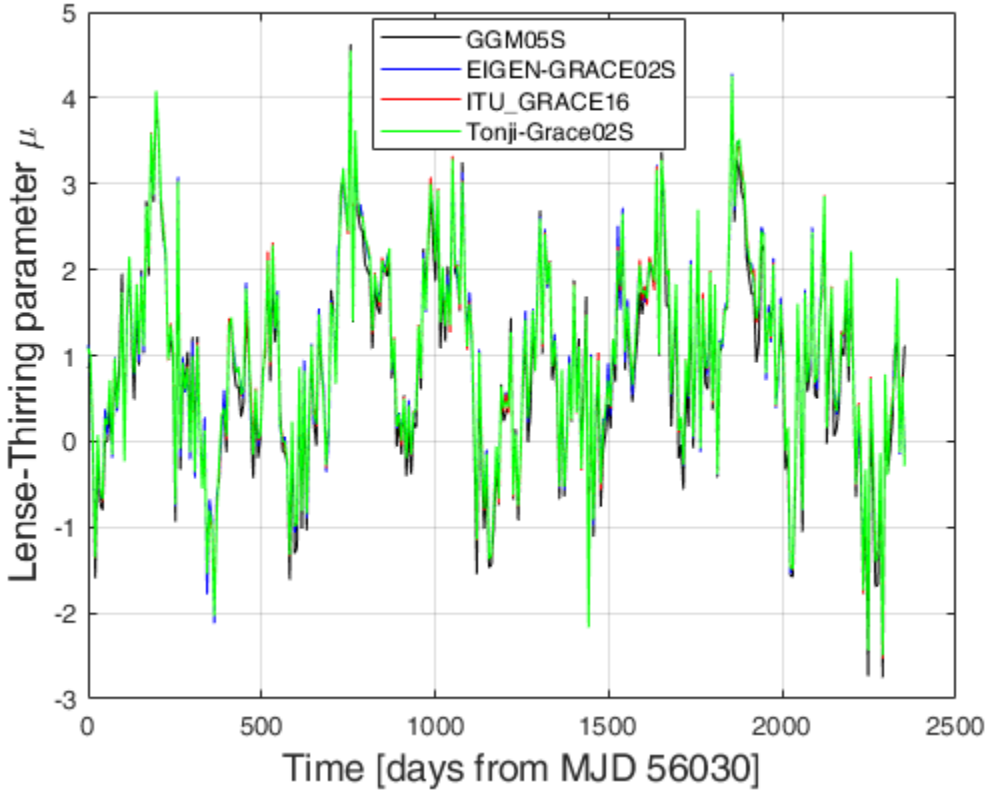

Cumulative sum for μ

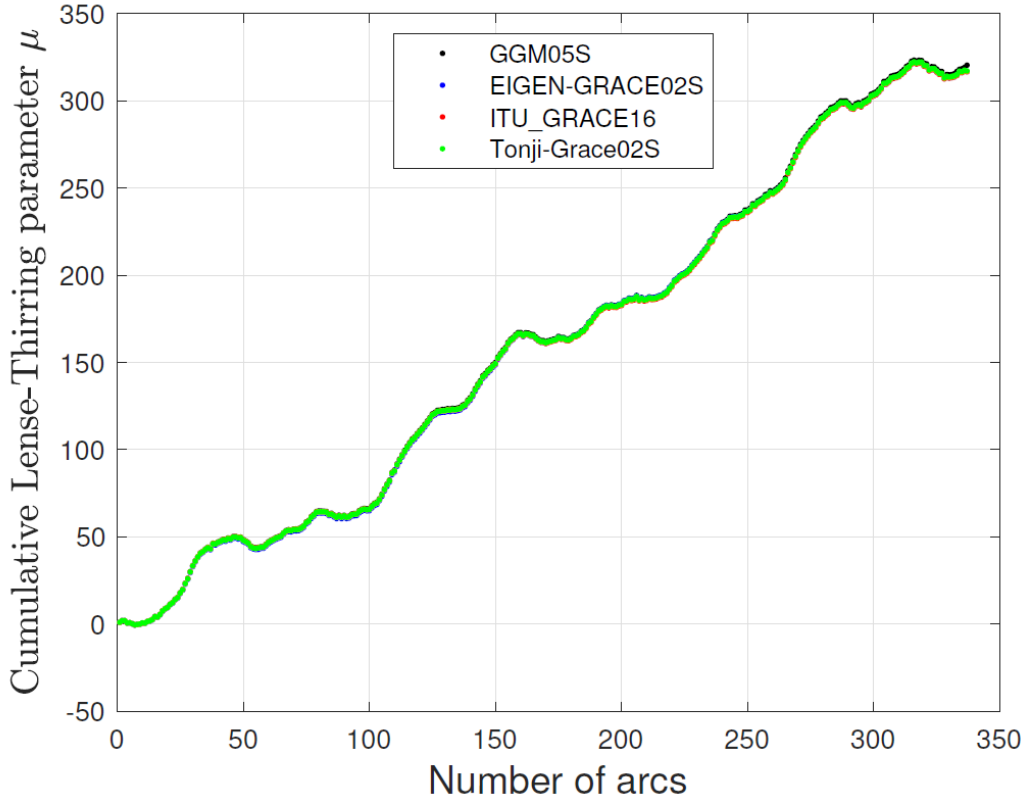

Measurements and constraints from the ascending node longitute

Einstein-Thirring-Lense effect measurement: frame dragging

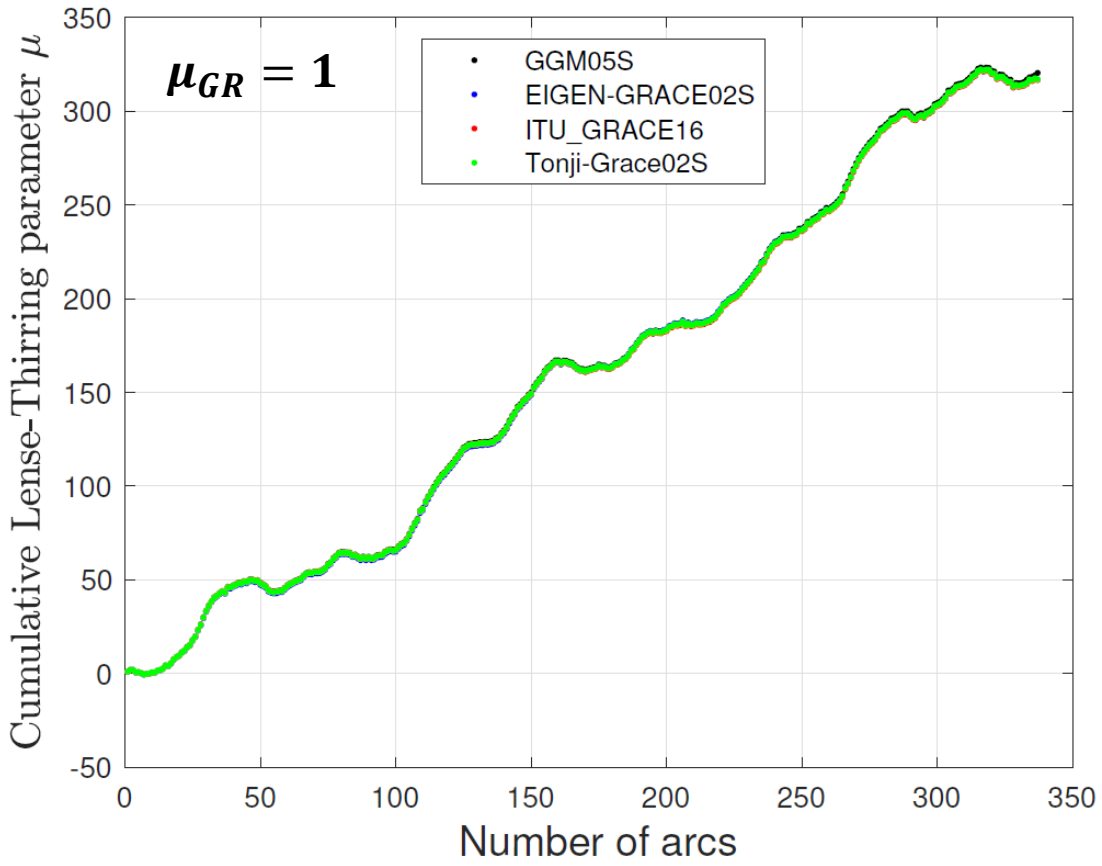

Errors @ 95% CL

Model	$\mu \pm \delta\mu$	$\mu - 1$
GGM05S	1.0053 ± 0.0074	$+0.0053$
EIGEN-GRACE02S	1.0002 ± 0.0074	$+0.0002$
ITU_GRACE16	0.9996 ± 0.0074	-0.0004
Tonji-Grace02s	1.0008 ± 0.0074	$+0.0008$

$$\boxed{\mu_{meas} - 1 = 1.5 \times 10^{-3} \pm 7.4 \times 10^{-3}}$$

This is indeed a very precise measurement

Measurements and constraints from the ascending node longitute

Main sources of systematic errors

Among the main perturbations to consider we have

- **The gravitational perturbations**
  - ❑ **Earth's gravitational field**
  - ❑ **Tides**
    - Ocean
    - Solid
  - ❑ **General relativity**
- **The non-gravitational perturbations**
  - ❑ **Direct solar radiation pressure, Earth's albedo and infrared radiation**
  - ❑ **Thermal thrust effects**

Measurements and constraints from the ascending node longitute

Main sources of systematic errors

Einstein-Thirring-Lense effect measurement: frame dragging

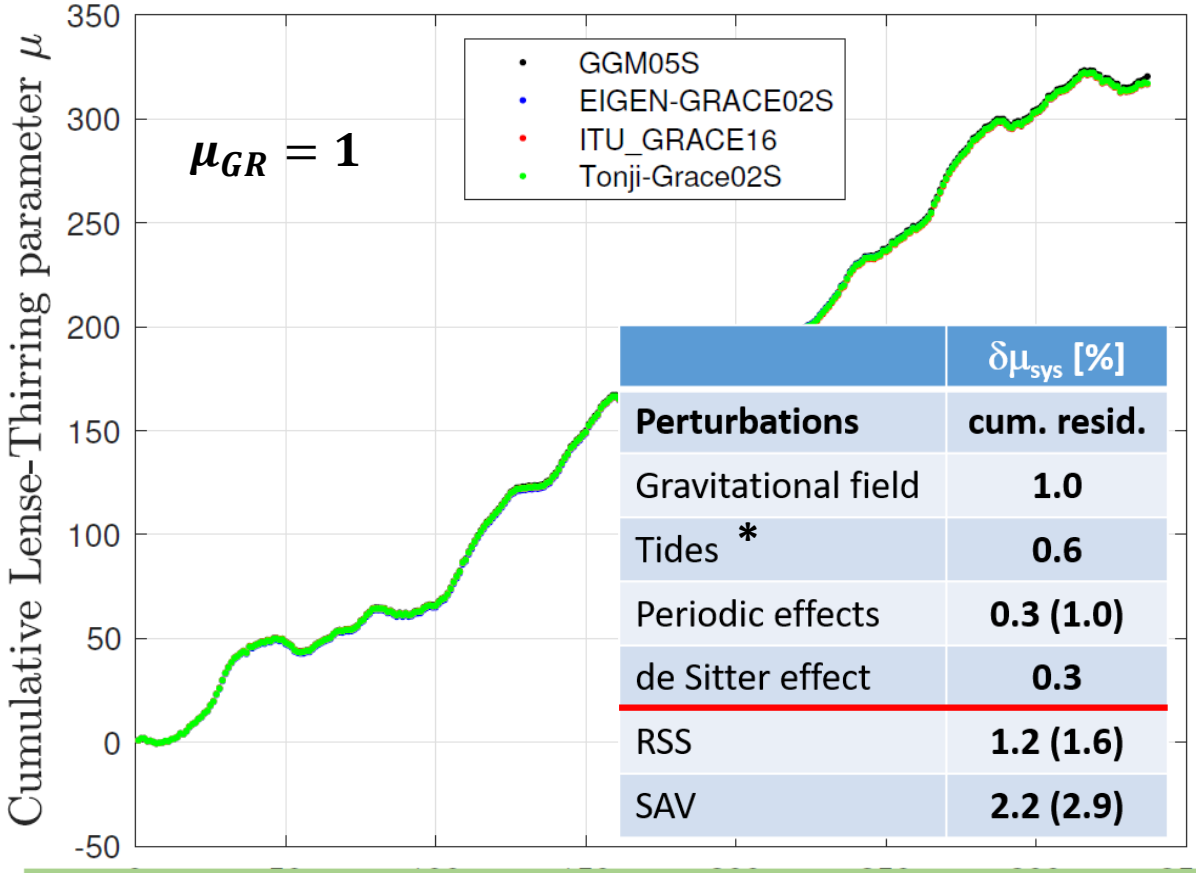

	$\delta\mu_{sys}$ [%]
Perturbations	**cum. resid.**
Gravitational field	**1.0**
Tides *	**0.6**
Periodic effects	**0.3 (1.0)**
de Sitter effect	**0.3**
RSS	**1.2 (1.6)**
SAV	**2.2 (2.9)**

Errors @ 95% CL

Model	$\mu \pm \delta\mu$	$\mu - 1$
GGM05S	1.0053 ± 0.0074	$+0.0053$
EIGEN-GRACE02S	1.0002 ± 0.0074	$+0.0002$
ITU_GRACE16	0.9996 ± 0.0074	-0.0004
Tonji-Grace02s	1.0008 ± 0.0074	$+0.0008$

$$\mu_{meas} - 1 = 1.5 \times 10^{-3} \pm 7.4 \times 10^{-3} \pm 16 \times 10^{-3}$$

Estimation of the systematic errors

This is indeed a very accurate measurement

D. Lucchesi, M. Visco, R. Peron, et al., *A 1% Measurement of the Gravitomagnetic Field of the Earth with Laser-Traked Satellites*. Universe 6, 139, doi:10.3390/universe6090139, 2020
*G. Pucacco, D. Lucchesi, *Tidal effects on the LAGEOS–LARES satellites and the LARASE program*. Celest. Mech. And Dyn. Astron., 130:66, https://doi.org/10.1007/s10569-018-9861-5, 2018

Measurements and constraints from the ascending node longitute

Einstein-Thirring-Lense effect measurement: frame dragging

$\boxed{\mu_{meas} = 1.0015 \pm 7.4 \times 10^{-3} \pm 0.016}$ **Linear Fit**

D. Lucchesi, M. Visco, R. Peron, et al., *An improved measurement of the Lense-Thirring precession on the orbits of laser-ranged satellites with an accuracy approaching the 1% level*. arXiv:1910.01941, doi:10.48550/arXiv.1910.01941, 2019

D. Lucchesi, M. Visco, R. Peron, et al., *A 1% Measurement of the Gravitomagnetic Field of the Earth with Laser-Traked Satellites*. Universe 6, 139, doi:10.3390/universe6090139, 2020

$\boxed{\mu_{meas} = 0.9910 \pm 0.02}$ **Linear Fit, after removing a few well known tidal signals from the nodes residuals**

I. Ciufolini, A. Paolozzi, et al., *An improved test of the general relativistic effect of frame-dragging using the LARES and LAGEOS satellites*. Eur. Phys. J. C, 79:872, doi.org/10.1140/epjc/s10052-019-7386-z, 2019

Measurements and constraints from the ascending node longitute

universe

MDPI

Article

A 1% Measurement of the Gravitomagnetic Field of the Earth with Laser-Tracked Satellites

David Lucchesi [1,2,3,*], Massimo Visco [1,3], Roberto Peron [1,3], Massimo Bassan [3,4], Giuseppe Pucacco [3,4], Carmen Pardini [2], Luciano Anselmo [2] and Carmelo Magnafico [1,3]

1 Istituto di Astrofisica e Planetologia Spaziali (IAPS)—Istituto Nazionale di Astrofisica (INAF), Via Fosso del Cavaliere 100, Tor Vergata, 00133 Roma, Italy; massimo.visco@inaf.it (M.V.); roberto.peron@inaf.it (R.P.); carmelo.magnafico@inaf.it (C.M.)

2 Istituto di Scienza e Tecnologie dell'Informazione (ISTI)—Consiglio Nazionale delle Ricerche, Via G. Moruzzi 1, 56124 Pisa, Italy; carmen.pardini@isti.cnr.it (C.P.); luciano.anselmo@isti.cnr.it (L.A.)

3 Istituto Nazionale di Fisica Nucleare, Sezione di Roma Tor Vergata, Via della Ricerca Scientifica 1, 00133 Roma, Italy; massimo.bassan@roma2.infn.it (M.B.); giuseppe.pucacco@roma2.infn.it (G.P.)

4 Dipartimento di Fisica, Università di Roma Tor Vergata, Via della Ricerca Scientifica 1, 00133 Roma, Italy

* Correspondence: david.lucchesi@inaf.it

Received: 16 July 2020; Accepted: 26 August 2020; Published: 31 August 2020

check for updates

Measurements and constraints from the ascending node longitute

Preliminary constraints on alternative theories of gravitation

The 2019-2020 result for the **Lense-Thirring precession** can be exploited to preliminary constrain some **ATG**, such as:

- a **scalar-tensor** theory, i.e., a metric theory of gravity
- a **torsion** theory, i.e., a non-metric theory of gravity

$$\dot{\Omega}_{LT} = \mu \frac{2G}{c^2 a^3} \frac{J_\oplus}{(1-e^2)^{3/2}}$$

$$\left[\begin{array}{l} \mu_{GR} = 1 \\ \mu_{New} = 0 \end{array} \right.$$

Discrepancy — Error @ 95% CL — Systematic error

$$\boxed{\mu_{meas} - 1 = 1.5 \times 10^{-3} \pm 7.4 \times 10^{-3} \pm 16 \times 10^{-3}}$$

D. Lucchesi, M. Visco, R. Peron, et al., *A 1% Measurement of the Gravitomagnetic Field of the Earth with Laser-Traked Satellites*. Universe 6, 139, doi:10.3390/universe6090139, 2020

Measurements and constraints from the ascending node longitute

Constraints to scalar-tensor theories

- An interesting case is that of extended gravity (**EG**) theories, where:
  - ❑ $R \rightarrow f(R)$
  - ❑ $R \rightarrow f\left(R, R_{\alpha\beta}R^{\alpha\beta}\right)$
  - ❑ $R \rightarrow f\left(R, R_{\alpha\beta}R^{\alpha\beta}, \phi\right)$

S. Capozziello, G. Lambiase, et al., *Constraining models of extended gravity using Gravity Probe B and LARES experiments*. PRD 91, 044012, 2015

$$S_{GR} = \frac{1}{16\pi G}\int R\sqrt{-g}d^4x + S_{ng}$$

$$S_{BD} = \frac{1}{16\pi G}\int \left(\phi R - \frac{\omega}{\phi}g^{\alpha\beta}\phi_{,\alpha}\phi_{,\beta}\right)\sqrt{-g}d^4x + S_{ng}$$

$$S_{EG} = \frac{1}{16\pi G}\int \left(f\left(R, R_{\alpha\beta}R^{\alpha\beta}, \phi\right) - \frac{\omega}{\phi}g^{\alpha\beta}\phi_{,\alpha}\phi_{,\beta}\right)\sqrt{-g}d^4x + S_{ng}$$

$\rightarrow$ Introduces effective masses: m_R, m_ϕ, m_Y

$$Y = R_{\alpha\beta}R^{\alpha\beta}$$

Where ϕ is a scalar field and ω represents the dimensionless Dicke's coupling constant: it is tested by the experiments

Measurements and constraints from the ascending node longitute

Constraints to scalar-tensor theories

- An interesting case is that of extended gravity (**EG**) theories, where:
  - ❑ $R \rightarrow f(R)$
  - ❑ $R \rightarrow f\left(R, R_{\alpha\beta}R^{\alpha\beta}\right)$
  - ❑ $R \rightarrow f\left(R, R_{\alpha\beta}R^{\alpha\beta}, \phi\right)$

S. Capozziello, G. Lambiase, et al., *Constraining models of extended gravity using Gravity Probe B and LARES experiments*. PRD 91, 044012, 2015

$$\boldsymbol{\mu_{meas} - 1 = 1.5 \times 10^{-3} \pm 7.4 \times 10^{-3} \pm 16 \times 10^{-3}}$$

$$\boldsymbol{\dot{\Omega}_{grav} = \dot{\Omega}_{LT}^{GR} + \dot{\Omega}_{LT}^{EG}}$$

$$\boldsymbol{\dot{\Omega}_{LT}^{EG} = -\frac{1 + m_Y r + (m_Y r)^2}{e^{m_Y r}} \dot{\Omega}_{LT}^{GR}}$$

$$\boldsymbol{m_Y > 1.9 \times 10^{-6}\, m^{-1}}$$

$$S_{GR} = \frac{1}{16\pi G}\int R\sqrt{-g}d^4x + S_{ng}$$

$$S_{BD} = \frac{1}{16\pi G}\int \left(\phi R - \frac{\omega}{\phi} g^{\alpha\beta}\phi_{,\alpha}\phi_{,\beta}\right)\sqrt{-g}d^4x + S_{ng}$$

$$S_{EG} = \frac{1}{16\pi G}\int \left(f\left(R, R_{\alpha\beta}R^{\alpha\beta}, \phi\right) - \frac{\omega}{\phi} g^{\alpha\beta}\phi_{,\alpha}\phi_{,\beta}\right)\sqrt{-g}d^4x + S_{ng}$$

$\rightarrow$ Introduces effective masses: m_R, m_ϕ, m_Y

$$Y = R_{\alpha\beta}R^{\alpha\beta}$$

Where ϕ is a scalar field and ω represents the dimensionless Dicke's coupling constant: it is tested by the experiments

Measurements and constraints from the ascending node longitute

Constraints to torsion theories

- **Torsional** theories are characterized by **non-symmetric affine connections**:
  - ❑ $\Gamma^{\alpha}_{\beta\gamma} \neq \Gamma^{\alpha}_{\gamma\beta}$

$$S^{\alpha}_{\beta\gamma} = \frac{\Gamma^{\alpha}_{\beta\gamma} - \Gamma^{\alpha}_{\gamma\beta}}{2}$$

Tensor that describes the **torsion** phenomena

$\boldsymbol{t_1, t_2, t_3, w_1, w_2, w_3, w_4, w_5}$ **torsion** parameters that must be constrained by measurements

$$\dot{\Omega}_{tor} = \langle \dot{\Omega}^{LT} \rangle_{sec} \left[\mu - \frac{w_2 - w_4}{4} \right] + \langle \dot{\Omega}^{dS} \rangle_{sec} \left[\frac{t_2}{2} \right]$$

March, R., Bellettini, G., Tauraso, R., Dell'Agnello, S., *Constraining spacetime torsion with LAGEOS*. Gen. Relativ. Gravit., 43, 3099–3126, 2011

$$-0.36 < \boldsymbol{w_2 - w_4} < +0.44$$

From a previous measurement of the Lense-Thirring effect with an estimated error budget of about 10%

Ciufolini, I.; Pavlis, E.C. *A confirmation of the general relativistic prediction of the Lense-Thirring effect. Nature*, 431, 958–960, 2004

Measurements and constraints from the ascending node longitute

Constraints to torsion theories

- **Torsional** theories are characterized by **non-symmetric affine connections**:
  - $\Gamma^{\alpha}_{\beta\gamma} \neq \Gamma^{\alpha}_{\gamma\beta}$

$$S^{\alpha}_{\beta\gamma} = \frac{\Gamma^{\alpha}_{\beta\gamma} - \Gamma^{\alpha}_{\gamma\beta}}{2}$$

Tensor that describes the **torsion** phenomena

$$\mu_{meas} - 1 = 1.5 \times 10^{-3} \pm 7.4 \times 10^{-3} \pm 16 \times 10^{-3}$$

$$\dot{\Omega}_{tor} = \langle \dot{\Omega}^{LT} \rangle_{sec} \left[\mu - \frac{w_2 - w_4}{4} \right]$$

$$\dot{\Omega}_{grav} = \dot{\Omega}^{GR}_{LT} + \dot{\Omega}^{GR}_{dS} + \dot{\Omega}_{tor}$$

$$w_2 - w_4 = -0.006 \pm 0.064$$

$t_1, t_2, t_3, w_1, w_2, w_3, w_4, w_5$ **torsion** parameters that must be constrained by measurements

$$\dot{\Omega}_{tor} = \langle \dot{\Omega}^{LT} \rangle_{sec} \left[\mu - \frac{w_2 - w_4}{4} \right] + \langle \dot{\Omega}^{dS} \rangle_{sec} \left[\frac{t_2}{2} \right]$$

March, R., Bellettini, G., Tauraso, R., Dell'Agnello, S., *Constraining spacetime torsion with LAGEOS*. Gen. Relativ. Gravit., 43, 3099–3126, 2011

$$-0.36 < w_2 - w_4 < +0.44$$

From a previous measurement of the Lense-Thirring effect with an estimated error budget of about 10%

Ciufolini, I.; Pavlis, E.C. *A confirmation of the general relativistic prediction of the Lense-Thirring effect*. Nature, 431, 958–960, 2004

Local Lorentz Invariance

Local Lorentz Invariance (**LLI**) represents a pillar of the **Standard Model** (**SM**) of particles and fields as well as of Einstein's theory of **General Relativity** (**GR**).

LLI states that the outcome of any **local** (in space and time) non-gravitational experiment is **independent** of the **velocity** of the **freely-falling** reference frame in which the experiment is performed.

Modern unification theories suggest that the gravitational long-range interaction between macroscopic bodies may be mediated, not only by the metric tensor field $\mathbf{g}_{\mu\nu}$ of **GR** but also by other fields, as **scalar**, **vector**, or **tensor** fields.

More generally, besides **GR**, any metrically coupled **tensor-scalar** theory of gravitation does not predict **any violation** of **local boost invariance**. This is for example the case of the **Brans-Dicke** theory of gravitation which predicts the existence of a scalar field ϕ.

However, in the case of theories that contain **vector fields** or other **tensor fields**, in addition to the metric tensor $\mathbf{g}_{\mu\nu}$, one expects that the **global distribution of matter** in the **Universe** to select a **preferred rest frame** for the local gravitational interaction.

In this case the **physical laws** could be **different** from a **moving observer** with respect to a **stationary one**, as well as from the orientation...

Local Lorentz Invariance

In **theories** of gravity with $\begin{cases} g_{\mu\nu} \\ \phi \end{cases}$ **LLI holds**, while in **theories** with $\begin{cases} g_{\mu\nu} \\ K^{\mu} \end{cases}$ or with $\begin{cases} g_{\mu\nu} \\ C_{\mu\nu} \end{cases}$ **LLI is violated**.

From the phenomenological point of view, and in the framework of the **Parametrized-Post Newtonian** (**PPN**) formalism [1,2,3], valid in the **weak-field** and **slow-motion** (**WFSM**) limit of **GR**, the **Preferred Frame Effects** (**PFE**) are described by the parameters **α1**, **α2** and **α3**, all equal to zero in **GR** and in tensor-scalar theories of gravity. In particular, in the case of the interaction of **N** ideal test masses, the **Lagrangian** depends on the two parameters **α1** and **α2**, that, if different from zero, will provide non-boost invariant terms depending on the **velocities** ($\boldsymbol{v}_a^0$) of the test masses with respect to some **gravitationally preferred rest frame** [4]:

$$\mathcal{L}^N = \mathcal{L}_{\beta,\gamma,\eta} + \mathcal{L}_{\alpha_1} + \mathcal{L}_{\alpha_2}$$

$$\mathcal{L}_{\alpha_1} = -\frac{\alpha_1}{4c^2} \sum_{a \neq b} \frac{G m_a m_b}{r_{ab}} \left(\boldsymbol{v}_a^0 \cdot \boldsymbol{v}_b^0 \right)$$

1. **Nordtvedt, K.** *Equivalence Principle for Massive Bodies. II. Theory*. Phys. Rev. **1968**, 169, 1017–1025
2. **Will, C.M.** *Theoretical Frameworks for Testing Relativistic Gravity. II. Parametrized Post-Newtonian Hydrodynamics, and the Nordtvedt Effect*. Astrophys. J. **1971**, 163, 611–628
3. **Will, C.M.; Nordtvedt, K.** *Conservation Laws and Preferred Frames in Relativistic Gravity. I. Preferred-Frame Theories and an Extended PPN Formalism*. Astrophys. J. **1972**, 177, 757–774
4. **Damour, T.; Esposito-Farese. G**. *Testing for preferred-frame effects in gravity with artificial Earth satellites*. Phy. Rev. D **1994**, 49, 4, 1693-1706

Local Lorentz Invariance

Local Lorentz Invariance is a key ingredient of the **Equivalence Principle**.

Einstein Equivalence Principle (EEP)
valid in **GR** and in all **metric theories** of gravity:

1. **WEP**
2. **LLI**
3. **LPI**

Strong Equivalence Principle (SEP)
valid in **GR**:

1. **GWEP**
2. **LLI**
3. **LPI**

GWEP = **Gravitational Weak Equivalence Principle**. It means that **WEP** is valid for **self-gravitating bodies** as well as for test bodies.

$$\mathcal{L}^N = \mathcal{L}_{\beta,\gamma,\eta} + \mathcal{L}_{\alpha_1} + \mathcal{L}_{\alpha_2}$$

$$G_{ab} = \mathrm{G}\left[1 + \eta\left(\frac{E_a^{grav}}{m_a c^2} + \frac{E_b^{grav}}{m_b c^2}\right)\right]$$

Nordtvedt effect

$$\eta = 4\beta - \gamma - 3 - \alpha_1 + \frac{2}{3}\alpha_2$$

$$\beta = \gamma = 1$$
$$\alpha_1 = \alpha_2 = 0$$

in **GR**

Local Lorentz Invariance

LLI and, consequently, **PFE**, are **well tested** in the context of **high-energy physics experiments** but are **much more difficult** to test in the context of **gravitation**, both in the **weak-field** regime and in the **strong-** or **quasi-strong-field** regime.

In 1994, **Damour** and **Esposito-Farese** have shown that the orbits of some **artificial satellites** have the potential to provide <u>improvements</u> in the **limit** of the **α1** parameter down to the **10^{-6}** level, thanks to the appearance of **small divisors** which enhance the corresponding **PFE**.

PHYSICAL REVIEW D VOLUME 49, NUMBER 4 15 FEBRUARY 1994

ARTICLES

Testing for preferred-frame effects in gravity with artificial Earth satellites

Thibault Damour
Institut des Hautes Etudes Scientifiques, 91440 Bures sur Yvette, France
and Département d'Astrophysique Relativiste et de Cosmologie, Observatoire de Paris,
Centre National de la Recherche Scientifique, 92195 Meudon, France

Gilles Esposito-Farèse
Centre de Physique Théorique, Centre National de la Recherche Scientifique,
Luminy, Case 907, 13288 Marseille Cedex 9, France
(Received 8 October 1993)

As gravity is a long-range force, one might *a priori* expect the Universe's global matter distribution to select a preferred rest frame for local gravitational physics. At the post-Newtonian approximation, two parameters suffice to describe the phenomenology of preferred-frame effects. One of them has already been very tightly constrained ($|\alpha_2| < 4 \times 10^{-7}$, 90% C.L.), but the present bound on the other one is much weaker ($|\alpha_1| < 5 \times 10^{-4}$, 90% C.L.). It is pointed out that the observation of particular orbits of artificial Earth satellites has the potential of improving the α_1 limits by a couple of orders of magnitude, thanks to the appearance of small divisors which enhance the corresponding preferred-frame effects. There is a discrete set of inclinations which lead to arbitrarily small divisors, while, among zero-inclination (equatorial) orbits, geostationary ones are near optimal. The main α_1-induced effects are (i) a complex secular evolution of the eccentricity vector of the orbit, describable as the vectorial sum of several independent rotations, and (ii) a yearly oscillation in the longitude of the satellite.

Local Lorentz Invariance

In our analysis:

- we concentrated upon the **yearly oscillation** of the **longitude** $(\omega + M)$ of the **LAGEOS II** satellite
- as **gravitationally preferred rest frame** we consider that of the **cosmic background radiation**
- **w** represents the speed of the **Sun** with respect to this reference frame with orientation given by the following ecliptic coordinates $(\lambda_{PF}, \beta_{PF})$:

$$w = 368 \pm 2\,\frac{km}{s} \qquad \begin{cases} \lambda_{PF} = 171°.55 \\ \beta_{PF} = -11°.13 \end{cases}$$

$$\mathcal{L}_{\alpha_1} = -\frac{\alpha_1}{4c^2}\sum_{a\neq b}\frac{Gm_a m_b}{r_{ab}}\left(\boldsymbol{v}_a^0 \cdot \boldsymbol{v}_b^0\right) \qquad \boldsymbol{v}_s^0 = \boldsymbol{v}_s + \boldsymbol{v}_\oplus + \boldsymbol{w}$$

$$\mathcal{L}_{\alpha_1} = -\frac{\alpha_1}{2c^2}\frac{GM_\oplus m_s}{r_{\oplus s}}\left(\boldsymbol{v}_\oplus + \boldsymbol{w}\right)\cdot\left(\boldsymbol{v}_s + \boldsymbol{v}_\oplus + \boldsymbol{w}\right)$$

Local Lorentz Invariance

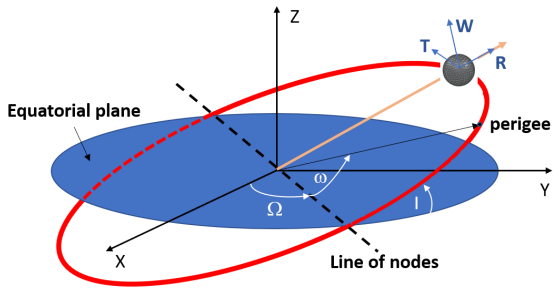

From **Lagrange's** perturbative equations we are able to extract the perturbative effect of a possible **PFE** on the **rate** of the **argument of pericenter** and on the **rate** of **the mean anomaly** of the satellite.

$$\frac{d\omega}{dt} = \frac{\sqrt{1-e^2}}{na^2e}\frac{\partial R}{\partial e} - \frac{\cot i}{na^2\sqrt{1-e^2}}\frac{\partial R}{\partial i}$$

$$\frac{dM}{dt} = -\frac{2}{na}\frac{\partial R}{\partial a} - \frac{1-e^2}{na^2e}\frac{\partial R}{\partial e}$$

R represents the perturbing funtion
$(a, e, i, \Omega, \omega, M)$ are the keplerian elements
n represents the satellite mean motion: $n = \sqrt{\frac{GM_\oplus}{a^3}}$

We finally obtain:

$$\left(\dot{\omega} + \dot{M}\right)_{\alpha_1} = -\alpha_1 n \frac{w v_\oplus}{c^2}(1 + \cos\varepsilon)\cos\beta_{PF}\sin(n_\oplus t - \lambda_{PF}) + \cdots$$

where ε represents the **obliquity** of the **ecliptic** with respect to the celestial equator ($\varepsilon \cong 23°.45$).

If **PFEs** exist, the quantity $\left(\dot{\omega} + \dot{M}\right)_{\alpha_1}$ must be present in the **residuals** of the two elements obtained from the satellite **POD**.

Local Lorentz Invariance

POD of the **LAGEOS II** satellite

- **GEODYN II s/w**
  - ❑ Timespan of 10311 days (about 28.3 years)
  - ❑ Arc length: 7 days
  - ❑ General Relativity: not modeled
  - ❑ Empirical accelerations, CR, …: not estimated
  - ❑ Non-gravitational perturbations: internal and external
  - ❑ Gravity field: from GRACE solutions
  - ❑ State-vector adjusted to best fit the tracking data
  - ❑ …

Local Lorentz Invariance

Procedure in the **time domain** to **extract** the **constraint** in the **PPN** parameter **α1**.

1. From the **POD** we estimated the satellite **state-vector** for each **arc**
2. From the **state-vectors** we obtain the **residuals** in the **rate** of the orbital elements: $\dot{\omega}$ and $\dot{M}$
3. From these **residuals** we build our **gravitational observable**: $\dot{\omega} + \dot{M}$
4. We remove from the **observable** the **predictions** of the **unmodeled relativistic precessions** of **GR**
5. We **Pass-Band filter** this new (corrected) observable around the **yearly frequency**
6. We apply a **Lock-in** to these data at the **expected frequency** (**the annual one**) for the effect described by the **α1** parameter and linked to the existence of the **PFE** due to the **cosmic background radiation**
7. We calculate the **mean** from this last operation and from this **mean**, suitably renormalized, we **extract** the value of the **PPN** parameter **α1**.

$$\left(\dot{\omega} + \dot{M}\right)_{\alpha_1} = -\alpha_1 n \frac{w v_{\oplus}}{c^2}(1 + \cos\varepsilon)\cos\beta_{PF}\sin(n_{\oplus}t - \lambda_{PF}) + \cdots = \alpha_1 K \sin(n_{\oplus}t - \lambda_{PF}) + \cdots$$

$$K = -n \frac{w v_{\oplus}}{c^2}(1 + \cos\varepsilon)\cos\beta_{PF}$$

Local Lorentz Invariance

Residuals in the two **observables** after the **POD**

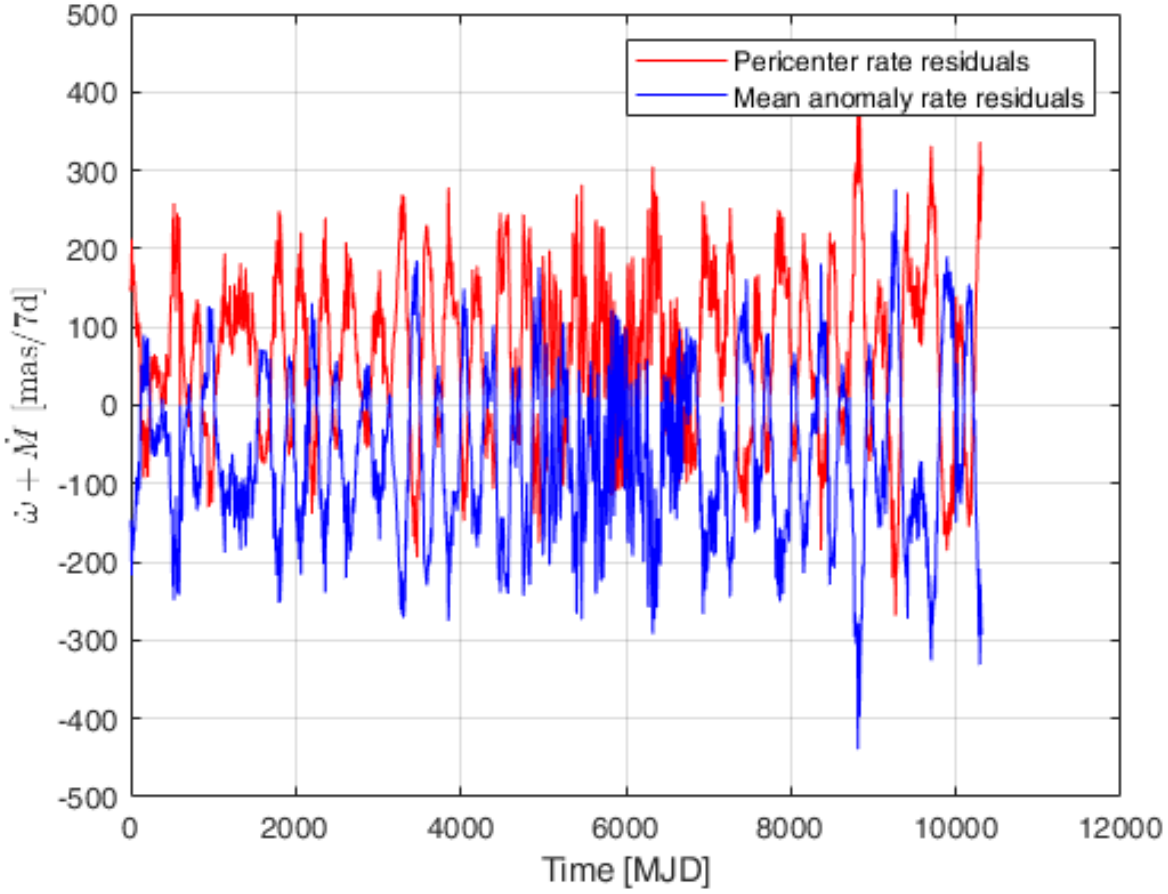

Relativistic precessions in the two **observables**

Rate (mas/yr)	LAGEOS	LAGEOS II	LARES
$\dot{\omega}_{Schw}$	+ 3270.78	+ 3352.58	+ 10,110.15
$\dot{\omega}_{LT}$	+ 31.23	– 57.33	– 124.53
$\dot{\omega}_{J2}^{dir}$	– 3.26	+ 2.85	– 23.38
$\dot{\omega}_{J2}^{indir}$	– 0.36	+ 0.16	– 2.65
Total	+ 3306.38	+ 3298.26	+ 9959.59
$\dot{M}_{Schw}$	– 3278.75	– 3352.26	– 10,110.14
$\dot{M}_{J_2 rel}$	– 0.92	+ 0.15	– 6.71
Total	– 3278.75	– 3352.11	– 10,116.85

$$\frac{d\omega}{dt} = \frac{\sqrt{1-e^2}}{na^2 e}\frac{\partial R}{\partial e} - \frac{\cot i}{na^2\sqrt{1-e^2}}\frac{\partial R}{\partial i}$$

$$\frac{dM}{dt} = -\frac{2}{na}\frac{\partial R}{\partial a} - \frac{1-e^2}{na^2 e}\frac{\partial R}{\partial e}$$

Local Lorentz Invariance

Residuals in the **observable** $\dot{\omega} + \dot{M}$

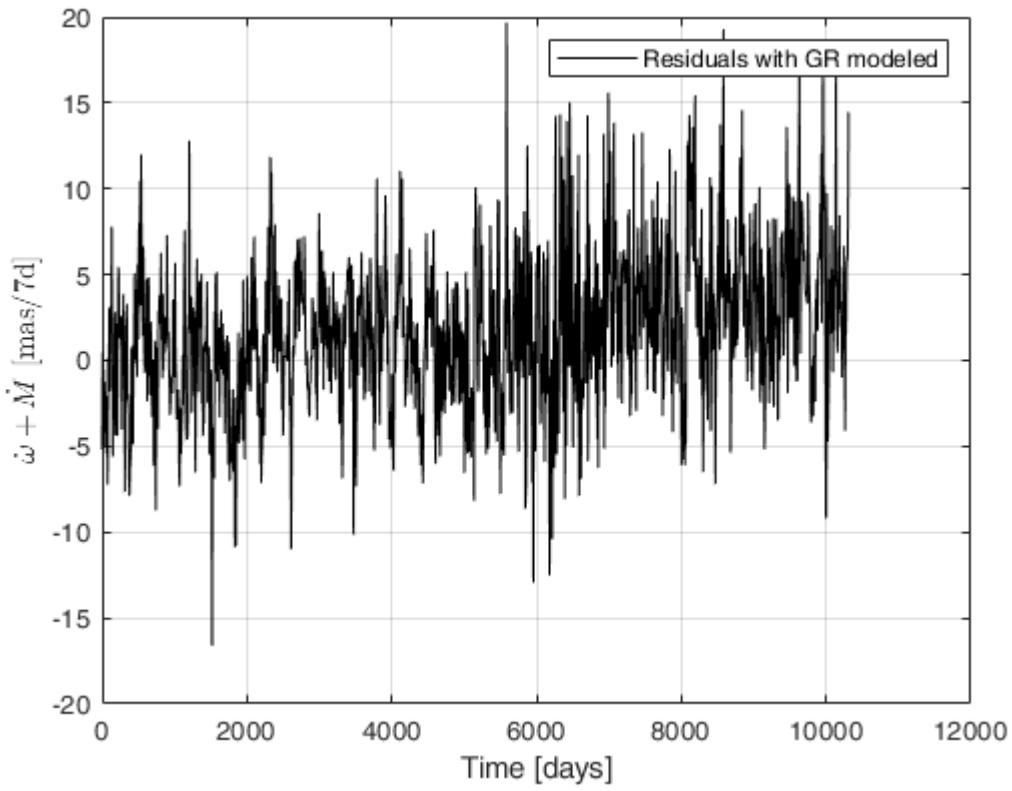

FFT of the **Residuals** in the **observable**

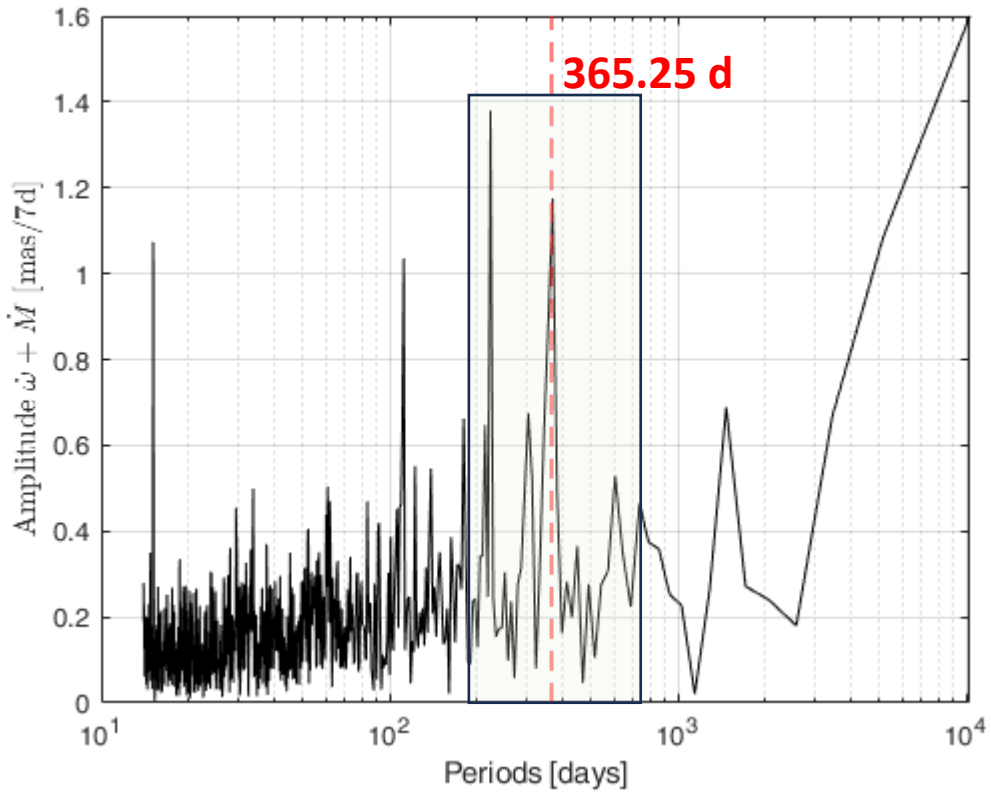

Local Lorentz Invariance

Residuals in the **observable** after Pass-Band filtering

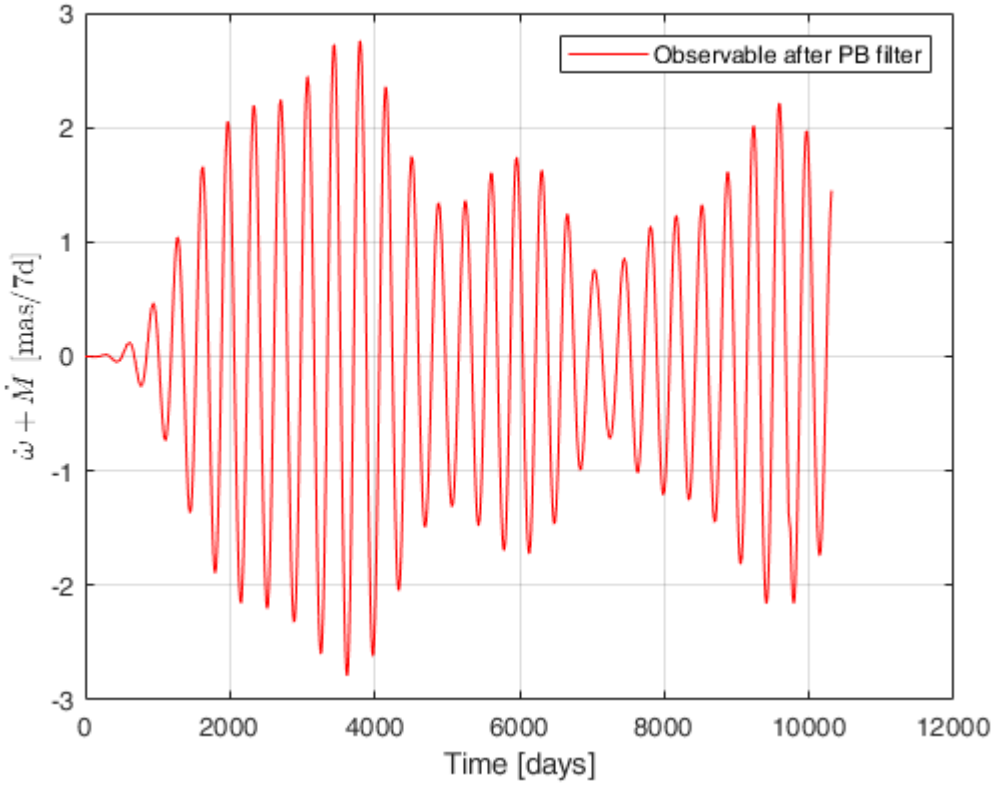

FFT of the **Residuals** in the **observable**

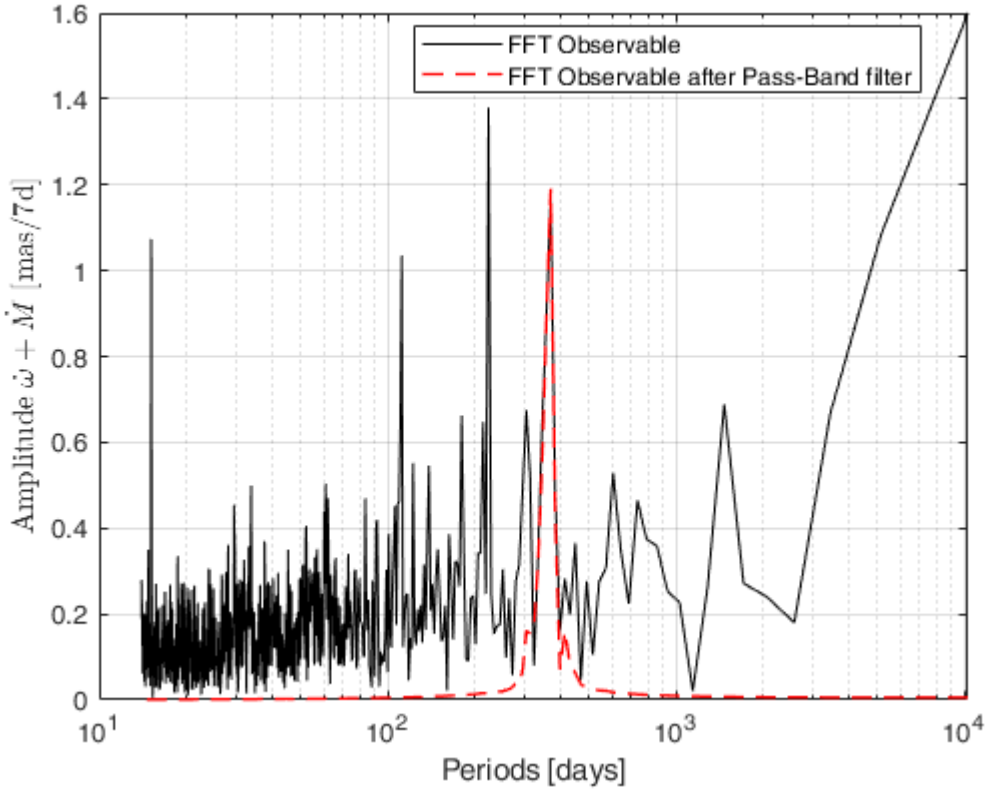

Local Lorentz Invariance

Lock-in analysis

$$\left(\dot{\omega} + \dot{M}\right)_{\alpha_1} = \alpha_1 K \sin(n_\oplus t - \lambda_{PF}) + \cdots \qquad K = -n\frac{w v_\oplus}{c^2}(1 + \cos\varepsilon)\cos\beta_{PF}$$

$$\sin(n_\oplus t - \lambda_{PF}) \cdot \left(\dot{\omega} + \dot{M}\right)_{res} = \alpha_1 \mathrm{K}(\sin(n_\oplus t - \lambda_{PF}))^2 + \cdots$$

Lock-in analysis, in this case more properly a **homodyne analysis** (**phase sensitive detection**), is mathematically based on **Werner's trigonometric formulas:**

$$\sin\alpha\sin\beta = \frac{1}{2}(\cos(\alpha - \beta) - \cos(\alpha + \beta))$$

$$\sin\alpha\cos\beta = \frac{1}{2}(\sin(\alpha - \beta) + \sin(\alpha + \beta))$$

$$\sin\alpha\sin\alpha = \frac{1}{2}(1 - \cos(2\alpha))$$

If **α=β**, as in our case, a **part of the signal** goes in **continuous** (**DC**) and a **part at twice the annual frequency**.

Local Lorentz Invariance

Lock-in analysis

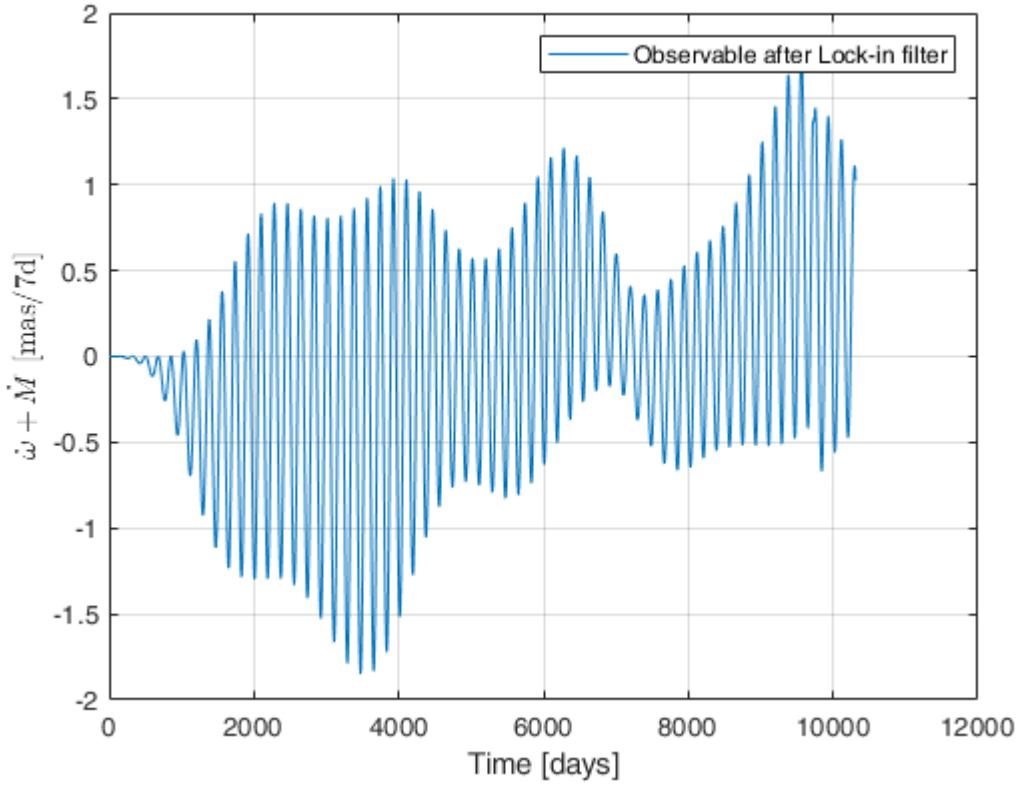

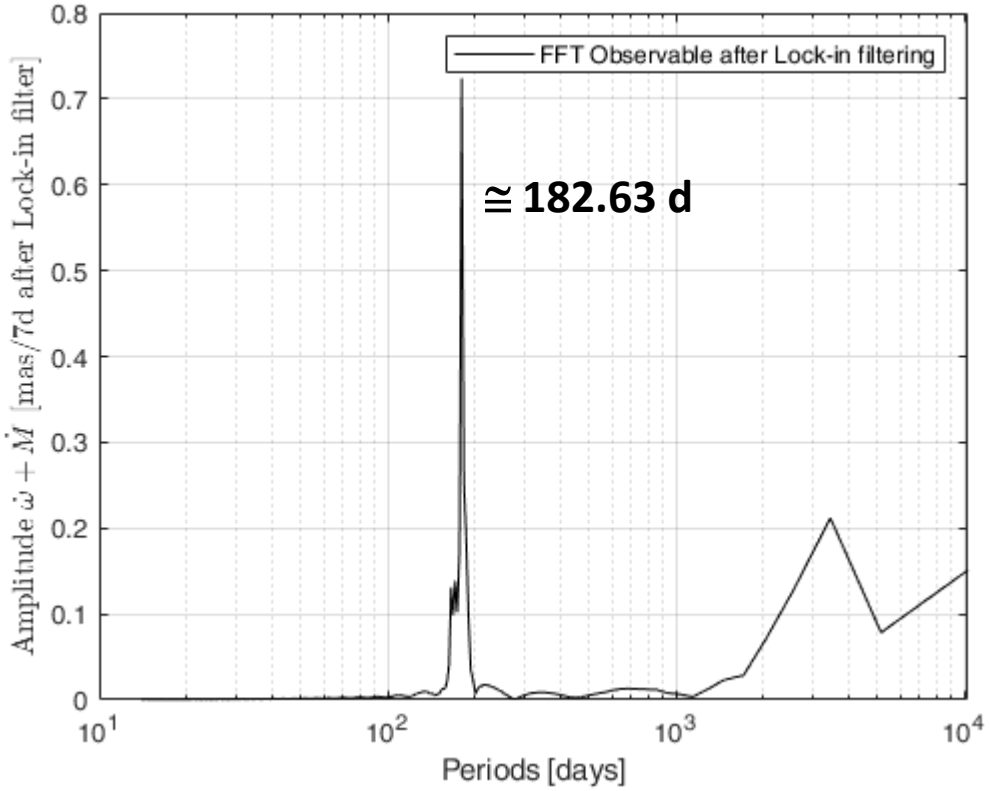

$$\alpha_1 = \left\langle \left(\dot{\omega} + \dot{M}\right)_{res} \right\rangle \frac{2}{K}$$

Local Lorentz Invariance

Preliminary result for the **PPN** parameter **α1** and constraints to alternative theories of gravitation:

$$\alpha_1 = +1.64 \times 10^{-6}$$

1. This result represents the **first constraint in α1** in the **field** of the **Earth** based on a **pure gravitational experiment**.
2. The result obtained, although preliminary, confirms the <u>validity</u> of the **LLI** for gravity and <u>strongly constrains</u> possible **PFEs** and, consequently, **vector-tensor theories of gravity**, at least in the **WFSM** limit of **GR: Einstein Æther theory.**

Local Lorentz Invariance

Preliminary result for the **PPN** parameter **α1** and constraints to alternative theories of gravitation:

$$\alpha_1 = +1.64 \times 10^{-6}$$

1. This result represents the **first constraint in α1** in the **field** of the **Earth** based on a **pure gravitational experiment**.
2. The result obtained, although preliminary, confirms the validity of the **LLI** for gravity and strongly constrains possible **PFEs** and, consequently, **vector-tensor theories of gravity**, at least in the **WFSM** limit of **GR: Einstein Æther theory.**
3. We have also performed a **sensitivity analysis** on the **value** of the **PPN parameter α1** by constructing a **distribution** of its values as **the Lock-in frequency** and signal **phase** vary **randomly** on a sample of **10^5 values** each. We consequently obtained a **two-parameter distribution** of **α1** for evaluating the possible violation signal of **GR**.

Results from the sensitivity analysis:

$\langle \alpha_1 \rangle = -3.2 \times 10^{-7}$

rms $(\alpha_1) = \sigma(\alpha_1) \cong 7.146 \times 10^{-5}$

max$(\alpha_1) = +1.1283 \times 10^{-4}$

median $(\alpha_1) = -9.9 \times 10^{-7}$

min$(\alpha_1) = -1.1283 \times 10^{-4}$

Local Lorentz Invariance

Sensitivity analysis:

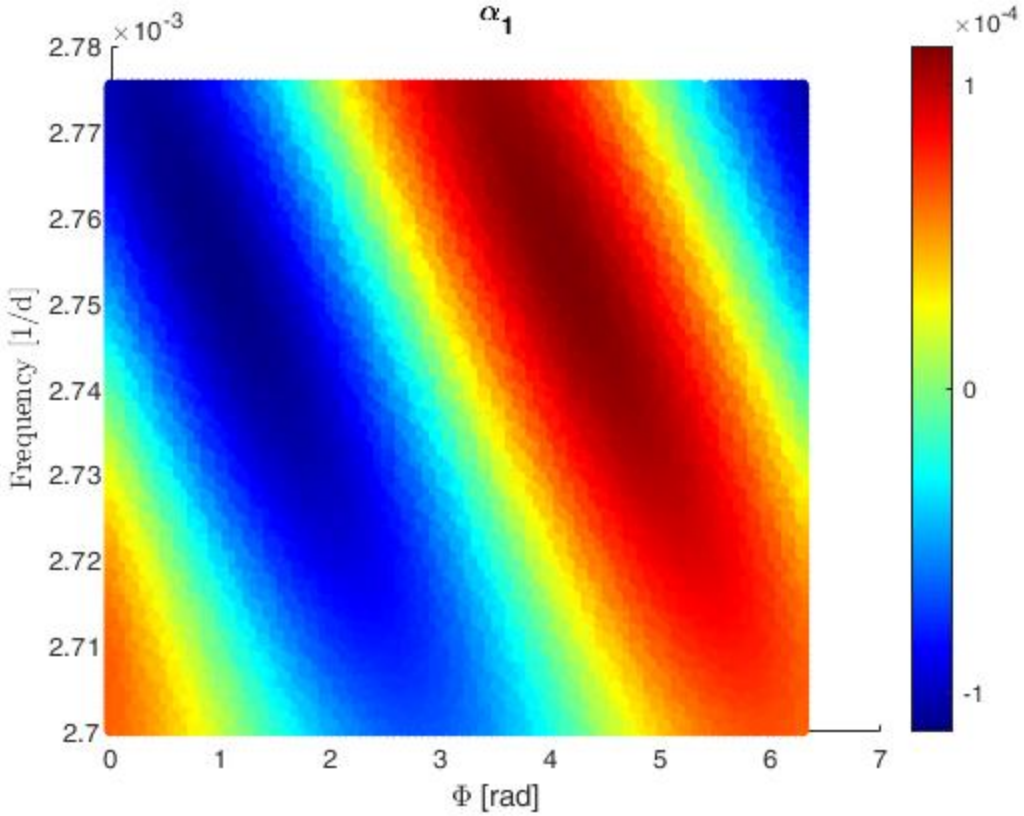

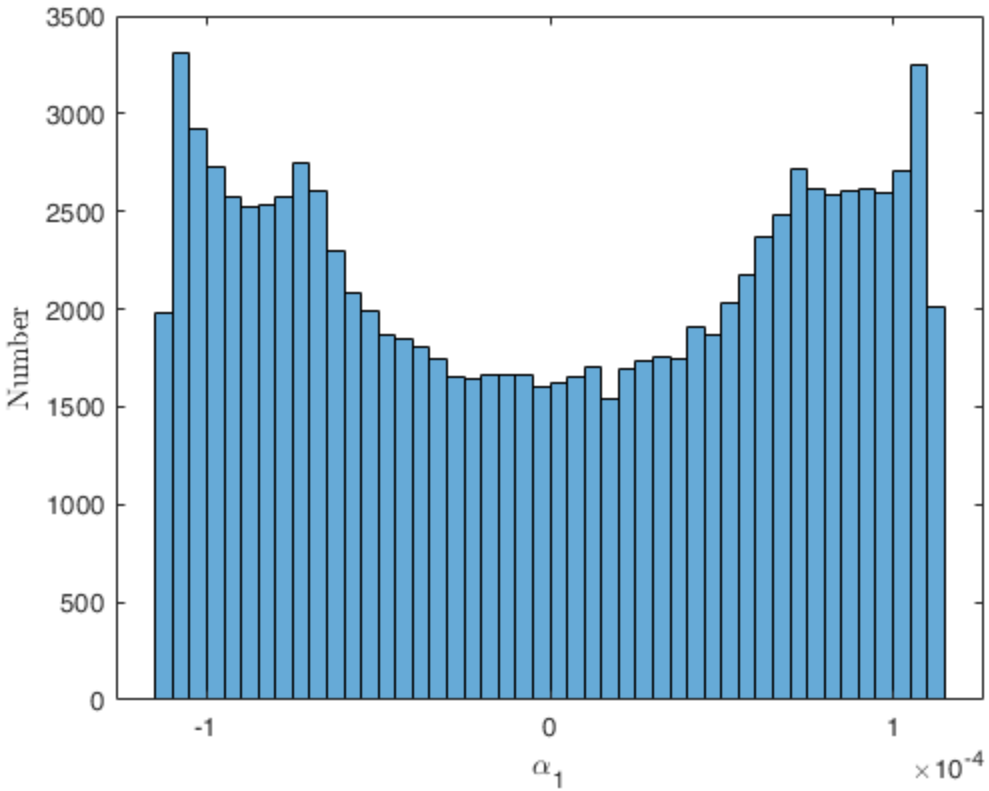

Local Lorentz Invariance

Preliminary **error budget** for the **systematic errors**:

1. **Gravitational field (quadrupole)** $\delta\alpha_1 \cong 2.47 \times 10^{-6}$
2. **Solid tides** $7 \times 10^{-9} < \delta\alpha_1 < 7 \times 10^{-8}$
3. **Ocean tides** $1.538 \times 10^{-6} < \delta\alpha_1 < 1.538 \times 10^{-5}$
4. **Non-Gravitational Perturbations:** $\delta\alpha_1 \cong 0$

$$\left.\begin{array}{c} \delta\alpha_1 \cong 2.47 \times 10^{-6} \\ 7 \times 10^{-9} < \delta\alpha_1 < 7 \times 10^{-8} \\ 1.538 \times 10^{-6} < \delta\alpha_1 < 1.538 \times 10^{-5} \end{array}\right\} \delta\alpha_1 \cong 1.6 \times 10^{-5}$$

Very preliminary evaluation of the measure on the constraint to the parameter **α1**:

$$\alpha_1 = +1.6 \times 10^{-6} \pm 7 \times 10^{-5}$$

From the measure

From the distribution

Local Lorentz Invariance

Comparison with the literature:

$\alpha_1 = +1.6 \times 10^{-6} \pm 7 \times 10^{-5}$	With **SLR** data from **LAGEOS II longitude**, 2023
$\alpha_1 = -7 \times 10^{-5} \pm 9 \times 10^{-5}$	With **LLR** data from the **oscillations** of the **Earth-Moon distance**, 2008
$\hat{\alpha}_1 = -4 \times 10^{-6} \pm 4 \times 10^{-5}$	From **binary Pulsar** data, 2012

Müller J, Williams J G and Turyshev S G, 2008. Lunar laser ranging contributions to relativity and geodesy. *Lasers, Clocks and Drag-Free Control: Exploration of Relativistic Gravity in Space (Astrophysics and Space Science Library* vol 349*)* ed H Dittus, C Lammerzahl and S G Turyshev p 457.

J. Müller, K. Nordtvedt, **D. Vokrouhlický**, *Improved constraint on the α_1 PPN parameter from lunar motion*. Phys. Rev. D, Vol. 54, No 10, 1996.

L. Shao, N. Wex, *New tests of Local Lorentz invariance of gravity with small-eccentricity binary pulsars*. Class. Quantum Grav. 29, 2012.

Conclusions

- The **activities** of the previous experiment **LARASE** (2013-2019) and of the ongoing experiment **SaToR-G** have been presented together with their **theoretical** and **experimental framework**

- We have obtained several **significant precise** and **accurate results** in testing **GR**, resulting in **interesting constraints** to **alternative theories of gravitation**

- **Passive geodetic satellites** represent indeed a very **powerful tool** (quasi ideal proof masses) to **test** the **gravitational interaction** in the field of the Earth and to **compare** the **predictions** of **GR** with those of **alternative theories of gravitation**.

The SaToR-G Team

@IAPS-INAF, Tor Vergata (RM)

David Lucchesi
Marco Lucente
Carmelo Magnafico
Roberto Peron
Feliciana Sapio
Massimo Visco

@Dept. Physics, Univ. Tor Vergata (RM)

Massimo Bassan
Giuseppe Pucacco

@ISTI-CNR, Pisa

Luciano Anselmo
Carmen Pardini

@IGN, Yebes (Spain)

José Carlos Rodríguez

Many thanks for your kind attention